PHOTOMETRY OF STAR CLUSTERS

Thomas Harry Hope Lloyd Evans

A Thesis Submitted for the Degree of PhD
at the
University of St Andrews

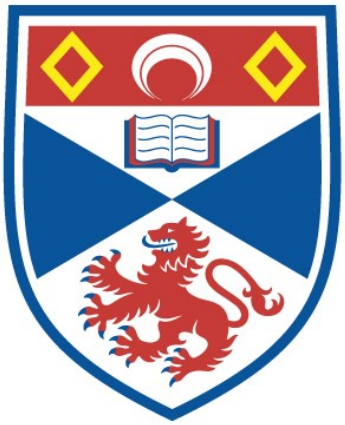

1968

PHOTOMETRY OF STAR CLUSTERS

BY

THOMAS HARRY HOPE LLOYD EVANS

A Thesis presented for the Degree
of Doctor of Philosophy in the
University of St. Andrews.

August, 1968.

Th ~~5609~~
5653

I hereby declare that the following Thesis is based upon the results of experiments carried out by me, that the Thesis is my own composition, and that it has not previously been presented for a higher degree. The research was carried out in the University Observatory, St. Andrews and the Radcliffe Observatory, Pretoria.

24 September 1968.

The Research undertaken by the Author comprises a study of the performance of the Cassegrain Schmidt telescopes of the St. Andrews University Observatory as applied to the photographic photometry of star clusters and an investigation of two Southern star clusters using the 74-inch reflector of the Radcliffe Observatory, Pretoria.

I was admitted as a Research Student under Ordinance General No. 12 from 1st August, 1963 and as a candidate for the degree of Doctor of Philosophy under Resolution of the University Court, 1966, No. 3 from October, 1964.

It is certified that the conditions of the Ph.D. Ordinance and Regulations of the University of St Andrews have been fulfilled in connexion with this Thesis by T.H.H. Lloyd Evans.

D.W.N. Stibbs
Napier Professor of Astronomy.

C O N T E N T S.

—oOo—

SUMMARY.

The suitability of the Cassegrain Schmidt telescopes at St. Andrews University Observatory for the measurement of stellar magnitudes and colours by in-focus multicolour photography has been examined. A major requirement is that the photographic plate should coincide with the focal surface. Thermal effects in the Scott Lang Telescope and optical and mechanical problems in the James Gregory Telescope cause difficulty in attaining this. These difficulties have been overcome in the case of the Scott Lang Telescope but no certain method for focussing the James Gregory Telescope was found. The photometric field, limited by field error, is approximately one degree in diameter in each case. Colour equations between the instrumental and standard B, V systems depend on magnitude and, in the case of the Scott Lang Telescope, on exposure time as well.

The methods used to measure UBV magnitudes and colours with the Radcliffe 74-inch reflector are described and the accuracy of the results discussed.

Magnitudes and colours of stars brighter than V = 15.5 in the open cluster IC 2581 have been measured, together with MK spectral types for a few of the brighter stars. The interstellar absorption provides a criterion for the recognition of cluster members. A discrepancy between the shape of the cluster main sequence and that of the zero age main sequence is attributed to an error in the derivation of the standard zero age main sequence. The cluster is found to be at a distance of 2500 parsecs and may form part of the η Carinae complex. The positions

of the brightest stars in the colour magnitude diagram are discussed in the light of modern theories of stellar evolution and an age of approximately 10 million years is deduced.

The colour magnitude diagram of the open cluster NGC 6383 has been obtained for stars brighter than V = 18.1; the limiting magnitudes in B and U are 19.7 and 17.9, respectively. MK spectral types have permitted the cluster membership of several bright B stars to be established; some stars of later type are non-members. The observations of this cluster are more complete than for most young clusters studied to date, but the poorness of the cluster and the unfavourable distribution of interstellar absorption with distance make it impossible to be certain of the membership of stars fainter than V = 13. The lack of stars fainter than V = 12.8 on the zero age main sequence indicates a contraction age of 5 million years. The distance is 1300 parsecs, like those of other young groups in the vicinity. The dense dust clouds which divide the Milky Way in Scorpius are immediately beyond this. Several faint variable stars may be of the T Tauri type.

ACKNOWLEDGEMENTS.

I am indebted to Professor D.W.N. Stibbs and to Dr. A.D. Thackeray for making the facilities of the St. Andrews University Observatory and the Radcliffe Observatory, respectively, available to me.

Professor Stibbs and Dr. A.J. Meadows each supervised this research for part of the time spent at St. Andrews. I am very grateful to them both for their valuable advice.

Dr. J. Cisar and Mr. T.B. Slebarski gave freely of their time in discussing problems encountered in using the Cassegrain Schmidt telescopes.

Dr. Thackeray suggested that I observe the open star clusters IC 2581 and NGC 6383. Dr. P.J. Andrews introduced me to the techniques of photoelectric photometry and shared in the necessary calibration work.

I am indebted to Mr. A.N. Argue, Dr. A.W.J. Cousins, Dr. V.C. Reddish and Dr. I.G. van Breda for helpful discussions and correspondence on photometric and instrumental problems.

Dr. P.W. Hill and Dr. D.H.P. Jones kindly advised me on the subject of computer programming.

I am most grateful to the members of the technical staff at the St. Andrews University Observatory and the Radcliffe Observatory and the staff of the Computing Laboratories at St. Andrews University and at the Council for Scientific and Industrial Research, Pretoria.

I wish to record my appreciation to the Carnegie Trust for the Universities of Scotland for a Scholarship while I was at St. Andrews and for additional grants which enabled me to attend scientific courses and meetings elsewhere.

LIST OF FIGURES.

—oOo—

LIST OF TABLES.

—oOo—

INTRODUCTION.

The critical testing of theories of stellar evolution has depended greatly on observations of star clusters which comprise a sample of stars of practically the same age but a wide range of mass and hence of evolutionary state. The Hertzsprung-Russel diagram of the cluster, in the form of a plot of magnitude against colour index, may be compared with the corresponding theoretical diagram. In practice it is usual to make observations in three wavebands so that the interstellar absorption in front of the cluster can be determined and allowed for. The two-colour diagram can, in favourable cases, provide a criterion of cluster membership for individual stars.

The investigation of a star cluster typically requires the measurement of the magnitudes of several hundred stars in each of three colours. The photographic plate may be used to record the brightness of all the stars at once, but the complexity of the photographic process makes it difficult to calibrate the magnitude and colour scales over the whole field. Photo-electric photometry can attain the requisite systematic accuracy, but the observation of individual stars is a time consuming process. It is customary to determine the magnitudes and colours photographically, using a relatively small number of stars observed photo-electrically to provide the calibration.

To make the best use of a photo-electric sequence it is evident that the photographic telescope must have a wide field. One such instrument

is the Cassegrain - Schmidt telescope, which is intended to combine the wide field of the classical Schmidt telescope with the flat and accessible focal surface of the conventional Cassegrain arrangement. Such an instrument could also be provided with bulky accessories such as a Cassegrain spectrograph or photometer. The Scott Lang and James Gregory Telescopes at St. Andrews University Observatory are of this type. Section I is devoted to an investigation of their properties in relation to the specific requirements of in-focus stellar photometry.

Section II is devoted to an account of the observing techniques employed at the Radcliffe Observatory in the study of star clusters by photographic and photo-electric photometry with the 74-inch reflector.

Section III describes the results obtained for the open cluster IC 2581 in Carina. This relatively young cluster contains several interesting evolving stars and lies in a region of particular importance to the study of galactic structure.

Section IV similarly describes the open cluster NGC 6383 in Scorpius. It was selected for study because it is one of the youngest clusters known; its relative freedom from bright nebulosity permits accurate photometric observations of fainter stars than in most objects of this type.

SECTION 1.

THE ST. ANDREWS CASSEGRAIN SCHMIDT TELESCOPES.

1. INTRODUCTION.

The theory of the Cassegrain Schmidt telescope has been developed by Linfoot (1943, 1944, 1955) on the basis of the plate diagram analysis developed by Burch (1942). The theory of this class of instruments has also been given by Baker (1940). Wayman (1952) later developed the theory to include fifth order aberrations. The ultimate optical performance, especially as regards the off-axis image quality, could not be predicted in complete detail when the St. Andrews telescopes were in the design stage. It was decided that the simplest type in this family of telescopes - the flat field aplanat with both mirrors spherical - should be tested experimentally, and the Pilot Model or Scott Lang Telescope was constructed to this end. (Linfoot, 1948; St. Andrews Observatory, 1950; E. Finlay - Freundlich, 1950). Finlay-Freundlich and Waland (1953) published a description of the telescope.

It was planned to design the 37-inch telescope after a critical evaluation of the performance of the Pilot Model. Linfoot (1956) published micro-photographs of the image quality taken by Dr. J. Cisar, but the study of the performance was never completed. The 37-inch telescope was completed with spherical mirrors, in spite of indications that it might be necessary to figure one of the mirrors.

The performance of the two instruments in 1963 - 1965, when they were used by the writer, were as follows.

The Scott Lang Telescope showed astigmatism which varied with

position angle as well as with distance from the centre of the field. This is understood to be the result of an error in figuring the corrector plate. The minimum image size at the centre of the field was approximately 30μ , or 5" of arc.

The James Gregory Telescope suffered from 20 wavelengths of spherical overcorrection, with a minimum image diameter of about 65μ , or 5" of arc. Optical misalignment caused strong coma which was not symmetrical about the centre of the field. A typical image had a small core with a displaced hollow comatic halo. Underexposed images showed only the core, while denser images appeared triangular.

It appears that

(1) The St. Andrews telescopes probably do not represent the optimum design of this class of telescopes.

(2) The performance of both instruments was marred by errors in figuring the corrector plates.

(3) The optical performance of the James Gregory Telescope was adversely affected by optical mis-alignment during the investigation described in this Section.

These considerations were not realised when the present work was started. The formation of photographic images is a complex process in any case and the photometric consequences of given optical imperfections are not readily predictable.

The ADH Baker Schmidt at the Boyden Observatory near Bloemfontein is another instrument of this type. According to Bowen (1960) the secondary mirror is not spherical. Accounts of its performance in photometric work have been published by Lindsay (1952), Hodge (1960), Vanysek (1964) and others. The corrector plate is normally used at full

aperture and in the absence of an internal stop the vignetting-free field is only about 1° in diameter. Hodge stopped down the corrector plate to reduce vignetting and claimed an essentially error-free photometric field of 2° 40' diameter. Other workers have referred to elongated images with consequent photometric errors, and it is generally accepted that the mechanical stability of the instrument is poor so that the optical performance may vary from time to time. The writer examined a number of plates taken with the ADH telescope in 1966: even the best of these showed some elongation of the images, probably due to coma. The aberrations are much less severe than those of the James Gregory Telescope and the small size of the images shows that the St. Andrews telescopes do indeed fall short of the ultimate possibilities of the design.

Some general points regarding the photometric properties of the Cassegrain Schmidt telescopes may be stated here. The St. Andrews telescopes have corrector plate and primary mirror of approximately equal diameter; a stop midway between them prevents vignetting over a field of several degrees. The location of the stop has some effect on the image quality and also controls the use of different parts of the optical components by different points in the field. The following table gives the area of a given optical component which is used in common by points 2° off axis in opposite directions as a percentage of the total area used by a given direction.

Telescope	Stop	Corrector	Primary	Secondary
SLT	15" midway	43	63	20
	15" on corrector	72	33	15
JGT	32" midway	48	72	23
	30" midway	40	60	18
	28" on corrector	64	19	6
f/4 Schmidt	16" on corrector	88	20	-

The importance of uniform reflecting surfaces is clear. The optical quality of the corrector plate must also be uniform.

An off-axis point will use an asymmetrical section of the corrector plate if the aperture stop is not on the corrector. This section will have a net prismatic effect causing transverse chromatic aberration. R.L. Waland observed this while testing the James Gregory Telescope. This may in principle lead to a colour equation which varies over the field.

Bowen (1960) has shown that the size of the chromatic image formed by a classical Schmidt is inversely proportional to the square of the focal ratio and directly proportional to the aperture. Furthermore the corrector plate of the James Gregory Telescope must be 3.1 times as powerful as that of the corresponding classical Schmidt. While exact calculations require more information on the optical properties of the corrector plate, it appears that the James Gregory Telescope, the A.D.H. and the 48-inch classical Schmidt at Mount Palomar will have a mean chromatic image diameter over the range 3600-5700A which is comparable to the image spread due to seeing. Changes in this image spread with wavelength within the medium wavebands used in cluster photometry may be a source of colour equations. In any case the greater power of the corrector plate of the Cassegrain Schmidt must worsen transverse chromatic aberration relative to that in the equivalent classical Schmidt.

The general layout of the Cassegrain Schmidt telescope is

FIGURE 1.

The Cassegrain Schmidt optical system, showing the principal dimensions given in Table 1.

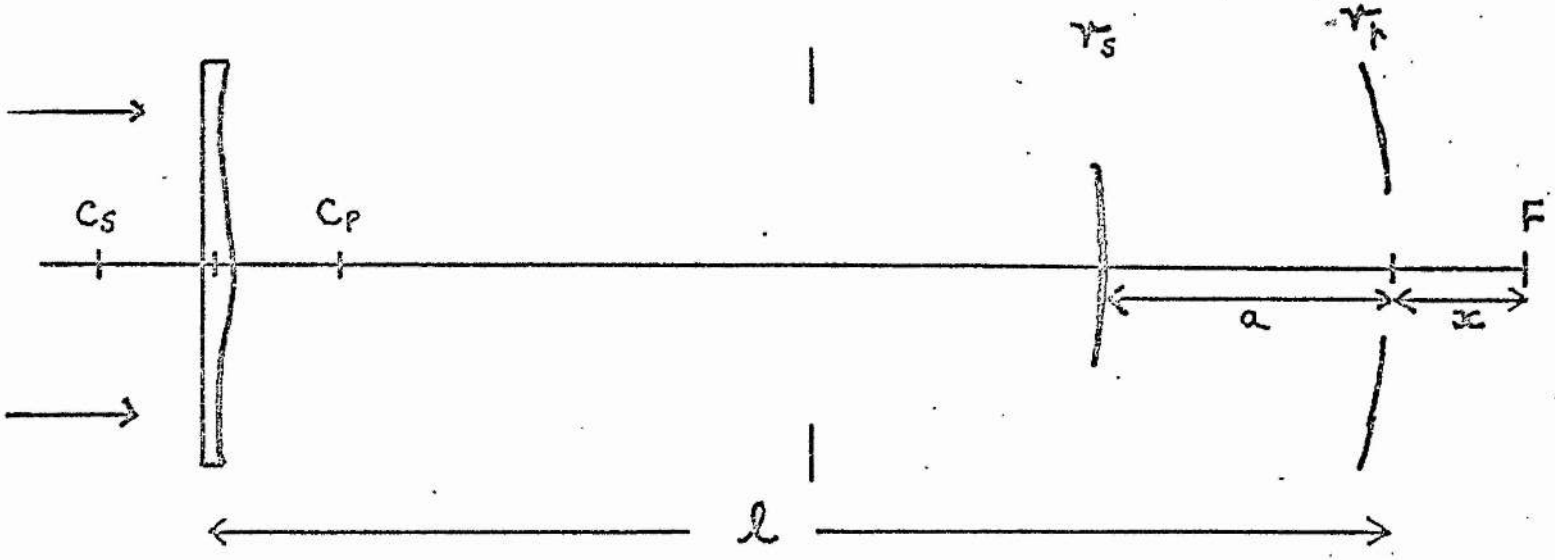
r_s
r_t
C_S
C_P
F
a
x
l

shown in Figure 1 and the principal dimensions of the St. Andrews telescopes are collected in Table 1.

2. The Requirements of In-Focus Stellar Photometry.

The following conditions have to be met if a telescope is to show no systematic field error :

1. The optical system must form images of the same structure over the required area of the focal surface.
2. There must be no vignetting and the reflecting surfaces must be uniformly aluminised.
3. The photographic plate must coincide with the focal surface within the corresponding depth of focus.

Investigations at several observatories have shown that classical Schmidt telescopes, when correctly adjusted, show no systematic field error exceeding a few hundredths of a magnitude across a field of 3° or 4° diameter. The present investigation follows the general lines of these studies. (Haffner (1955), Argue (1960, 1961), Ahmed (1963)).

It was mentioned in Chapter 1 that the first condition is not fulfilled, but the photometric consequences are not readily deduced. The optical system is designed to have no vignetting; the reflecting surfaces are not accessible for measurement. Long exposure plates of fields far from the Milky Way, taken by Mr. C. W. Fraser, were micro-photometered to find the degree of uniformity of illumination of the field. The illumination of the Scott Lang Telescope (SLT) field decreases by about $0^{m}.03$ from the centre to the edge of the photometric field, and that of the James Gregory Telescope (JGT) by about $0^{m}.06$.

(The photometric field is taken to be 3° in diameter). The UBV filters were tested in the Joyce Loebl micro-densitometer. None had transmission differences greater than $0^m.03$ between opposite sides of the field, and errors will seldom exceed $0^m.01$ - $0^m.02$.

The consequences of given focus errors have been investigated extensively in the case of classical Schmidt telescopes. Iris photometry of focal sequences shows, in the case of images more than about 2 magnitudes above the plate limit, a parabolic dependence of magnitude difference on focus error. Light which would otherwise be wasted on the saturated part of the image can contribute to the blackening and make the out-of-focus image stronger. (Haffner 1955). Near the plate limit an image point which would have had an exposure appropriate to the linear part of the characteristic curve of the emulsion falls on the toe, and the total blackening in the out-of-focus image is less. The blackening is insensitive to focus error for a narrow range of magnitudes around the "optimum point". (Weaver 1962). The same arguments apply to other sources of image spread.

A figure of $0^m.02$ was set as the permissible field error across the plate. The corresponding depth of focus was found from the iris photometry of focal sequences on the coarse grained OaO plates to be used for observational projects. Without attempting to cover an excessive range of magnitudes on a single plate, the depth of focus is :

SLT $\pm$ 0.001 inch (1 thou)

JGT $\pm$ 0.002 inch (2 thou)

The next four chapters describe the work devoted to the attainment of these tolerances.

FIGURE 2.

(a) The focus-temperature plot for the Scott Lang Telescope, based on focus plates taken in the period January- August, 1964.

(b) The focus-temperature plot for the Scott Lang Telescope, based on knife-edge tests made in the Spring of 1965.

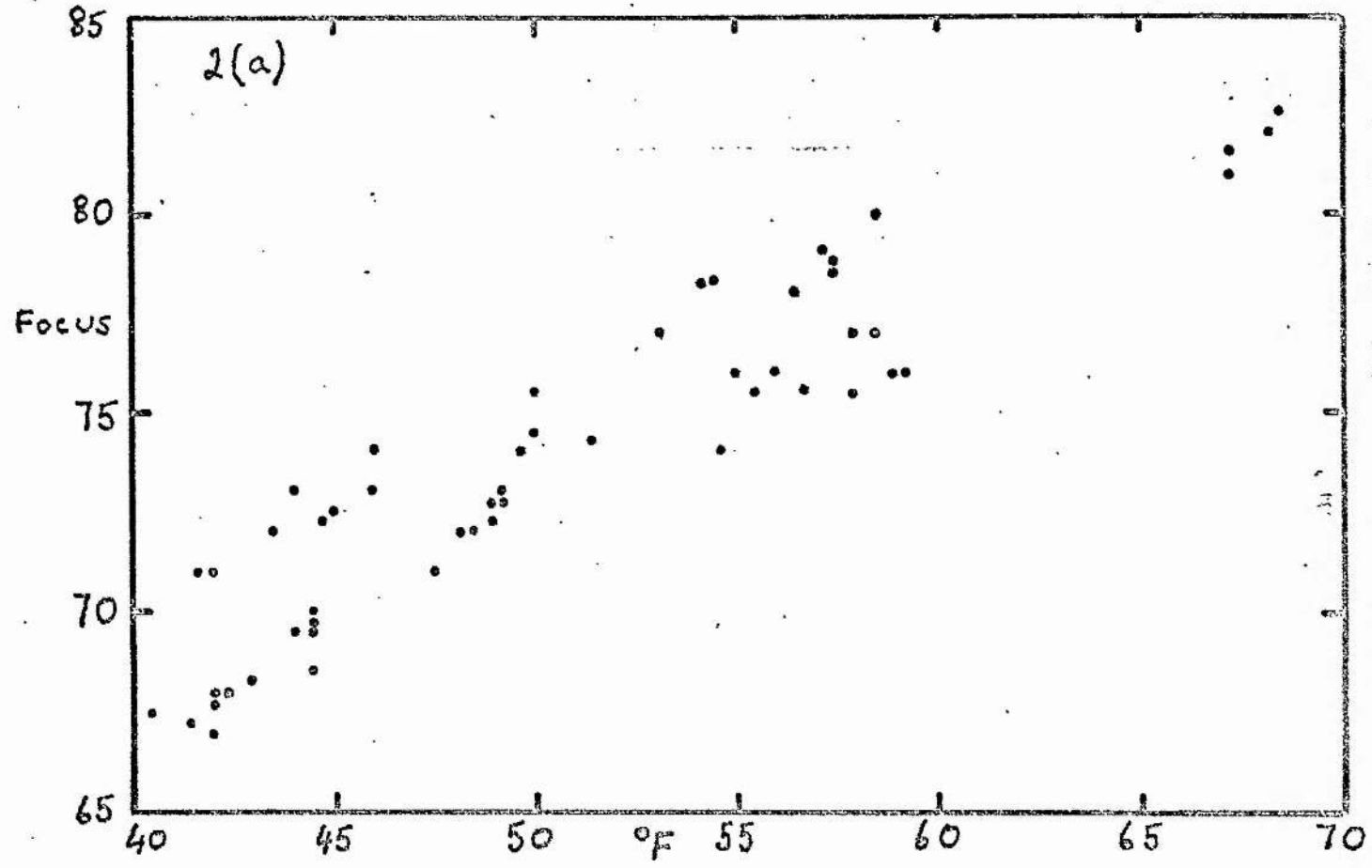
2(a)
85
80
75
70
65
Focus
40
45
50
°F
55
60
65
70

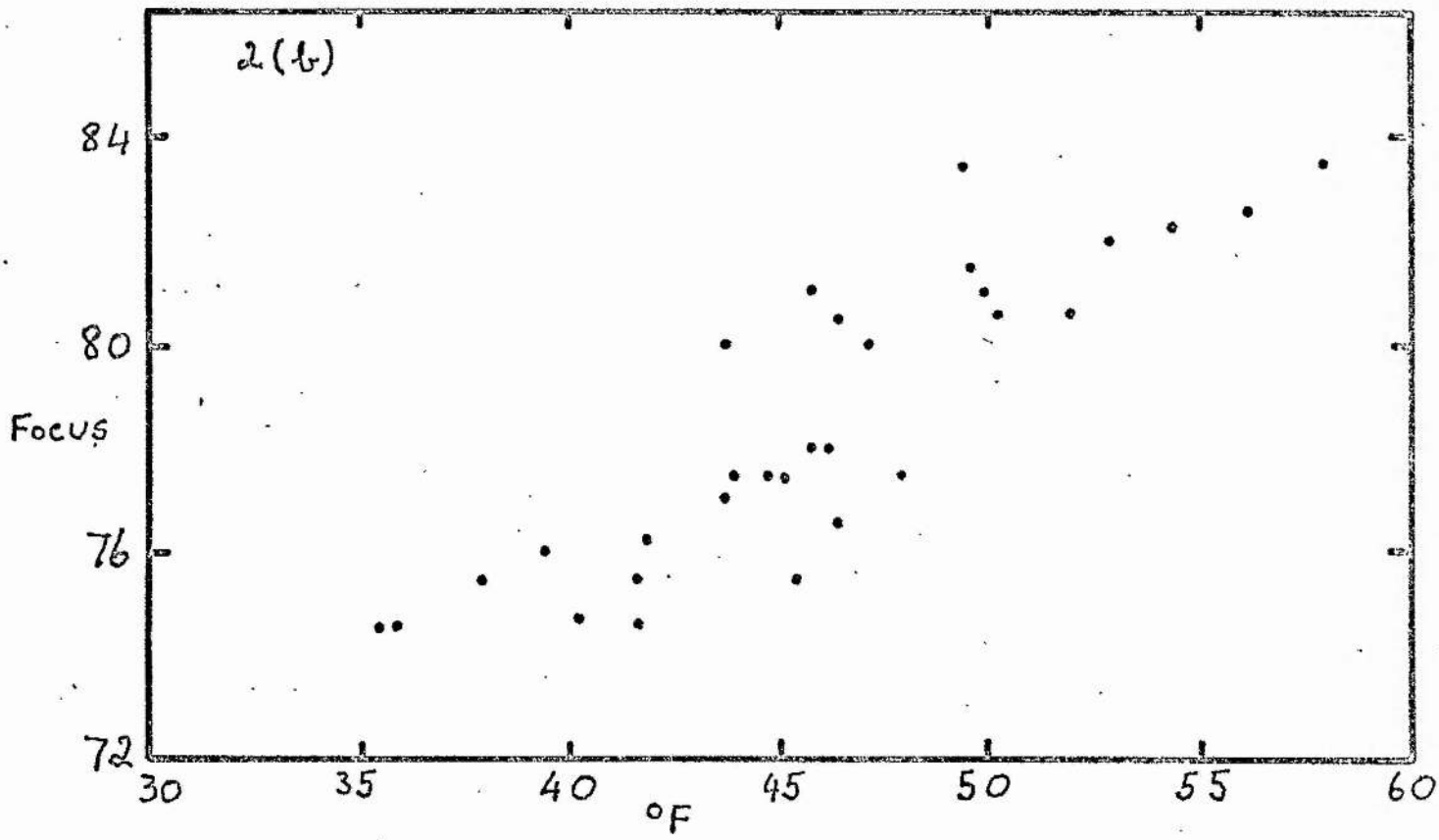
2(b)
84
80
76
72
Focus
30
35
40
45
50
55
60
°F

3. Focussing Problems with the Scott Lang Telescope.

The focussing procedure used in 1963 was to set the focus wheel in accordance with a formula which gives the focus reading as a linear function of temperature. The thermometer is located inside the tube and so indicates the temperature of the mirrors and their supporting structure, insofar as these may be said to have a single temperature. A second thermometer at the top end of the tube was not used. Both telescopes are fitted with vapour pressure thermometers, whose slight dependence on telescope attitude is unimportant.

Inconsistent results lead to a lengthy investigation of the focussing problem. Both focus plates and knife edge tests were used. Figures 2(a) and 2(b) show plots of focus readings from focus plates taken in the first 8 months of 1964 and from knife edge tests made in the spring of 1965, respectively, as a function of temperature. One scale division on the focus wheel is equal to 1 thou change in focus. The focus may be determined by either method with a standard deviation of about $\pm \frac{1}{2}$ thou. The comparison of focus values from focus plates and knife edge tests made in quick succession gives a mean difference of 0.0 ± 0.2 thou (Fig. 3). It is important to set the focus wheel so that the plateholder assembly is pulled up against gravity, otherwise errors of up to 5 thou may result from play in the screw.

Figure 2 shows that

1) The relation between focus and temperature is not linear. The data can be represented by two straight lines, with a slope of + 0.7 thou /° F below 50° F and + 0.4 thou /° above 50° F.

2) There is a shift in zero point of about 6 thou between the two periods. This cannot be attributed to changes in plateholder

FIGURE 3.

The frequency distribution of residuals, focus plate - Foucault, for focus determinations made in quick succession.

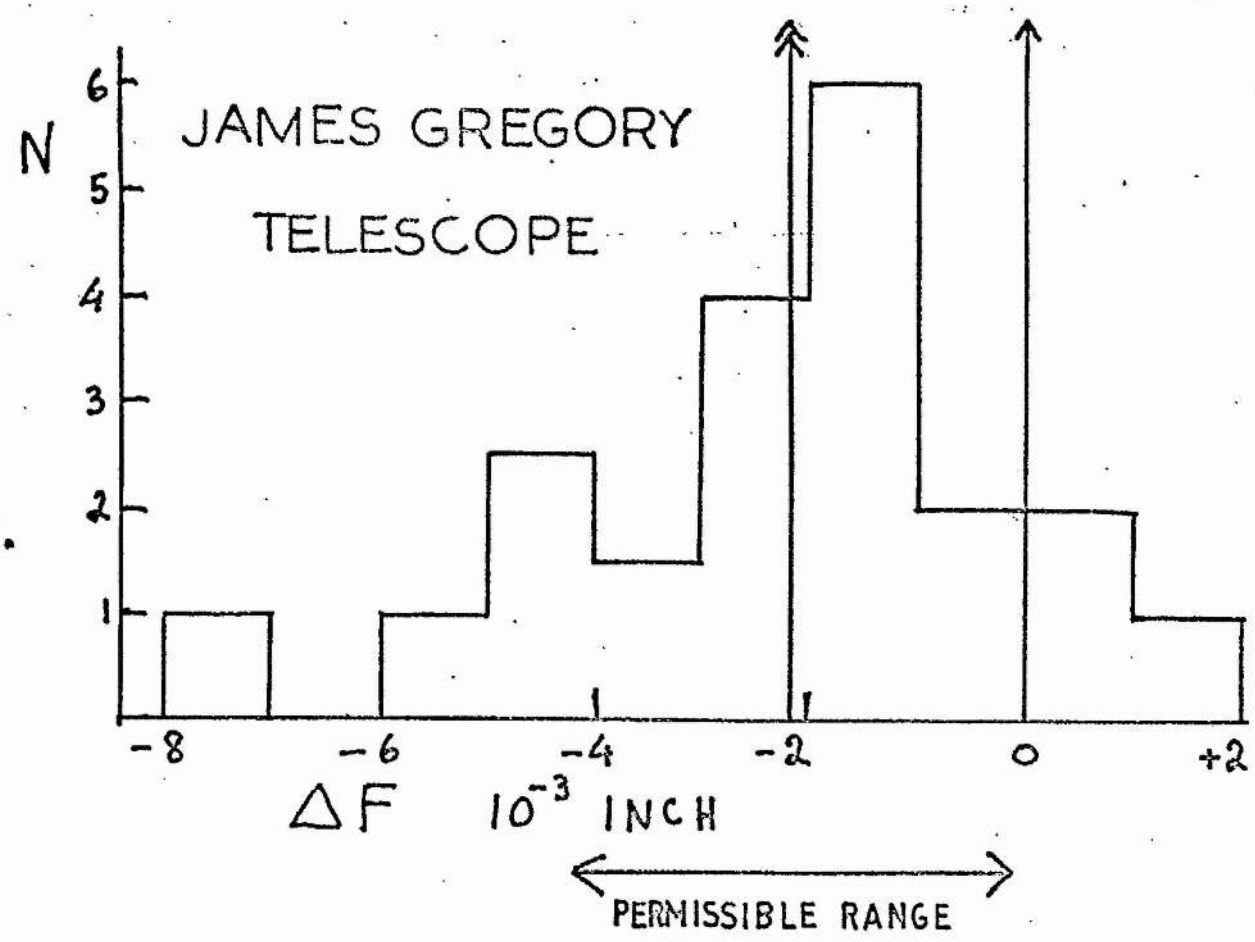
JAMES GREGORY
TELESCOPE
N
6
5
4
3
2
1
-8
-6
-4
-2
0
+2
ΔF 10⁻³ INCH
PERMISSIBLE RANGE

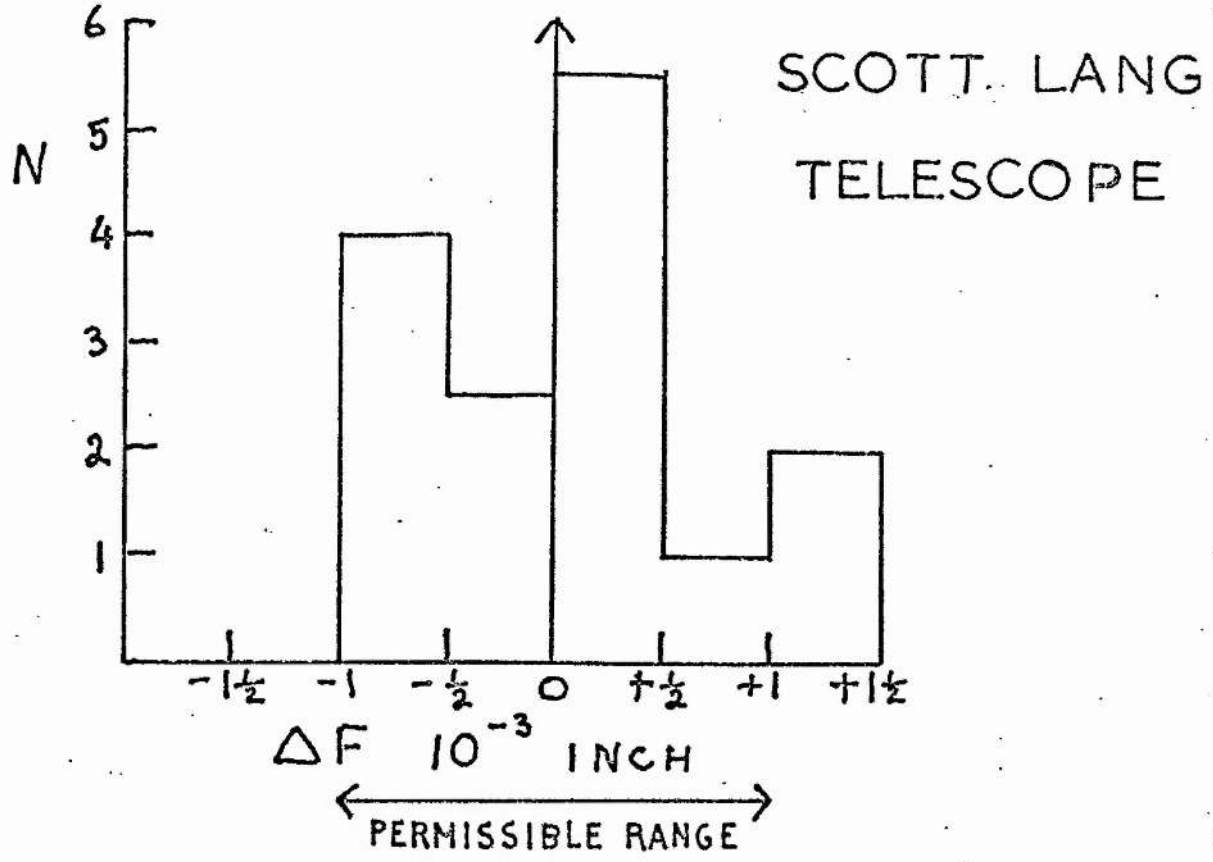
SCOTT. LANG
TELESCOPE
N
6
5
4
3
2
1
-1½
-1
-½
0
+½
+1
+1½
ΔF 10⁻³ INCH
PERMISSIBLE RANGE

settings. It could, for example, be due to a gradual shift of the secondary mirror along the axis. The change is thought to have occurred by stages, starting in August or September 1964.

3) The scatter in each of the plots 2(a) and 2(b) is far in excess of the depth of focus. It cannot be accounted for by measuring error, and the fact that points near the upper and lower envelopes were obtained throughout the first period rules out effect 2) as a major contributor. Experiments described in the next chapter show that thermal lag effects are responsible.

4. Thermal Properties of the Scott Lang Telescope.

The points in Fig. 2(a) show a tendency to fall near the upper or lower envelopes of the distribution. When the points are classified as High, Medium or Low, a relation with time since the dome was opened is found :

Number of points	H	M	L
Dome open less than 4 hours	21	6	14
Dome open more than 4 hours	1	1	16

This behaviour suggests a dependence on temperature. The Low foci occurring in the first 3 hours were all on nights when the temperature was falling unusually slowly. A sustained fall of temperature throughout the night may result in the lower envelope never being reached. The lower envelope is evidently the focus-temperature relation appropriate to equilibrium conditions. The telescope requires 4 hours from the time the dome is opened to reach this state on a typical night.

Series of knife edge tests were made on a number of nights in winter 1964-65. Figure 4 shows a few examples. While there are some

FIGURE 4.

The change of focus with temperature on individual nights. Scott Lang Telescope.

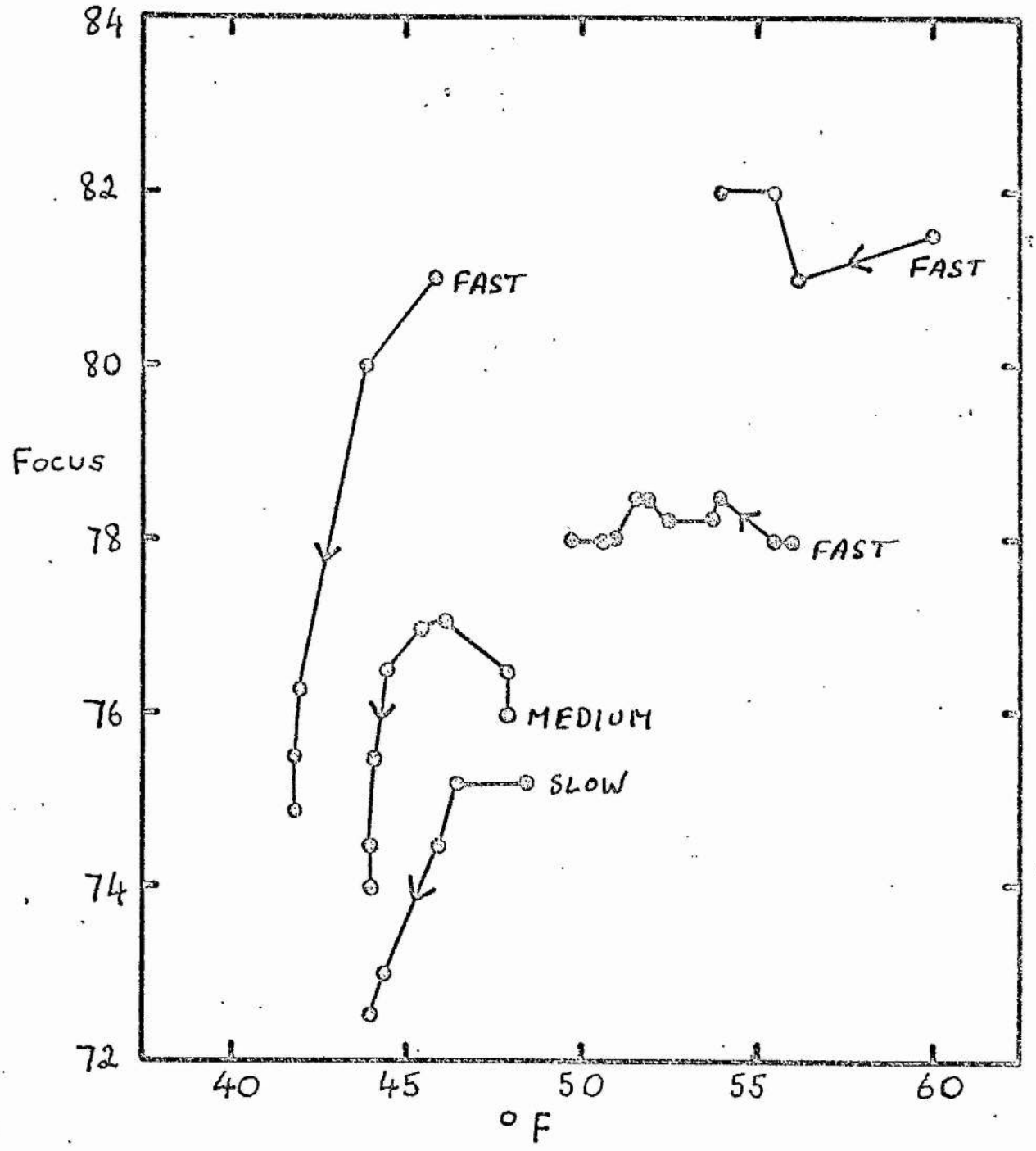
84
82
80
78
76
74
72
Focus
40
45
50
55
60
°F
FAST
FAST
FAST
MEDIUM
SLOW

anomalies, the usual situation is that the focus is maintained at a nearly constant value when the temperature is falling fast, while a slow temperature change produces a more rapid fall in focus reading. In some cases the focus reading actually rose to begin with, even though the temperature of the telescope fell.

These phenomena can be explained as the result of thermal lag within the telescope structure.

In the notation of Fig. 1 the distance from the primary vertex to the focus is

$$x = -\frac{r_s(\frac{1}{2}r_p - a)}{r_p - r_s - 2a} - a$$

where we have neglected the small influence of the corrector plate on the focus position. Partial differentiation gives for the two telescopes

	SLT	JGT
$\partial x/\partial r_s$	-0.40	-0.33
$\partial x/\partial r_p$	+1.79	+1.64
$\partial x/\partial a$	-4.58	-4.28

While the construction materials of the SLT are not known exactly, we note that the coefficient of thermal expansion of steel is about 3 times larger than that of Hysil glass, and taken with the large value of $\partial x/\partial a$ it appears that the separation of the mirrors is the crucial factor.

The observed behaviour can be explained in terms of the action of the bimetallic compensator which is built into the secondary mirror mount. This acts to maintain the separation of the mirrors as the temperature falls, giving a nearly constant focus for some time.

(Waland, 1964). It effectively provides a negative thermal coefficient. It does not cool so rapidly as the tube, which protects it from the cold outside, but its effect predominates when equilibrium is attained and the overall temperature coefficient has the opposite sign to that which would result if the secondary mirror were simply attached to the tube. The initial rise in focus reading which has sometimes been noticed is due to the tube cooling before any marked change occurs in the temperature of the compensator.

It is clear that the bimetallic compensator cannot be relied upon to meet the accuracy required for in-focus photometry.

5. Focussing for Photometric Observations.

The accuracy attained by the knife edge method meets the requirements of in-focus photometry. It is only necessary to determine the focus once each hour or so to keep the focus within the tolerance of $\pm$ 1 thou at the centre of the plate.

The different plateholders were adjusted relative to a standard so that differential tilts across the field did not exceed $\pm \frac{1}{2}$ thou; the standard plateholder was squared on relative to the focal plane to a similar tolerance. The adjustment of plateholders was done easily using an arrangement suggested by Dr. V.C. Reddish. The plateholder was mounted face down in a replica of the plateholder mount which was attached to a tripod with adjustable legs. A dial test indicator on a steel block could be moved freely on a polished granite slab with its probe in contact with a plate in the holder and the legs adjusted to give the same reading all over the plate. A second plateholder, with the same plate inserted, then replaced the first, and its

adjusting screws were set to give the same reading overall.

Finlay-Freundlich and Waland (1953) reported that the secondary mirror could tilt slightly as the telescope's orientation was altered, leading to a change in image quality and a tilt of the focal surface relative to the plate. No effect of this nature was noticed in the present study; the appearance of the astigmatic off-axis images, which is very sensitive to focus changes, remains unchanged over a wide range of telescope attitude.

The corrections required for the UBV filters were determined from several knife edge tests and focus plates to an estimated $\pm \frac{1}{4}$ thou. In practice each filter was used with a particular plateholder and the appearance of the images far from the optical axis used to deduce small corrections from operational plates. The focus error for a particular plateholder + filter combination should not exceed $\pm \frac{1}{2}$ thou.

The test gear described above was used to determine the profile of unexposed photographic plates. It was found that plates are normally concave on the emulsion side, in accordance with earlier investigations by others. The depth of the concavity between the plate centre and the mean of the three support points was measured for 3 different plate batches :

103aD	9 plates	0.2 thou.
0a0	7 plates	0.5 thou.
0aJ	12 plates	1.0 thou.

Individual plates may depart considerably from the mean; it might be desirable to press the plates flat or to use specially selected flat glass plates.

It is considered that the required accuracy of focus is attainable with the Scott Lang Telescope.

6. Focussing Problems with the James Gregory Telescope.

The methods used to study the focus problems and thermal properties of the Scott Lang Telescope were applied to the James Gregory Telescope during 1965. The softness and complexity of the images reduces the accuracy of focus determinations from focus plates; it is only with difficulty that the focus can be judged to the nearest 2 thou. The spherical aberration means that there is no position of the knife edge for which the whole aperture goes dark at once, so that it is necessary to estimate the focus for the same aperture zone each time. Individual knife edge and focus plate estimates of the focus differed by up to 6 thou, with differences greater than 2 thou in 40% of the cases, and even larger errors were sometimes deduced from the image quality of intended photometric plates set on a knife edge focus. Figure 3 shows a histogram of the difference between the focal positions derived from the two methods applied in quick succession.

The 8 inch square plateholders were adjusted early in 1965. Apparatus of the type used for the SLT was not available. The plateholder was placed with its three set screws on the granite slab and a dial test indicator on a long arm attached to a steel block was moved over the upper (rear) surface of a standard plate in the holder. The accuracy attained is thought to be within the depth of focus - possibly 1 thou tilt across the field.

The study of the thermal properties of the JGT was hampered by abrupt changes in focus. The first of these was caused by a change in

plateholder register, but subsequent shifts must be attributed to a mechanical shift within the telescope. Thermal lag does not seem to be a possible cause, as the changes were large and the temperature conditions were not abnormal. These changes, in the sense of departures from the focus-temperature relation applicable before the change, were

1965	April	Reading up by 4 thou.
	early October	down by 6-8 thou.
	late October	up by 6-8 thou.

The focus-temperature relation for three overlapping temperature intervals has a linear coefficient :

24	-	42° F	-0.6 thou/° F.
30	-	40° F	-0.3 thou/° F.
38	-	56° F	-0.3 thou/° F.

The secondary mirror is free to move along the tube, its distance from the primary being maintained by invar rods even though the tube expands or contracts. The overall dependence of focus on temperature should be in the range -0.1 to +0.2 thou/° F, where the major uncertainty is the thermal coefficient of the particular specimen of invar used. (Kaye and Laby, 1964). The dependence of focus on temperature evidently can be eliminated by a suitable choice of materials. The average measured value of -0.4 thou/° F falls well outside this range and suggests that the mechanism may have been inoperative. The measured co-efficient is not far from that which would be expected if the mirror separation were controlled by the steel tube.

Thermal lag effects have not been observed and probably do not cause

a spread in focus of more than 2 thou at a given temperature.

A curvature of the focal plane relative to a plate, amounting to 2 thou between the centre and edge of the field, was suspected. The focal surface appears to be concave to the telescope, opposite to the spurious field curvature which would result from concavity of the photographic plate. The profile of 8 inch square plates has not been measured.

The photometric plates were focussed on the average of the readings from the current focus formula and from the knife edge test. Only about 30% of all such plates were within the required tolerance of $\pm$ 2 thou, as judged from focus plates taken at the time.

7. Photometry in the Coma Cluster.

Argue (1964) has published a photo-electric sequence on the UBV System specially for the purpose of testing Schmidt or other wide field telescopes. The sequence comprises 179 stars in a $3^{o}.3$ diameter field centred on the Coma open cluster. The magnitude scale from V = 6.5 to V = 15.6 is defined by 47 stars in the colour range $0.35 < (B-V) < 0.68$ which are confined to a small, slightly off-centre area of the field. A further 51 stars of magnitudes 11 and 12, confined to the same colour range but spread over the field, are intended to determine the field error. The remaining 81 stars, distributed over the field, are suitable for the determination of the colour equation at several magnitude levels. Figure 5 shows the colour magnitude diagram of the "scale" and "colour" stars.

Satisfactory plates were taken with both telescopes in the period

FIGURE 5.

The colour magnitude diagram for the stars of the photo-electric sequence in the Coma field. The "Scale" and "Colour" sequence stars are denoted by crosses and dots, respectively.

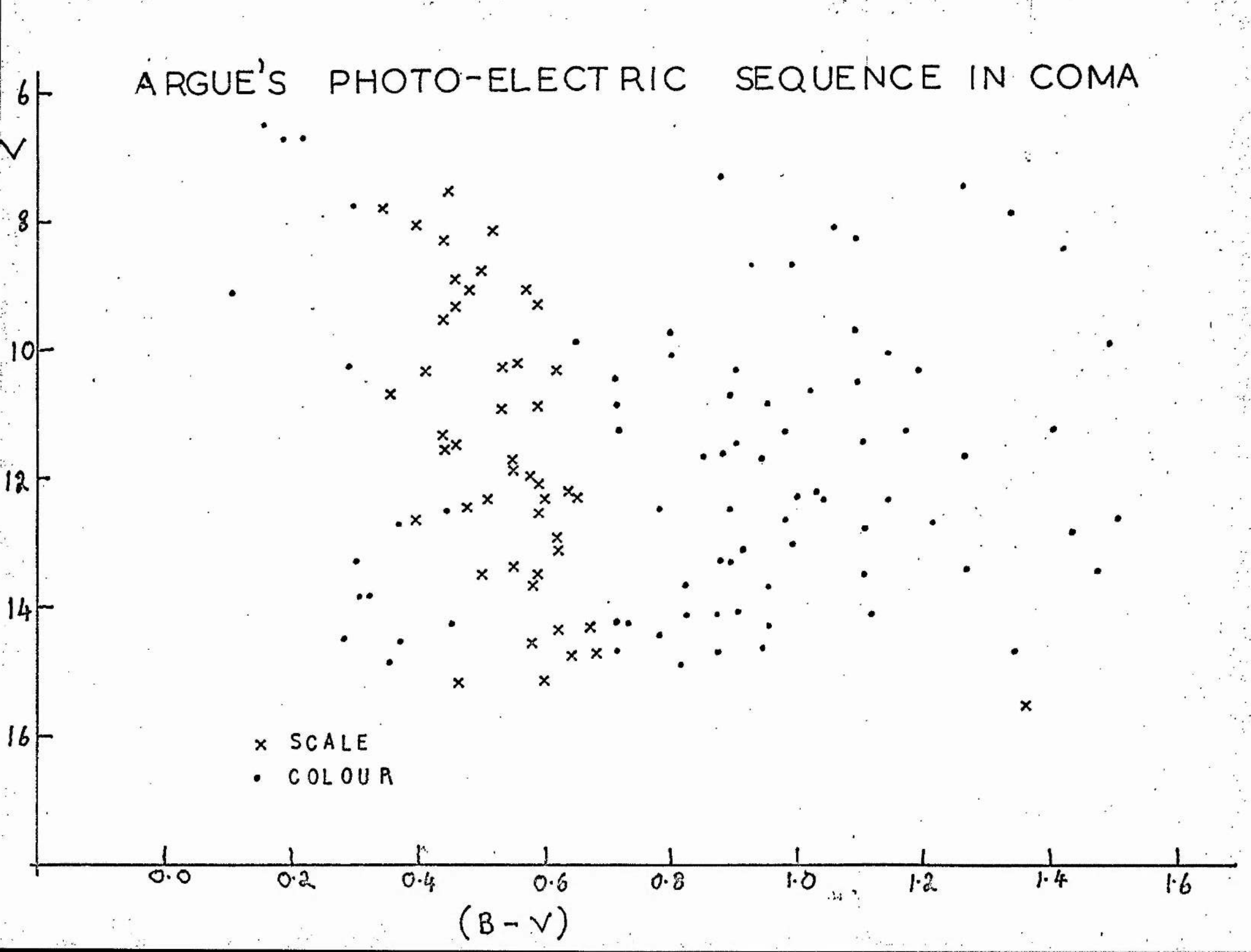
ARGUE'S PHOTO-ELECTRIC SEQUENCE IN COMA
V
6
8
10
12
14
16
× SCALE
• COLOUR
0·0
0·2
0·4
0·6
0·8
1·0
1·2
1·4
1·6
(B - V)

February - April 1965. The weather was generally poor at that time and many of the plates were taken on nights of low but not noticeably patchy transparency. The exposure time was usually 5 minutes.

The plate-filter combinations and the number of plates taken with each instrument are given in the following table.

Colour.	Plate	Filter.	Number of Plates
		SLT	
V	103aD	Pilkington OY 6	12
B	OaO	Schott G G 13	9
		JGT	
V	103aD	Schott G G 14	7
B	OaO	Schott G G 13	11

Details of the individual plates, including the focus error estimated from focus plates or from subsequent knife edge tests, are given in Table 2. Several of the plates taken with the JGT are out of focus by more than the estimated depth of focus.

The plates were developed for 5 minutes at 68° F in D19b, being brushed or vigorously rocked.

The plates were measured with the Askania - Becker iris photometer at the University Observatory. The power supply to the measuring lamp was rectified to reduce A/C ripple on the Cathode Ray Oscilloscope trace. Drift corrections were applied in some cases. These corrections were determined as the average drift measured for three images of different strength, though it is suspected that the drift was not completely independent of image strength.

The iris curves were drawn by hand for the scale stars only and the deviation in magnitudes read off for all the other stars.

Measuring errors were estimated as follows :

A. Standard deviation of a single measure of a given image, deduced from repeated measures on the same plate. (Iris photometer measuring error).

B. Standard deviation of a single measure of a given star on a given plate, deduced from the interagreement of magnitudes deduced for the same star on several plates. Any variable systematic plate error will contribute to this but a field error common to all plates will not.

C. Standard deviation in the photo-electric measures according to Argue (single observation).

	SLT (B plates)		JGT (B plates)		
B	A	B	A	B	c
8-9	± 0.02	± 0.08	± 0.05	± 0.07	± 0.03
9-10	0.03	0.07	0.02	0.09	0.04
10-11	0.03	0.07	0.02	0.07	0.04
11-12	0.03	0.07	0.02	0.07	0.07
12-13	0.03	0.07	0.03	0.06	0.10
13-14			0.02	0.05	0.10
14-15	0.05	0.10	0.03	0.07	0.10
> 15			0.05	0.09	0.10

FIGURE 6.

The field error of the Scott Lang Telescope, averaged over all V plates of the Coma field. The residuals $V = V_{pg} - V_{pe}$ are plotted against the angular distance from the centre of the field for stars in each of the four quadrants N, S, E and W.

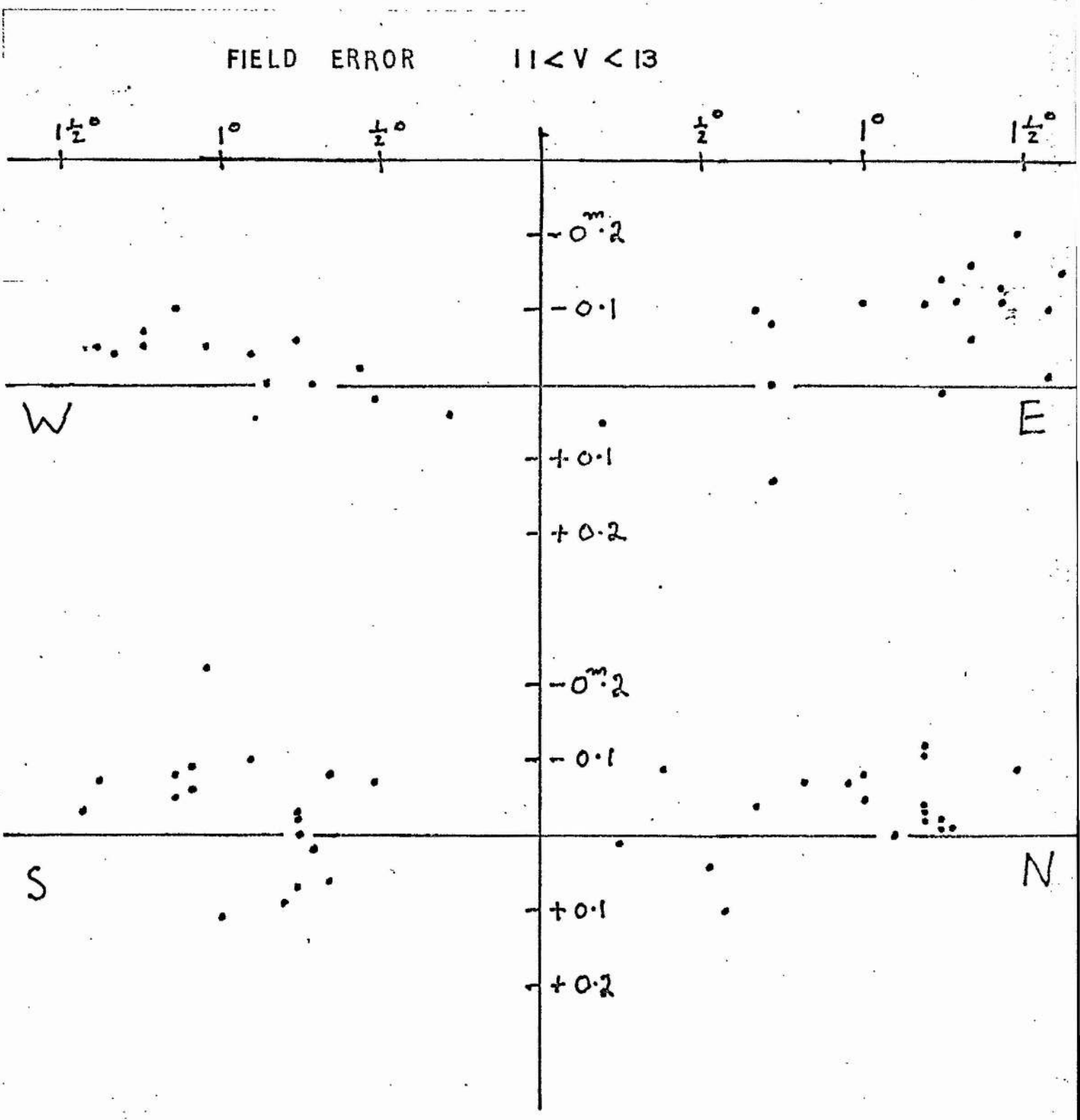
FIELD ERROR 11 < V < 13
1½°
1°
½°
½°
1°
1½°
-0m.2
-0.1
W
E
+0.1
+0.2
-0m.2
-0.1
S
N
+0.1
+0.2

8. Field Error.

The deviations for the Field stars show that both instruments have field errors, though of opposite sign. It should be borne in mind that the centre of the distribution of the scale stars is in the fourth (SW) quadrant. Figures 6 and 7 give the mean field error as a function of angular distance from the centre of the field for the 4 quadrants for each instrument.

The field error of the SLT is such that stars away from the optical axis are measured too bright. This is in the sense to be expected for stars several magnitudes above the plate limit if the error were due to the increasing size of the astigmatic images with distance from the centre of the field.

Stars are measured fainter the farther they are from the centre of the field of the JGT. The error is about 0^{m}.06. A plot of one against the other shows a scatter diagram; however the errors of determination of either field error are quite large. One possibility is that the stellar field error is due to the interaction of the stellar image with the sky background, as occurs in the photometry of star fields with a variable nebulous background.

Alternatively the variations in image structure over the field may be responsible. The 11 blue plates are divided into 3 groups, characterised by

a) Good seeing, good focus. (3 plates)

b) Poor seeing, good focus. (4 plates)

c) Average seeing, poor focus. (4 plates)

The first group appears to have a larger field error than the other two;

FIGURE 7.

The field error of the James Gregory Telescope, averaged over all B plates of the Coma field. The residuals $\Delta B = B_{pg} - B_{pe}$ are plotted against the angular distance from the centre of the field for stars in each of the four quadrants N, S, E and W.

FIELD ERROR 11 < B < 13

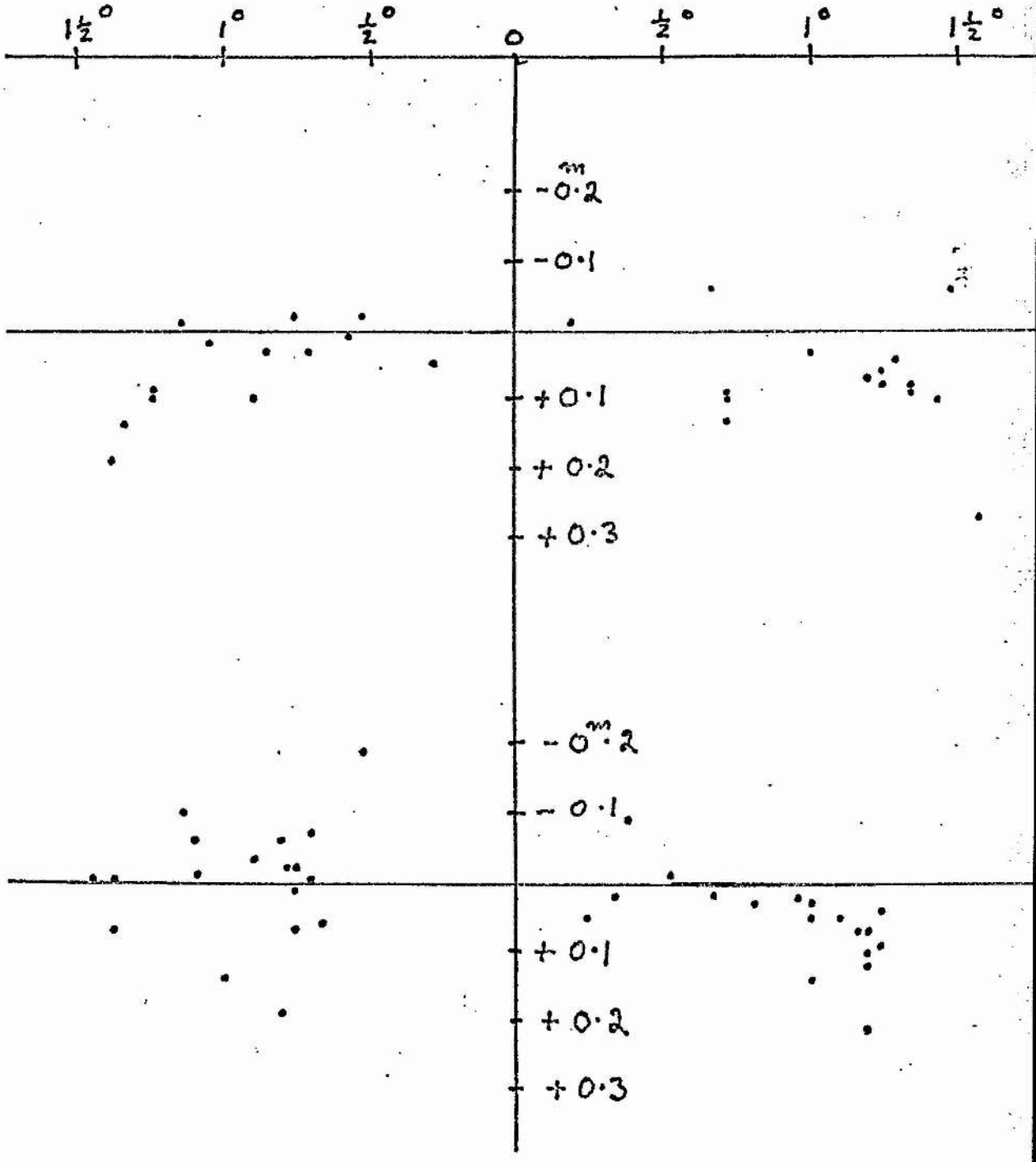

this might be attributed to the sharper images.

Re-measurement of 4 V plates with a larger iris showed no appreciable difference.

If some of the light is scattered very widely in off-axis images by the large optical aberrations, the normal magnitude-focus error relation would not apply and all stars might be measured faint off-axis.

It does not appear possible to reach a final decision as to the cause of the field error in the JGT.

Both telescopes give a satisfactorily small field error over a field of 1° diameter.

This study does not settle the question regarding the suitability of Cassegrain Schmidt telescopes for in-focus stellar photometry, since neither instrument provides the ultimate performance possible with the design.

9. Photographic Colour Equations.

The colour equation was determined from the stars in a 2° diameter circle whose centre was displaced from the centre of the plate towards the centre of the concentration of scale and colour stars in the SW quadrant. Eleven stars which gave excessive residuals in the same sense with both telescopes and whose photo-electric magnitudes were noted as uncertain by Argue were rejected.

Sample colour equation curves are shown in Figure 8. The colour equation was represented by a linear function of (B-V) fitted by least squares in order to eliminate personal bias. The calculations were repeated for various magnitude intervals and field rejection criteria

FIGURE 8.

The dependence of the residuals $\Delta V = V_{\lambda g} - V_{\lambda e}$ on colour (B-V) for three magnitude intervals. Photometry of the Coma cluster field with the Scott Lang Telescope.

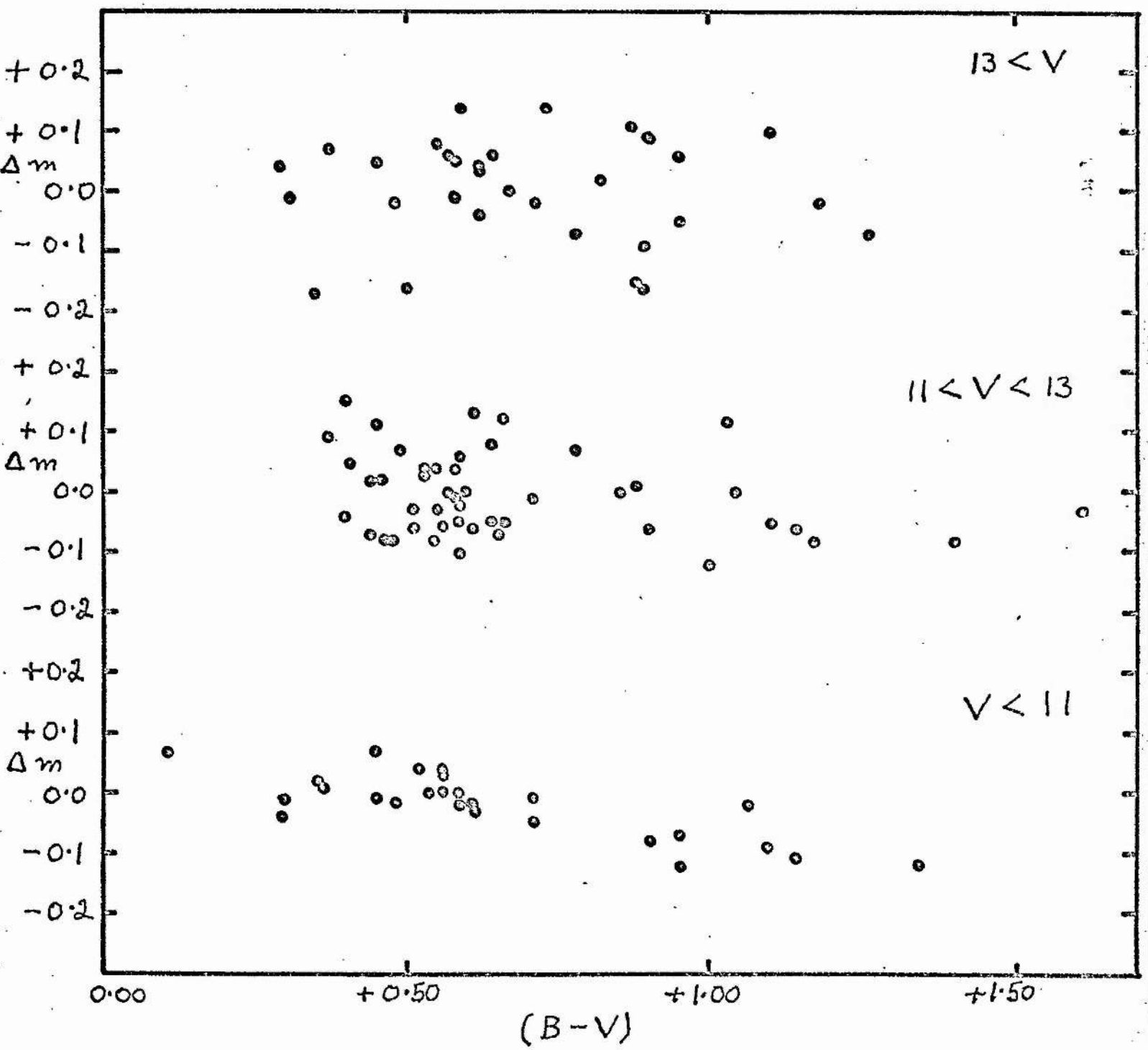
13 < V
11 < V < 13
V < 11
+0·2
+0·1
Δm
0·0
−0·1
−0·2
0·00
+0·50
+1·00
+1·50
(B−V)

as a check; the standard error of each mean colour coefficient is ± 0.02, except for the faintest group where the scatter is large. The following Table gives a_1 where $m = m_{pg} + a_1 (B-V-a_o)$

	SLT	JGT
$B < 11.5$	+ 0.10	- 0.10
$11.5 < B < 13.5$	0.00	- 0.05
$13.5 < B < 15$	0.00	+ 0.02
$V < 11.0$	+ 0.14	+ 0.13
$11.0 < V < 13.0$	+ 0.04	+ 0.13
$13.0 < V < 15$	+ 0.04	+ 0.07

The filters were those recommended by Johnson (1955), except for the Pilkington OY6 used to reproduce the V magnitudes with the SLT. It has a short wavelength cut-off at about 150 A to the violet of the cut-off of the photo-electric V band and about 100 A to the violet of that of the Schott GG 11 or GG 14 filters recommended for photographic use.

Experience with the Radcliffe 74 inch reflector shows that adherence to Johnson's precepts does not guarantee the absence of a colour equation in photographic photometry. The interest in the present colour equations lies in the difference between the two telescopes and in the dependence on magnitude.

Additional observations of the open cluster NGC 752 were made with the SLT in November 1965. Kodak IIaO plates were used for the B magnitudes; the same filters and 103aD plate batch were used as in Coma.

A total of 7 plates in each colour were taken with 3 minute exposures and 10 with 30 second exposures. Most of the plates were taken in quick succession on one night.

The standard stars are contained in an area approximately 1° in diameter, eliminating field error. The close agreement of the photo-electric measures by Johnson (1953) and by Eggen (1963) supports Johnson's claim of an internal standard error of a single observation of $\pm$ $0^{m}.01$. A small systematic difference between the respective scales was allowed for in deriving mean magnitudes for the present study. The main uncertainty in the colour equations found is caused by the sparseness of standard stars at the bright end of the magnitude scale, especially in V. (See Fig. 9). The magnitude ranges used were $8.0 < V < 10.5$ and $8.0 < B < 11.0$.

Two independent reductions were made: a hand curve fitted graphically to the mean iris readings for all plates of a set and a polynomial of second or third degree fitted by least squares to the iris readings of each plate. Linear colour equations were fitted by least squares. The values of a_1 in the following Table are the mean of the values from the two reductions. The standard error of each mean colour coefficient, judged from the inter-agreement of the values for different plates, is $\pm$ 0.01.

Exposure	B	V
10 sec.	- 0.03	+ 0.08
3 min.	+ 0.20	+ 0.10

These colour equations cannot be attributed to a mismatch of wave-bands, which would affect stars of different magnitudes and of different

FIGURE 9.

The colour magnitude diagram for the photo-electric standards in NGC 752.

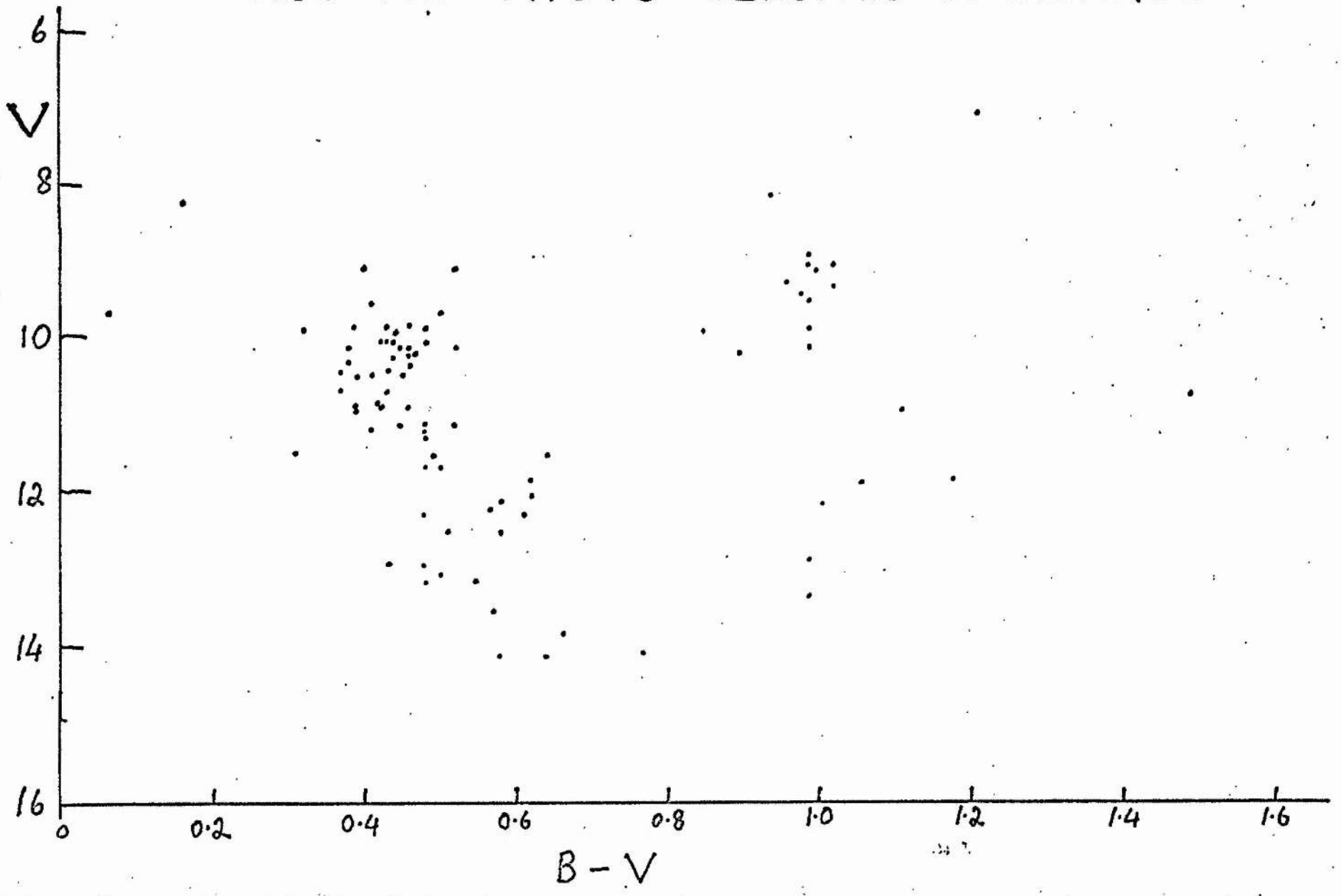
NGC 752 PHOTO-ELECTRIC STANDARDS
V
6
8
10
12
14
16
0
0·2
0·4
0·6
0·8
1·0
1·2
1·4
1·6
B − V

exposures equally. The difference between the colour equations for long and short exposures of NGC 752 is not due to different atmospheric extinction. The distributions in the two-colour diagram of stars used for the determination of colour equations in different magnitude intervals in the Coma field are very similar, so it is unlikely that the change in colour equation with magnitude is caused by a change in the stellar properties with apparent magnitude. The variation with exposure time of the B colour equations in NGC 752 must be of instrumental origin as the same stars were used to find the colour equations for long and short exposures.

Possible causes of magnitude dependent colour equations, sometimes referred to as the photographic Purkinje effect, have been discussed by Weaver (1962) and by Stock and Williams (1962). The effect arises from a wavelength dependence of the image structure, which may be caused by chromatic aberration in the optical system or by wavelength dependent scattering in the photographic emulsion. The change in image structure affects the total blackening and hence the deduced magnitude in the same way as the focus errors discussed in Chapter 2. The generally small colour terms for the faintest magnitude group in Coma may be attributed largely to the mismatch of the photographic colour system (neglecting image structure) and of the B, V system defined by the photo-electric photometry.

The V colour equations with the two telescopes are not strictly comparable since different filters were used. The main change in colour equation occurs at a fainter magnitude in the case of the JGT. The opposite signs of the trends with magnitude in the B colour equations

suggest either that different physical phenomena are responsible or that optical differences are the cause. The instrumental profile of the JGT is large compared to the image size which would result from emulsion scattering alone, so it seems likely that chromatic aberration is important. The excessive power of the corrector plate, with a refractive index which is greater the shorter the wavelength, means that within the B or V waveband the resulting image spread must be greater at shorter wavelengths. This is in accordance with the sign and magnitude dependence of the B colour term but not with those of the V colour equation. The situation in the SLT is not clear; it is probable that light scattering in the emulsion is relatively more important, though even on-axis images are larger than would be the case if this were the only instrumental cause of image spread.

A difference of 0.1 in colour coefficient when different O emulsions are used for the B waveband may not be unusual. The change in colour coefficient with exposure time in NGC 752 is surprisingly large and contrasts with the near equality of the V colour coefficient for the two exposure groups.

Argue (1963) reported a photographic Purkinje effect in his own photometry of the Coma cluster with the Cambridge Schmidt, while Lawrence and Reddish (1965) found large colour equations in V in their photometry of Cygnus II with the Hamburg and Edinburgh Schmidt telescopes.

The colour equations reported here would lead to serious photometric errors if they were not correctly allowed for. Unless the source of such effects can be found and eliminated, accurate photometry will require sufficient photo-electric standards to allow the calibration of

the whole magnitude and colour range of the photographic instrument. (Argue 1963).

10. Conclusions.

The presence of optical and mechanical defects in the St. Andrews telescopes prevents an assessment of their ultimate potentiality for in-focus stellar photometry. The error-free field was approximately 1° in diameter when the writer tested them (1965). The presence of complicated colour equations requires numerous photo-electric standards to calibrate the colour system, and these telescopes would be uneconomical when compared with a classical Schmidt having a useful field of perhaps 3° in diameter.

A more useful application of these telescopes is in survey programmes. The Scott Lang Telescope has been used to detect very red stars by taking yellow and infra red plates of Milky Way fields. The V-I index of late M stars is large compared to the photometric errors. The dominance of instrumental over seeing image spread is advantageous in enabling one to take plates with closely comparable image quality, an important consideration if it were desired to search for variables.

SECTION 2.

PHOTOGRAPHIC AND PHOTO-ELECTRIC PHOTOMETRY WITH THE RADCLIFFE 74 INCH REFLECTOR.

1. Introduction.

The Radcliffe Observatory is situated on a ridge 5,000 feet above sea level and 4 miles from the centre of Pretoria. Artificial lighting is responsible for the high sky brightness near the zenith of V = 20.6, B = 21.6, U = 21.5 magnitudes per square second of arc, respectively. Slag-pouring operations at the Iscor Steel Works, 6 miles West of the Observatory, are carried out at irregular intervals when they cause a rapidly fluctuating sky brightness for 10 minutes or so. This is a serious hindrance to the photo-electric photometry of faint stars. Industrial smoke, from Iscor and other sources, is a frequent nuisance in winter. The weather is strongly seasonal with almost continually clear conditions in winter but much cloud in summer.

The 74-inch telescope is a conventional paraboloidal reflector built by Grubb Parsons. The $f/18$ Cassegrain focus is used for photo-electric and spectroscopic work; direct photography is carried out at the Newtonian focus, using a 44-inch aperture stop to give a focal ratio of $f/8.2$. The primary mirror is pyrex and the secondaries are fused quartz. The reflecting surfaces are aluminised. The cylindrical turret is effectively thermally insulated so that the instrument is not usually subject to serious thermal effects.

2. The Photo-electric Photometer.

The photo-electric photometer, a single channel instrument of conventional design (Feast et al, 1960) is mounted in place of the spectrograph field eyepiece at a broken Cassegrain focus. There are thus 3 aluminised reflecting surfaces in the optical train. The Fabry lens is of fused quartz and the window of the EMI 6256 A photomultiplier tube is also quartz. The filters used to define the UBV system are

U : Corning 9863

B : Schott BG 12 + GG 13

V : Omag 303

The focal plane diaphragms used have circular holes of diameter 37".9, 19".1 and 11".6, holes 5, 4 and 3 respectively. All observations of faint stars were made with hole 3, which was also used for bright cluster stars unless the seeing required the use of hole 4. Hole 5 was used mainly for standard star tie-ins under poor seeing conditions.

The output from the cell is taken via a short low noise co-axial cable to the amplifier, which is bolted to a faceplate just below the photometer on the spectrograph casing. The output is taken to a Brown recorder on the observing floor; the EHT unit for the photomultiplier is mounted with it. A D.C. Amplifier built in the Royal Observatory workshops was used until August 1966, when a General Radio 1230-A D.C. amplifier became available. The R. O. amplifiers had insufficient gain to provide full scale deflection on the recorder chart for stars fainter than about V = 13 and the observations of faint stars described here would not have been possible with them.

The amplifiers were calibrated at least every 2 or 3 months,

using as input either a D.C. source of high internal resistance or the signal from the photomultiplier when a Sr^{90} source was placed in the filter slide. Different calibrations of the GR amplifier showed a maximum difference of approximately 5% over the full range; no dependence on temperature was found and it is possible that the differences are due to calibration errors of a random nature.

The photometer field eyepiece was provided with a graticule with 10 second squares; the star was centred on this and could then be centred more accurately if necessary by looking through the focal plane diaphragm with a microscope. Very faint stars were located by measuring offsets from a bright star on a direct photograph and setting the bright star at the appropriate position on the graticule (Arp, 1958_a). This procedure generally sufficed to position a star near the centre of hole 3.

3. Photo-electric Observing Methods.

Procedures prescribed by Dr. P.J. Andrews were used for all Radcliffe observations in the interests of uniformity and to minimise the time spent on calibration observations.

The extinction was assumed to be independent of colour. Observations were confined to moderate values of sec Z - up to 1.3 for NGC 6383 when 3 hours off the meridian and 1.65 for IC 2581 at 4 hours West. The colour system was determined by observing UBV standards, mainly from the E regions (Cousins, 1961), at sec Z of approximately 1.1. If there is a term of 0.04 (B-V) in k_{by}, as found elsewhere, an error of $0^m.02$ for each magnitude difference in (B-V) between standard and programme

star would result at sec Z = 1.6. The very red stars are very faint and generally not cluster members, so that an error of this size is not considered important.

The colour system was calibrated every few months as the mirrors aged by observations of about 50 standard stars. These observations were made jointly by Dr. Andrews and the writer, usually on nights of poor seeing and above average transparency. The observations for winter 1967 are shown in Fig. 10, together with the adopted curves. The transformation for U-B is not completely satisfactory. This is a long standing problem in UBV photometry. Dr. A.W.J. Cousins, who has been responsible for most of the work on standard stars in the Southern sky, has even suggested that precise transformation is impossible so that each observer might as well use his own colour system, defining his own standard relationships for intrinsic lines and reddening. The system would not be constant for a given instrument, because changes in the instrumental system as the mirrors age can be greater than the difference between the standard system and the transitory instrumental system which best reproduces it.

The difficulties are especially severe for reddened blue stars: entering the graph for the correction f_{ub} with (U-B) and (B-V), the value deduced for a given star would depend on the reddening. Much of the change in f_{ub} must be due to differences in the Balmer jump; in applying the relation defined by little reddened dwarf stars (very few reddened stars are available as standards) to reddened stars, an attempt has been made to use the value appropriate to the unreddened colours if this lead to a substantial difference. The total amplitude of fub sometimes

FIGURE 10.

The colour transformation curves for photo-electric UBV photometry with the 74-inch reflector, determined in April, May and June, 1967. These are based on observations of standard stars in E6, E7 and E8.
The sense is that these corrections have to be added to the instrumental magnitude or colour of a programme star. The adopted curves are shown.

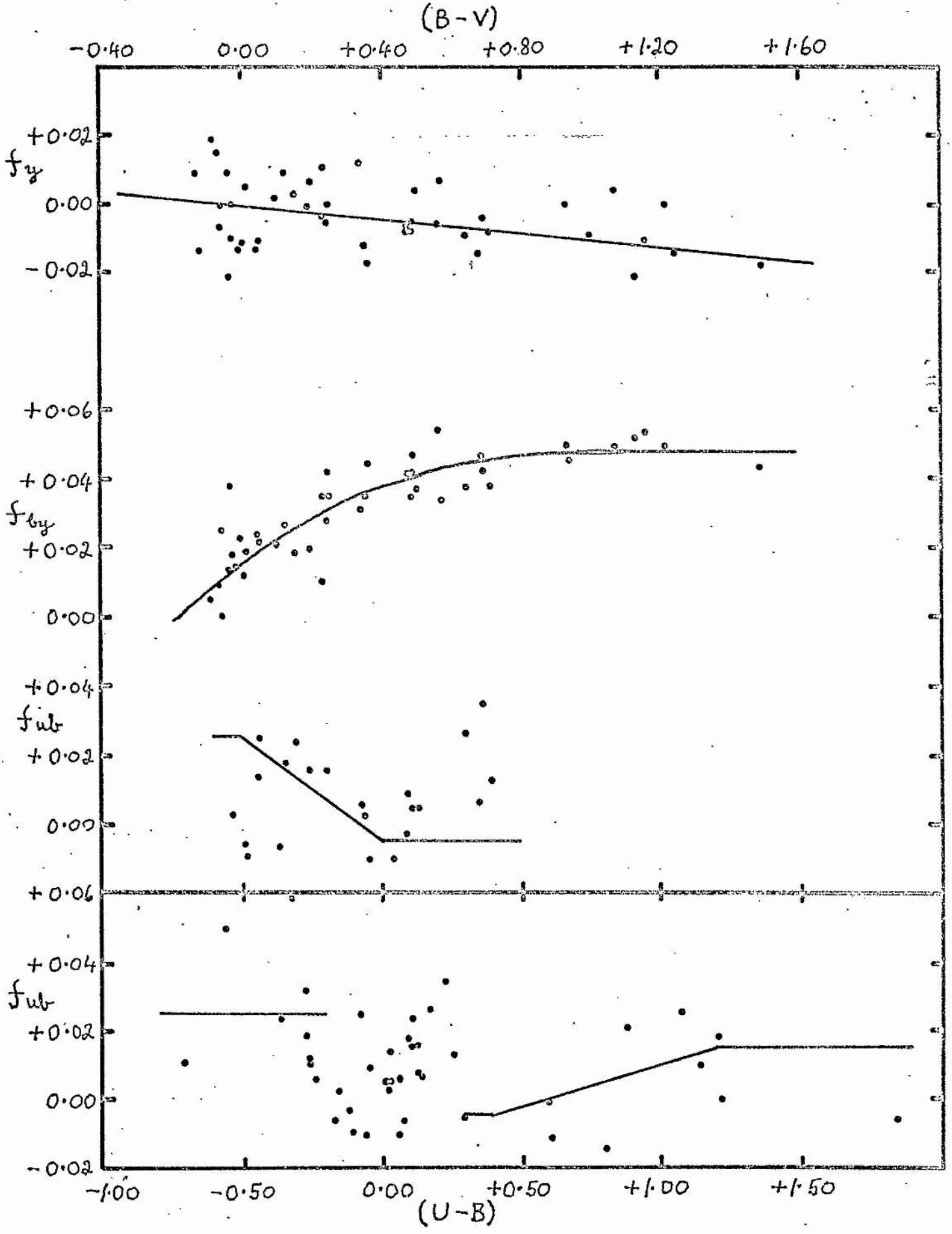
(B-V)
-0.40
0.00
+0.40
+0.80
+1.20
+1.60
+0.02
f_y
0.00
-0.02
+0.06
+0.04
f_{by}
+0.02
0.00
+0.04
f_{ub}
+0.02
0.00
+0.06
+0.04
f_{ub}
+0.02
0.00
-0.02
-1.00
-0.50
0.00
+0.50
+1.00
+1.50
(U-B)

reaches $0^m.08$.

Cousins (1967) has found slightly different curves of the correction f_{by} against B-V for reddened and unreddened stars. The difference is of the order of $0^m.01$ and is ignored.

Local standards within the cluster fields were observed on good nights, using E region stars and some additional stars at higher declination (Cousins and Stoy, 1964) as standards. The extinction was measured when possible, otherwise the average values $k_y = k_{ub} = 0.30$, $K_{by} = 0.15$ were used. The individual determinations generally agreed to $\pm 0^m.01$ but with larger differences in the (U-B) tie-ins for IC 2581. Uncertainties in the standard star values, especially for (U-B) (Cousins, 1968) may be responsible. Uncertainties in colour transformations may also be important. Star 6 in NGC 6383 was observed on 7 nights in 1966 and 2 nights in 1967 relative to stars in E region 7. The total range of the individual values of V, (B-V) and (U-B) was only $0^m.02$ in either season but there were differences, in the sense (1967-1966), of $+0^m.01$, $-0^m.01$ and $+0^m.03$ respectively. It seems likely that the true uncertainty in the zero points is set by these effects, which are larger than the formal standard errors of individual tie-ins would suggest.

The observations of all other stars were made relative to these local standards, which had to be assumed constant in light (but see later). Extinction and colour corrections were allowed for before determining the zero points.

4. Photometry of Faint Stars.

Single deflections on stars fainter than V = 15.5 do not give

sufficient accuracy. It is difficult to centre a star fainter than V = 16.0 on the graticule directly. The observations of fainter stars were therefore made by offsetting from the position of a nearby bright star and making repeated measures of star and sky.

The reference star must be within 2' in each co-ordinate but not so close as to contribute appreciably to the measured light; a star with $11 < V < 13$ is most suitable. These requirements imposed a severe limitation on the choice of faint sequence stars in NGC 6383. It is also necessary to find a sky position free from faint stars. It is possible that the systematic errors which are suspected in the U magnitudes fainter than U = 17.9 in NGC 6383 are the result of a failure to ensure equality of the diffuse background (whether nebulous or scattered starlight) in star and sky positions.

Repeated measures are essential not only to reduce random errors per se but because it occasionally happens that "star + sky" gives a smaller deflection than "sky" alone. Where only single deflections are made such measures are rejected (to avoid log of a negative quantity) and the resulting magnitude scale is biased to brighter magnitudes. The usual procedure was to observe in the order ...V* B* Bs Vs V* ....., with each deflection lasting up to one minute. The U magnitude was then measured on a higher gain.

Drifting thin cloud or smoke illuminated by city lights and the periodic Iscor outbursts, for which watch was kept from a window, are the main external sources of error. If either was noticed the observation was terminated and a local standard star observed. Checks on bright stars showed that the centring was generally accurate, though a

FIGURE 11.

Part of the Brown recorder trace for V and B observations of NGC 6383 - 135 on 5 August, 1967.

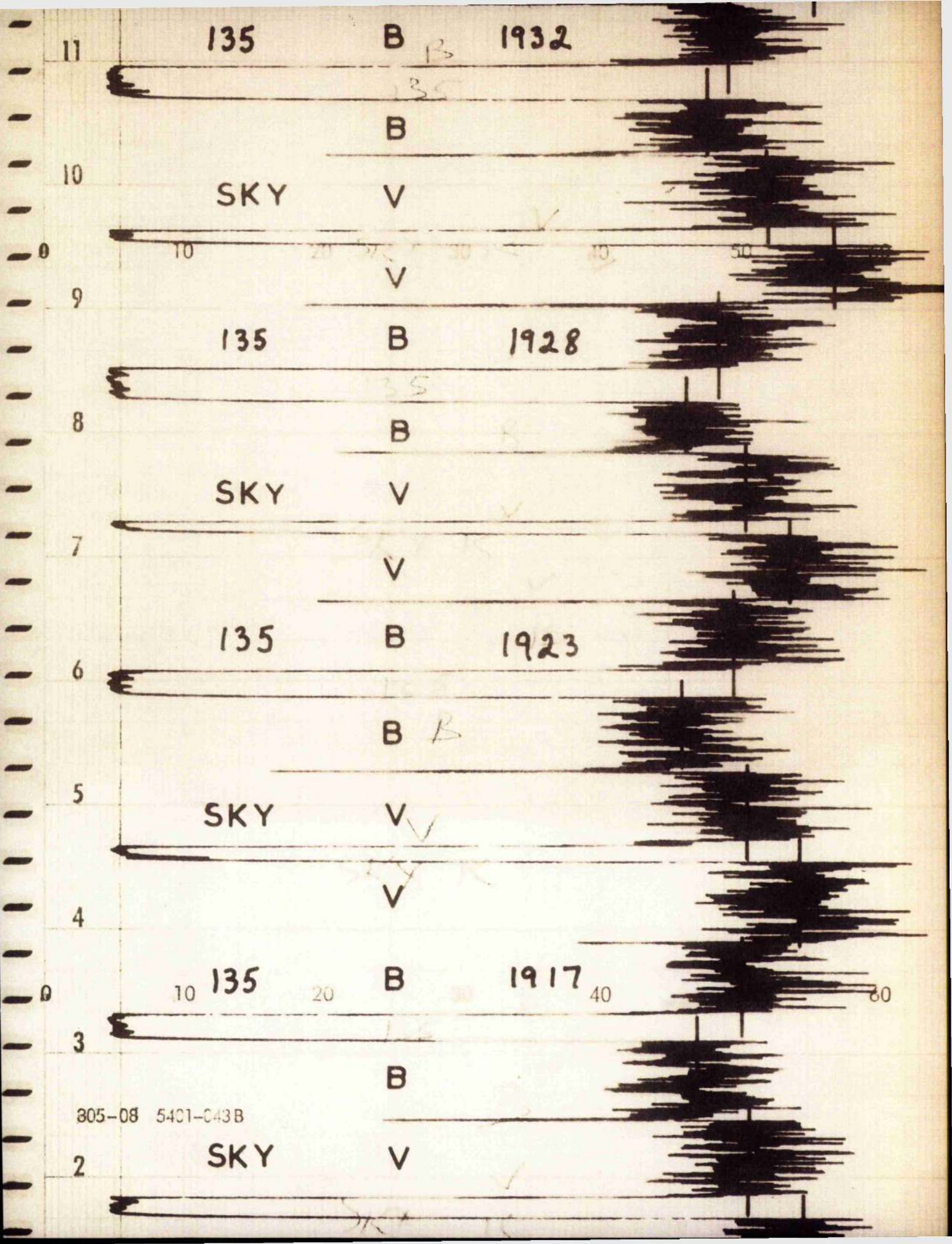
11
135 B 1932
B
10
SKY V
10 20 30 40 50
0
V
9
135 B 1928
8
B
SKY V
7
V
135 B 1923
6
B
5
SKY V
V
4
135 B 1917
10 20 40 60
0
3
B
805-08 5401-043B
2
SKY V

few observations were rejected because of poor centring manifested by erratic results.

A sample Brown recorder tracing of a faint star is reproduced in Figure 11.

5. Comparison with Previous Observations.

The differences between the present photo-electric observations in IC 2581 and those of Fernie (1966) are plotted in Figure 12. The new observations indicate that the stars are fainter and slightly redder in (B-V); the ultraviolet observations are not comparable, as Fernie used a refractor. The small standard deviation of individual points about the iris curves (Chapter 11) suggests that the large scatter in Figure 12 is not attributable to the new observations. The values of V and (B-V) given for star 2 (HD 90706) by Cousins and Stoy (1964) agree well with those found here for this local standard, while the internal consistency of all the zero point transfers for stars 2, 3 and 7 excludes the possibility of a large zero point error in V. It is concluded that most of the difference between the present observations and those by Fernie is attributable to errors in the latter.

The differences between the present photo-electric observations in NGC 6383 and those of Eggen (1961) are shown in Figure 13. There appears to be a scale difference in V, a systematic difference (possibly colour dependent) in (B-V) and a large scatter in (U-B). It does not seem possible to account for the differences in V and (B-V) as the result of errors in the present observations, although the problem of transforming instrumental to standard (B-V) colours of reddened early

FIGURE 12.

The differences, present - Fernie, in V and (B-V) for photo-electric sequence stars in IC 2581 observed by Fernie (1966) and by the writer.

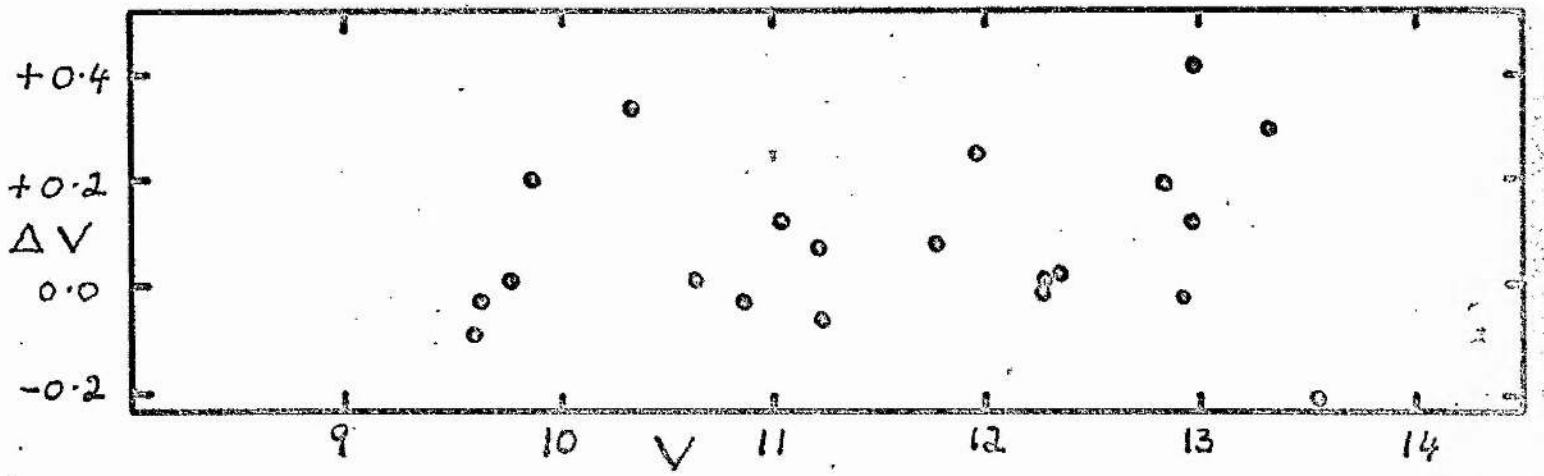
+0·4
+0·2
ΔV
0·0
−0·2
9
10
V
11
12
13
14

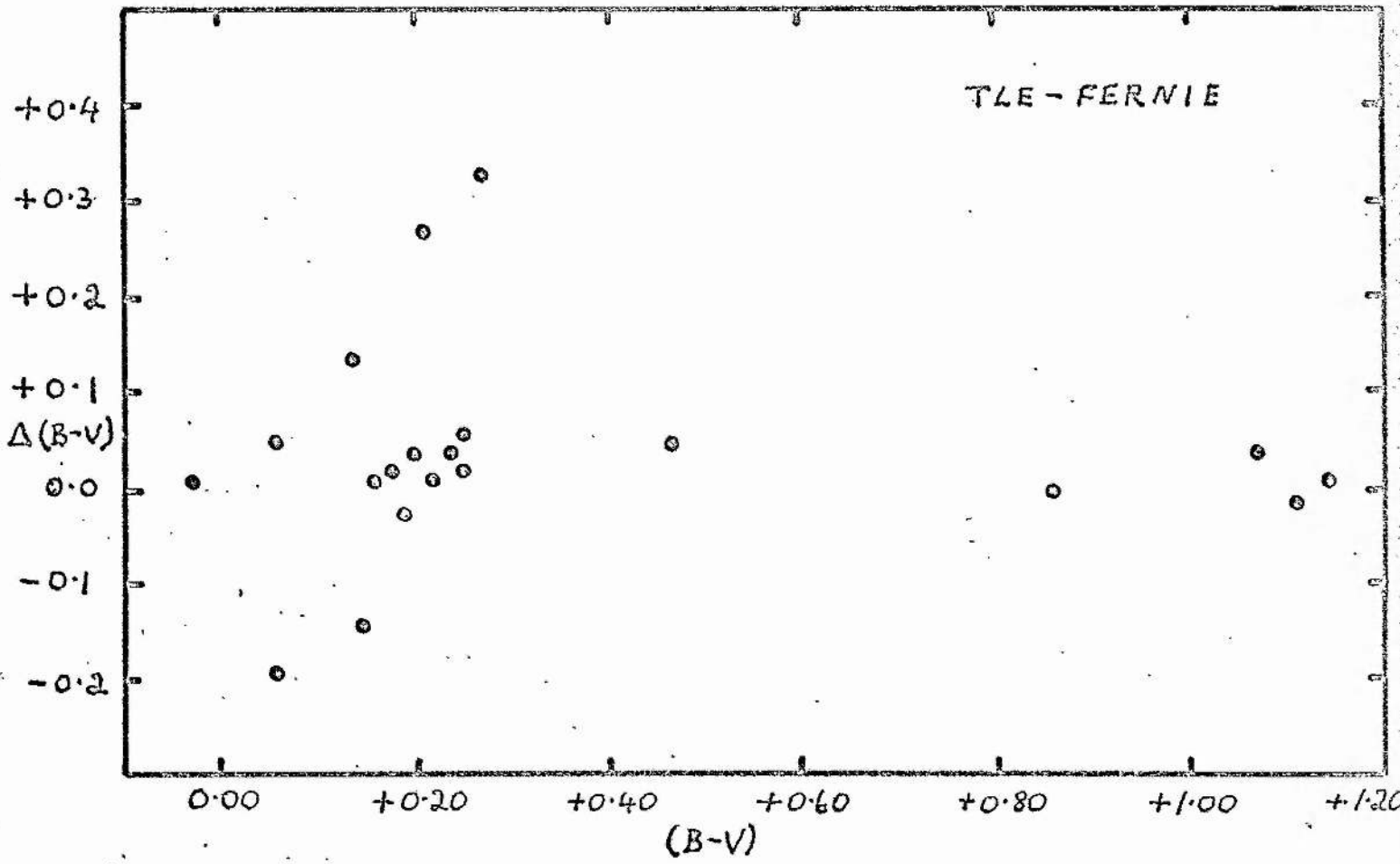
TLE - FERNIE
+0·4
+0·3
+0·2
+0·1
Δ(B-V)
0·0
−0·1
−0·2
0·00
+0·20
+0·40
+0·60
+0·80
+1·00
+1·20
(B-V)

type stars may have led to larger errors than the interagreement of individual observations would suggest. The large differences in (U-B) may be attributable in some cases to the difficulties introduced by the scattered light of HD 159176.

6. Photographic Observations.

The 74-inch reflector is used with a 44-inch stop to reduce coma to negligible proportions over a field of 16' diameter (Arp, 1958a). The Newtonian flat is adjusted in daylight at the start of each run. The collimation is determined from symmetry and the squaring-on of the plateholder is checked by viewing the Cassegrain baffle in front of the primary mirror with a small telescope mounted in the plateholder. The two adjustments are made by moving the plateholder mount perpendicular to the optical axis using the XY guiding motions and by rotating the secondary mirror mount about the optical axis of the primary. The 45° tilt of the secondary mirror and the squaring-on adjustments of the breechpiece and plateholders are kept fixed. The optical axis may deviate from the plate centre by as much as 2'-3' in practice. This is only apparent on plates taken at full aperture.

The depth of focus has not been measured. Extrapolation from the values quoted for Schmidt telescopes, assuming an inverse dependence on the square of the focal ratio, gives a value of 5 thou. This is in accordance with the appearance of focal sequences. Knife edge focussing gives an internal error of about $\pm$ 0.1 mm (4 thou); focus plate determinations agree within this tolerance and the tilt across the field is not larger than this. The focus changes only very slightly during

FIGURE 13.

The differences, present - Eggen, in V, (B-V) and (U-B) for photo-electric sequence stars in NGC 6383 observed by Eggen (1961) and by the writer.

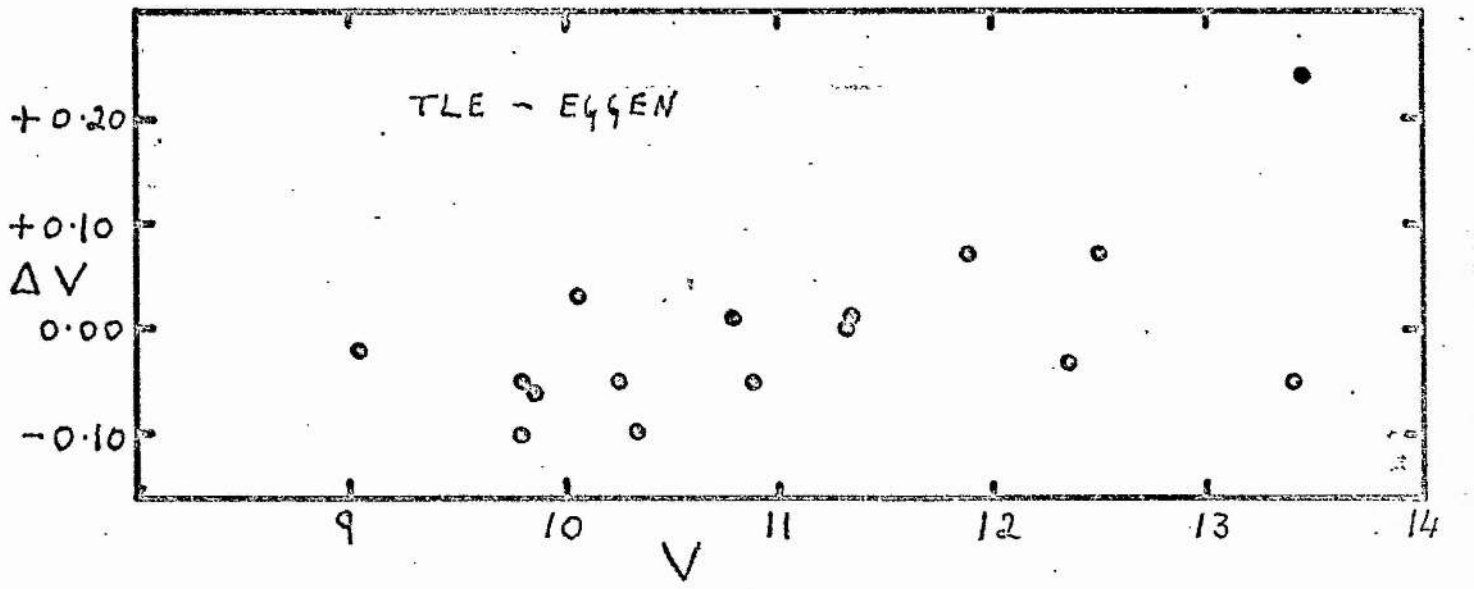
TLE - EGGEN
+0·20
+0·10
ΔV
0·00
−0·10
9
10
11
12
13
14
V

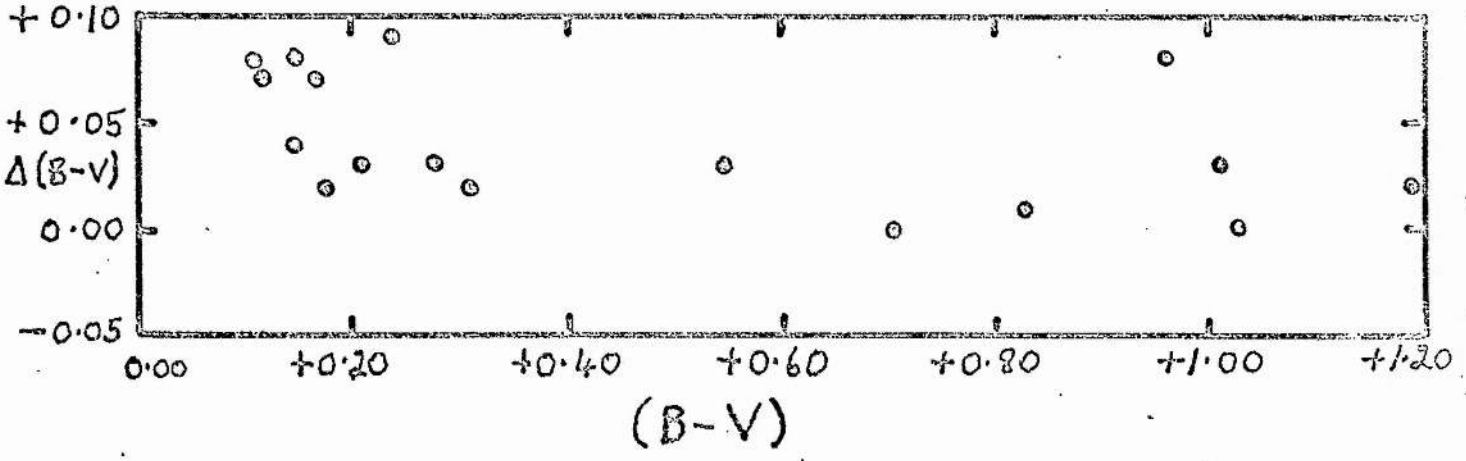
+0·10
+0·05
Δ(B-V)
0·00
−0·05
0·00
+0·20
+0·40
+0·60
+0·80
+1·00
+1·20
(B-V)

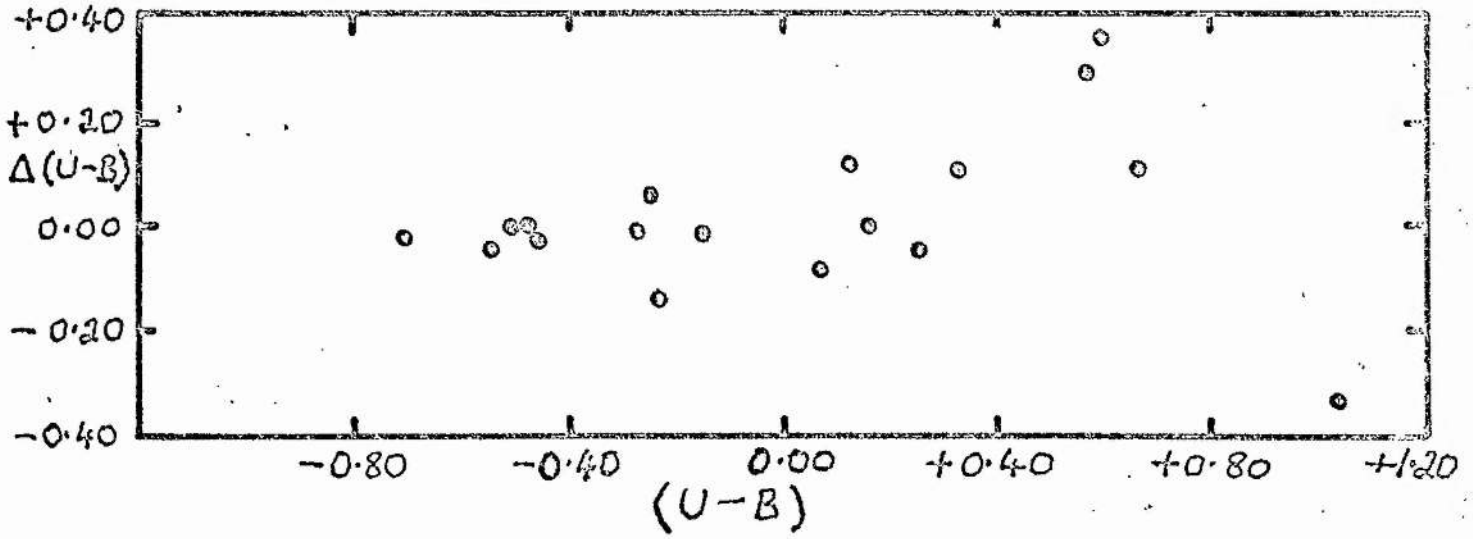
+0·40
+0·20
Δ(U-B)
0·00
−0·20
−0·40
−0·80
−0·40
0·00
+0·40
+0·80
+1·20
(U−B)

the night unless there is an unusually rapid fall in temperature.

Slight astigmatism is probably always present; strong astigmatism occurs at hour angles in excess of those used for photometric plates. Exposures were restricted to the region within 3 hours of the meridian.

Guiding is by means of the XY motions on the plateholder mount; an off-axis guide star is viewed through one of two eyepieces mounted on slides.

The telescope has an open frame tube. Stray light from sky or ground is kept off the plate by means of a black cloth wound round part of the top section of the tube, a wooden baffle between the breechpiece and the 44-inch aperture, a second black cloth round the breechpiece itself and the wind blind.

The plate and filter combinations were :

V	103aD + GG 11	or	103aG + GG 11
B	103aO + GG 13	or	IIaO + GG 13
U	IaO + UG 2		

The plate size is $3\frac{1}{4}$ inch x $4\frac{1}{4}$ inch.

Table 3 contains details of all the plates of IC 2581 and NGC 6383. A range of exposure times was used to ensure that each star could be measured on more than one plate under favourable conditions regarding image strength, scattered light and crowding.

7. Reduction Procedures.

The plates were measured with the Sartorius iris-diaphragm photometer. The stability of this instrument is excellent, with no drift when it is properly aligned. All the stars above the plate limit

(usually rather conservatively estimated) or the faint end of the sequence and within a circle of diameter 16' (IC 2581) or 20' (NGC 6383) were measured. Sky fog measures were made on the long exposure plates of NGC 6383 and for stars in the vicinity of bright stars on the remaining plates.

The long exposure plates of NGC 6383, on which the fog density varied due to faint nebulosity and scattered light from the O8 star HD 159176, were reduced graphically. The iris curves for the 2 hour U exposures were plotted with the iris readings corrected for the local sky fog to avoid biasing the curve. The deviations in magnitudes of individual standards on the remaining plates were plotted against the local plate fog density and corrections made to the magnitudes of other stars on the basis of the mean relationship.

The remaining plates were reduced using the IBM 360 Model 40 Computer at the Numerical Analysis Laboratory of the Council for Scientific and Industrial Research in Pretoria. Two programmes were used. The first determined the relation between the iris readings and magnitudes of the standard stars. The standard magnitudes had first been placed on the natural system of the plate by applying the colour equations, assumed linear in (B-V) in the case of B and V, which were found graphically from a small sample of the plates. No correction was applied to the U magnitudes. The hand drawn iris curves also permitted the rejection of stars which showed excessive deviations from the mean curve, usually because of background fog near bright stars.

The programme, like that used for the NGC 752 reductions, is based

on the 1620 Library Program 7.0.002, Polynomial Curve Fitting. The first, second and third order polynomials of magnitude as a function of iris reading are fitted by least squares for the standards in predetermined intervals of magnitude and colour. A colour equation, linear in (B-V) for V and B, linear in (U-B) for U, is fitted for all the standards in each magnitude range to take up any remaining mismatch of colour systems. The polynomial coefficients, the average standard deviation of the standards from the curve and the individual residuals are printed out.

The division of the total magnitude range on a plate into several independent shorter intervals has the following advantages :

1) The order of the best fitting polynomial will in general be lower than that for the whole range.

2) The problem of weighting created by the great increase of standard error at fainter magnitudes is largely avoided.

3) Any change of colour equation with magnitude is handled automatically.

4) It is possible to select the scale stars for a given magnitude range from a narrow range in colour, avoiding the trend of mean colour with magnitude which would otherwise be present. This is less satisfactory in the U band in the two clusters studied here.

The best order iris curve is selected on the basis of standard deviation and lack of correlation between magnitude and residual.

The second programme calculates a magnitude on the plate system for each iris reading from the appropriate polynomial. The magnitude

FIGURE 14.

The colour dependence of the residuals $m_{pg} - m_{pe}$ of the adopted photographic magnitudes from the photo-electric values for IC 2581.

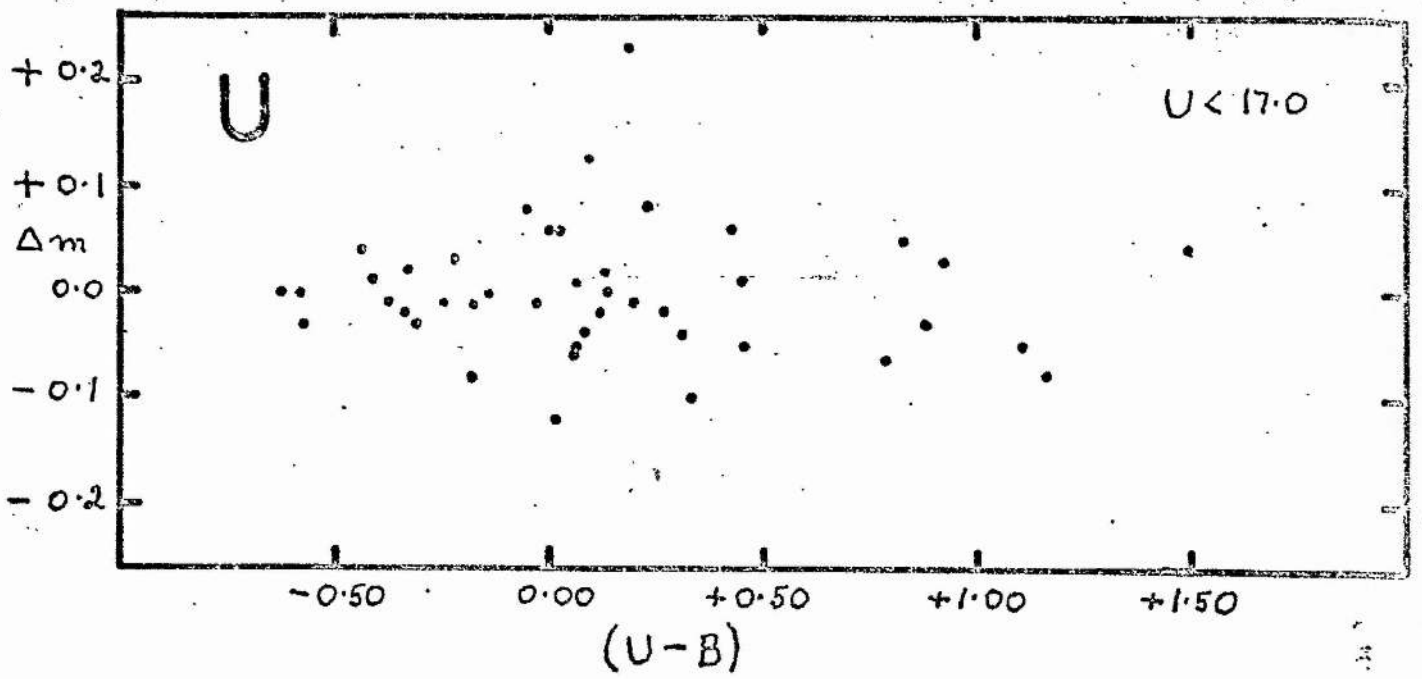
U
U < 17·0
+0·2
+0·1
Δm
0·0
−0·1
−0·2
−0·50
0·00
+0·50
+1·00
+1·50
(U−B)

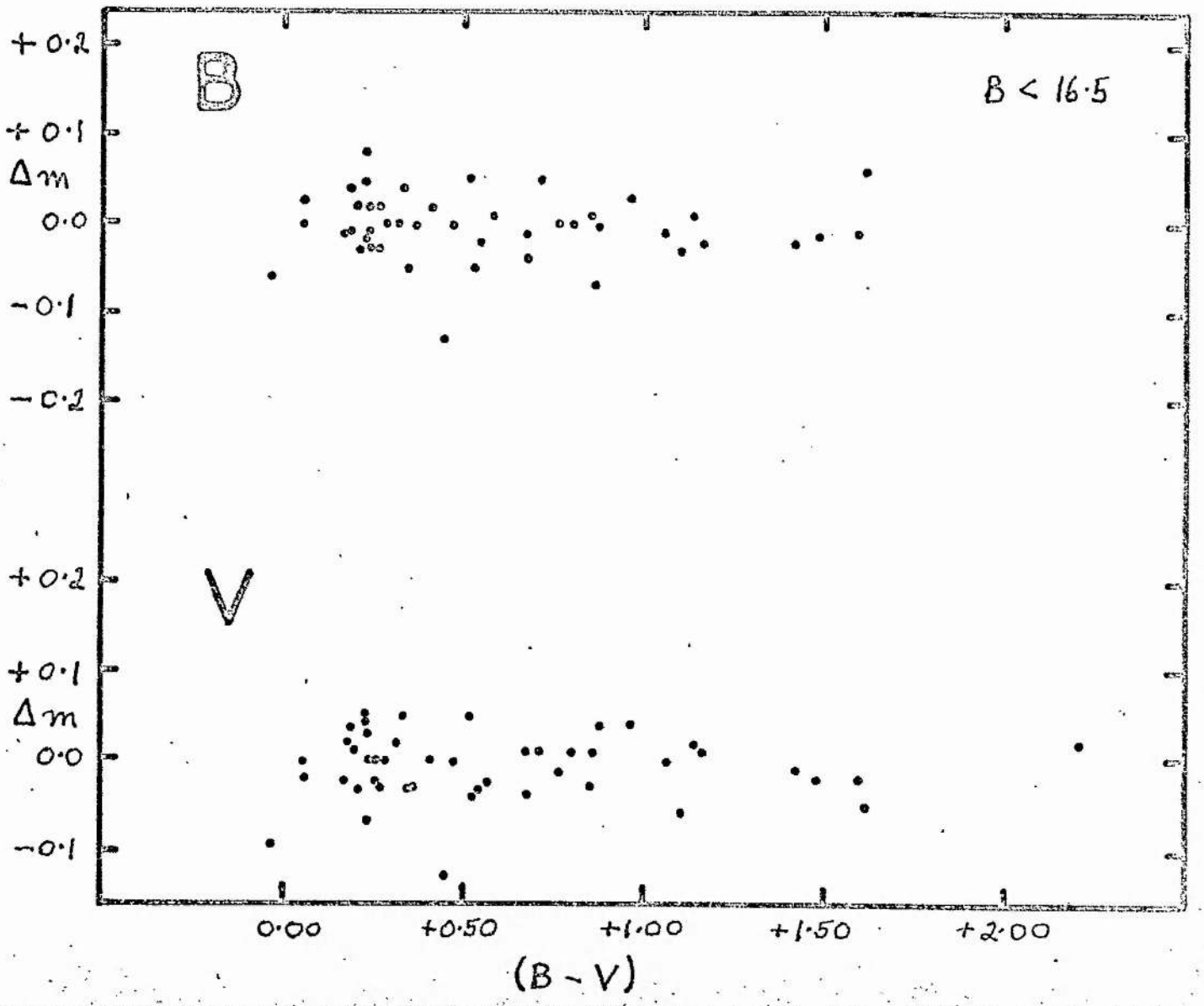
B
B < 16·5
V
+0·2
+0·1
Δm
0·0
−0·1
−0·2
0·00
+0·50
+1·00
+1·50
+2·00
(B−V)

of a given star on all the plates in a particular colour and exposure group are averaged and (B-V) calculated. The small colour equations in B and V are removed to place the magnitudes on the natural system of the corrected photo-electric standards, then the colour term assumed initially is removed. The final mean magnitudes and colours are printed out with the corresponding standard deviations. The uncorrected magnitudes read directly from the iris curve for each plate may also be printed out. No colour equation is applied to the U magnitudes, as it is likely to be a complicated function of both (U-B) and (B-V).

The mean magnitudes from the various exposure groups have been averaged to give final mean magnitudes. The stars which are crowded or which are close to the bright central star are in general measured fainter on the shorter exposure. The faintest magnitude found is adopted in the former case, though in some instances this will still be too bright. The same procedure has been used for stars on a bright background where standards in a similar location are not available.

8. Colour Equations.

Table 4 contains the mean total colour equations found for the various exposure time groups and magnitude intervals in each of the three colours. The coefficients are defined by

$$V_{pg} = V + \alpha(B-V)$$
$$B_{pg} = B + \beta(B-V)$$
$$U_{pg} = U + \gamma(U-B)$$

Figures 14 and 15 show the residuals for the photographic

FIGURE 15.

The colour dependence of the residuals $m_{pg} - m_{pe}$ of the adopted photographic magnitudes from the photo-electric values for NGC 6383.

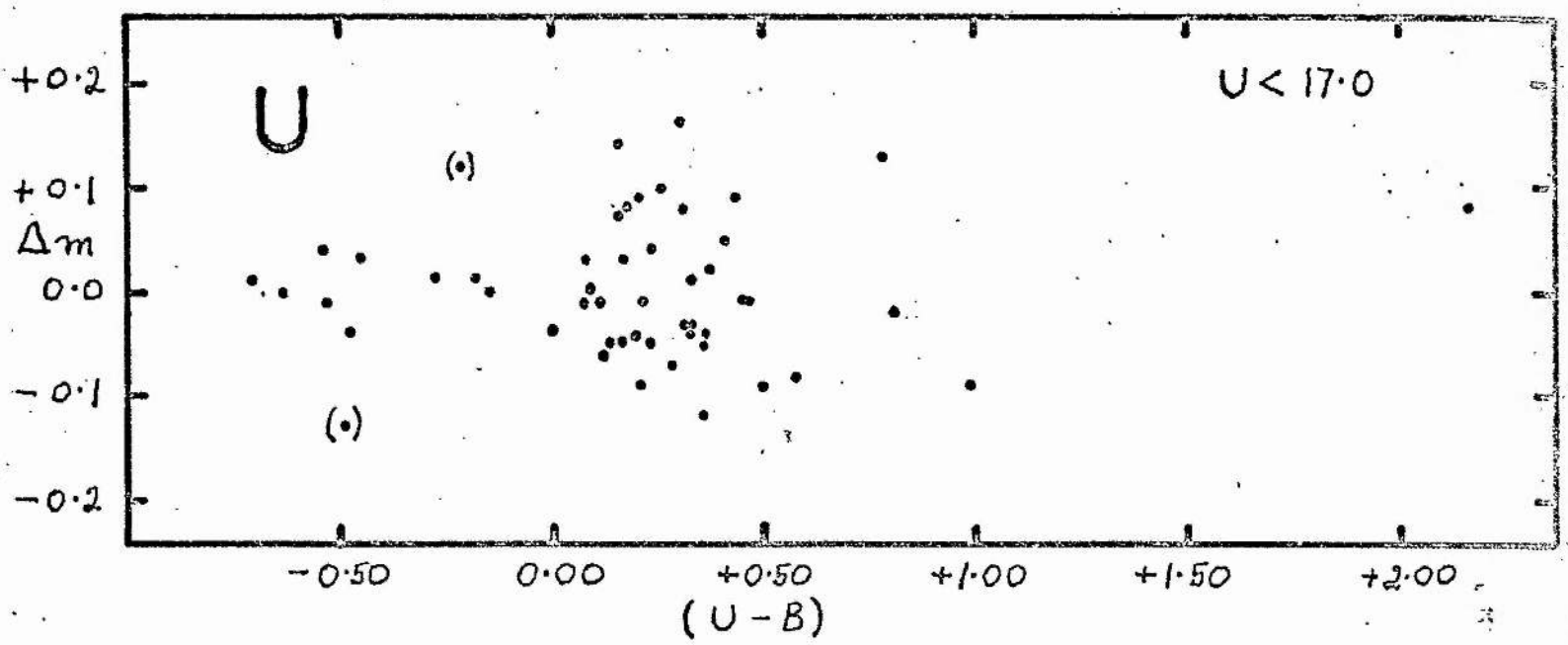
U
U < 17·0
(•)
(•)
+0·2
+0·1
Δm
0·0
−0·1
−0·2
−0·50
0·00
+0·50
+1·00
+1·50
+2·00
(U − B)

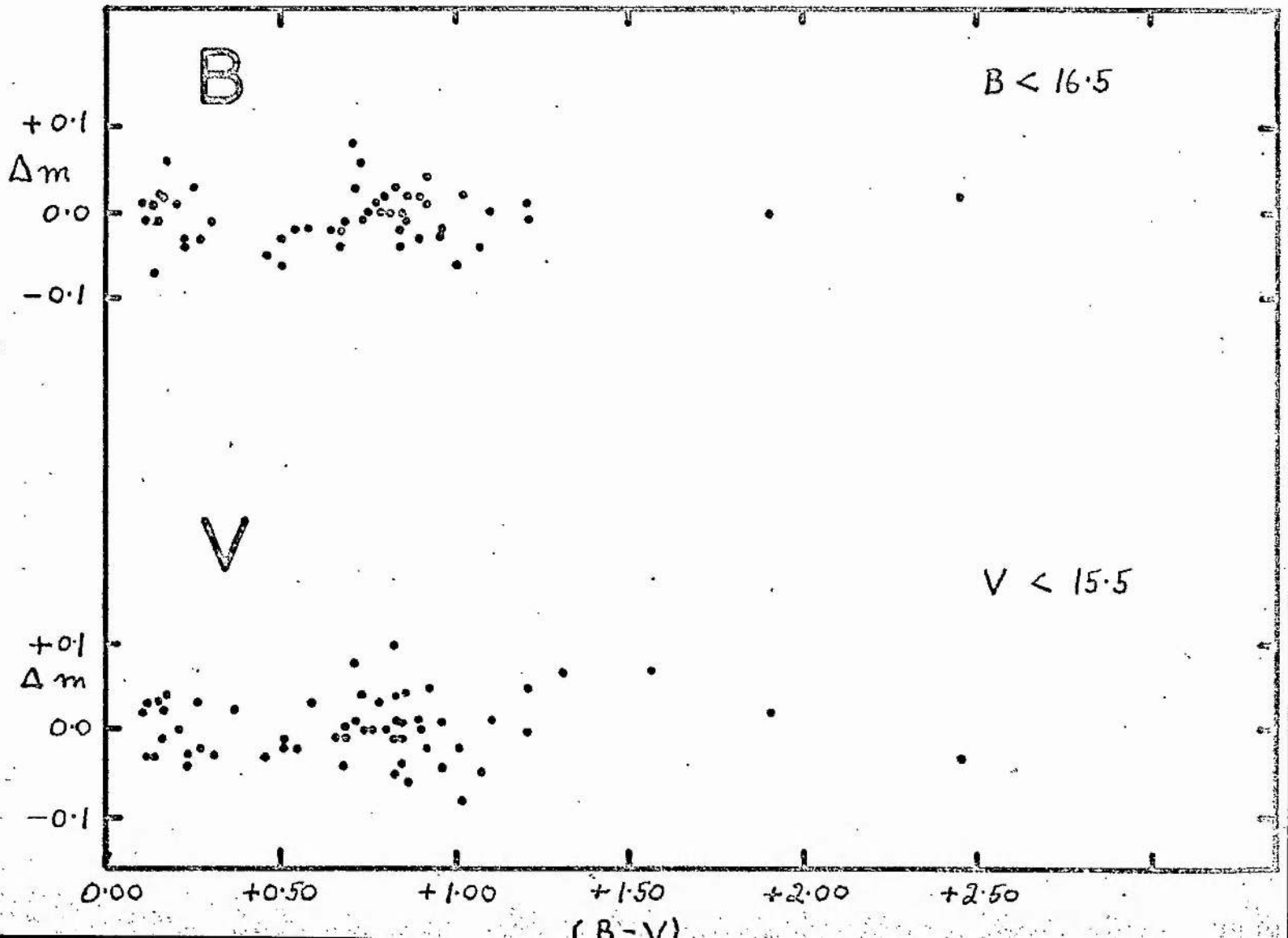
B
B < 16·5
+0·1
Δm
0·0
−0·1
V
V < 15·5
+0·1
Δm
0·0
−0·1
0·00
+0·50
+1·00
+1·50
+2·00
+2·50
(B − V)

magnitudes adopted for the standard stars after averaging the results of the various exposure groups of IC 2581 and NGC 6383, respectively. The residuals in V and B are plotted against (B-V); those in U are plotted against (U-B).

The colour equations computed for the different magnitude groups cannot readily be compared because the mean colour of the standards changes with magnitude. There does not appear to be any appreciable photographic Purkinje effect. The photographic colour equations for the faintest magnitude groups are often dominated by random error; the colour equations from the brighter magnitude groups have been applied in such cases.

The colour equations of the photographic B magnitudes found using 103aO or IIaO plates respectively are different. Neither the 103aD nor the 103aG plates used with a Schott GG 11 filter reproduces the V waveband very closely. Comparison of the V magnitudes for stars brighter than V = 15.0 in NGC 6383 as found with the two types of plate shows no systematic difference exceeding $0^{m}.01$ after colour corrections linear in (B-V) have been applied.

The residuals in U do not show a marked dependence on (U-B). The computer reductions for IC 2581, where the distribution in colour of the standards is more favourable than in NGC 6383, show a linear term of about 0.02 (U-B) in the sense that red stars are measured faint. The scatter is quite large and may mask a more complicated colour equation. Walker (1964) has pointed out that the Schott UG 2 filter gives rise to a more marked S bend in the two colour diagram than does the Corning 9863 filter originally used to define the U waveband. The

reason is the more effective elimination of the spectral region longward of the Balmer discontinuity by the UG 2 filter. The presence of stars above the hump of the standard curve in the two colour diagram of IC 2581 may indicate that this has occurred in the present work. The photographic colour system, unlike its photo-electric prototype, is not defined by a large number of standard stars covering the full range of colours within a limited range of magnitudes. This restriction is imposed by the limited range of types of star available at a given magnitude in a limited field and by the large amount of telescope time required to provide such a calibration. The result in practice is that uncorrected colour equations may be absorbed into the U magnitude scale and that stars of equal U may not have equal U_{pg}.

The U magnitudes have been left on the instrumental system.

It is not possible to make the common claim that systematic errors are minimised because the standards belong to the cluster and share the distribution in magnitude and colour of cluster members in general. The analysis shows that the standards, which were selected with a variety of criteria (in particular that they be uncrowded and, in the case of the faintest ones, not on a bright background, so that they are often far from the central star and in an empty part of the field) are only predominantly cluster members in the brightest few magnitudes.

9. Field Error.

The dependence of the residuals on distance in minutes of arc from the centre of the field is shown for IC 2581 in Figure 16 and for NGC 6383 in Figure 17. Field errors will to some extent be taken up

FIGURE 16.

The magnitude residuals $m_{pg} - m_{pe}$ of the photographic magnitudes from the photo-electric values as a function of angular distance from the centre of IC 2581.

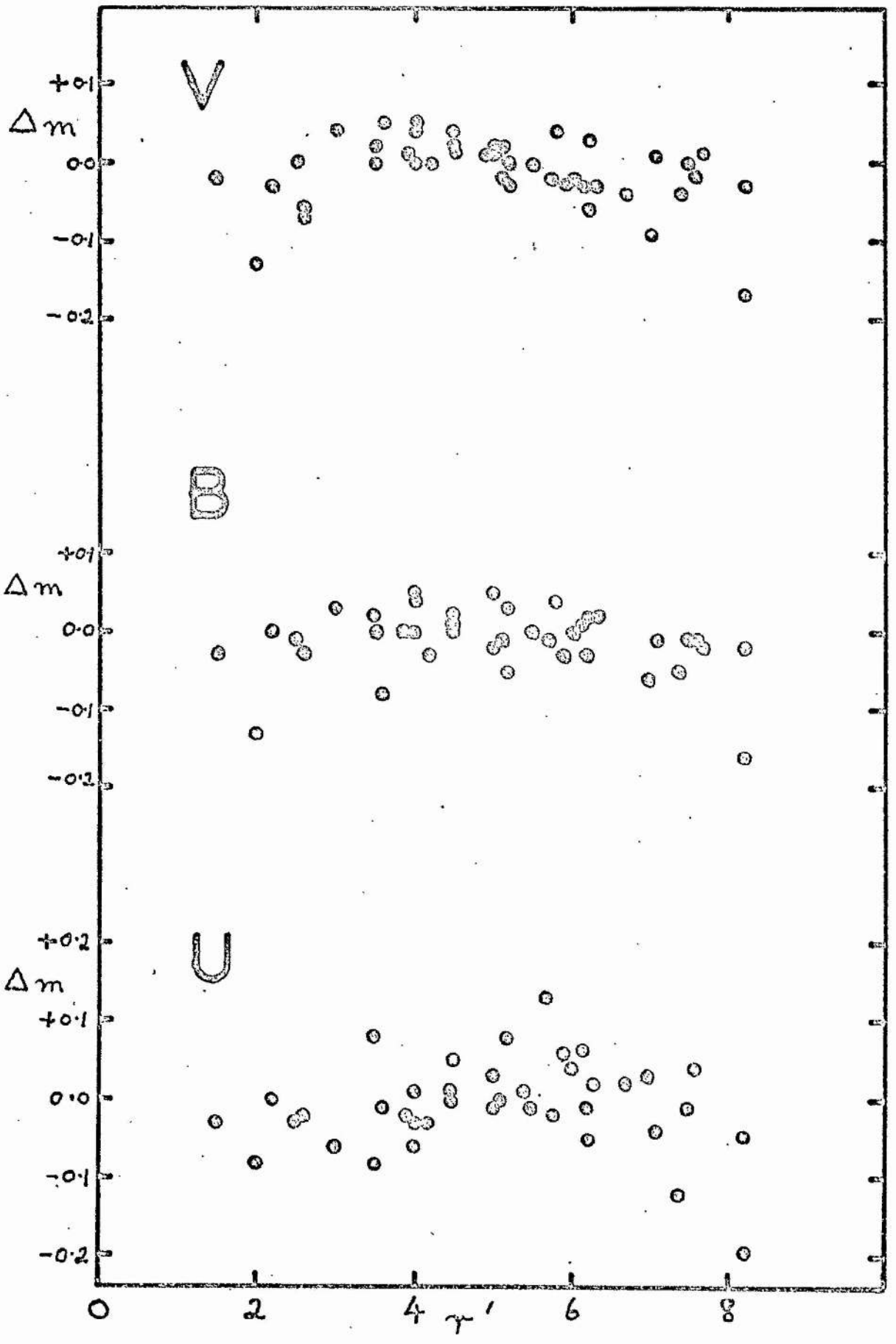
V
B
U
Δm
+0.1
0.0
−0.1
−0.2
+0.2
0
2
4
6
8
φ'

in the scale and colour system, because these stars - except for a few which deviated from the trial iris curves and those outside the 16' diameter field - were used to define the system. The 16' field is seen to be practically free of field error and the error amounts to about $0^m.1$ at a distance of 12' from the centre. This field error is the average of several Newtonian runs; it seems likely that if the error in achieving coincidence between the optical axis and the centre of the plate were eliminated, the error-free field would be slightly larger. Stars are measured bright off axis, as would be expected if the error were due to coma.

An error due to image structure will depend on magnitude. The indicated correction has been applied only to the few bright stars between 8' and 12' from the centre.

10. Errors.

The following errors are tabulated:

1. The standard error of a single photo-electric observation (V, (B-V), (U-B))

2. The standard deviation of the individual points about the iris curves for a given plate. (V, B, U)

3. The standard error of the mean of all the measures of a star on the plates (usually 3 or 4 in number) of a given exposure time. (V, B, U)

These random errors are given as a function of magnitude for IC 2581 and NGC 6383 in Tables 5 and 6, respectively. The internal

FIGURE 17.

The magnitude residuals $m_{pg} - m_{pe}$ of the photographic magnitudes from the photo-electric values as a function of angular distance from the centre of NGC 6383.

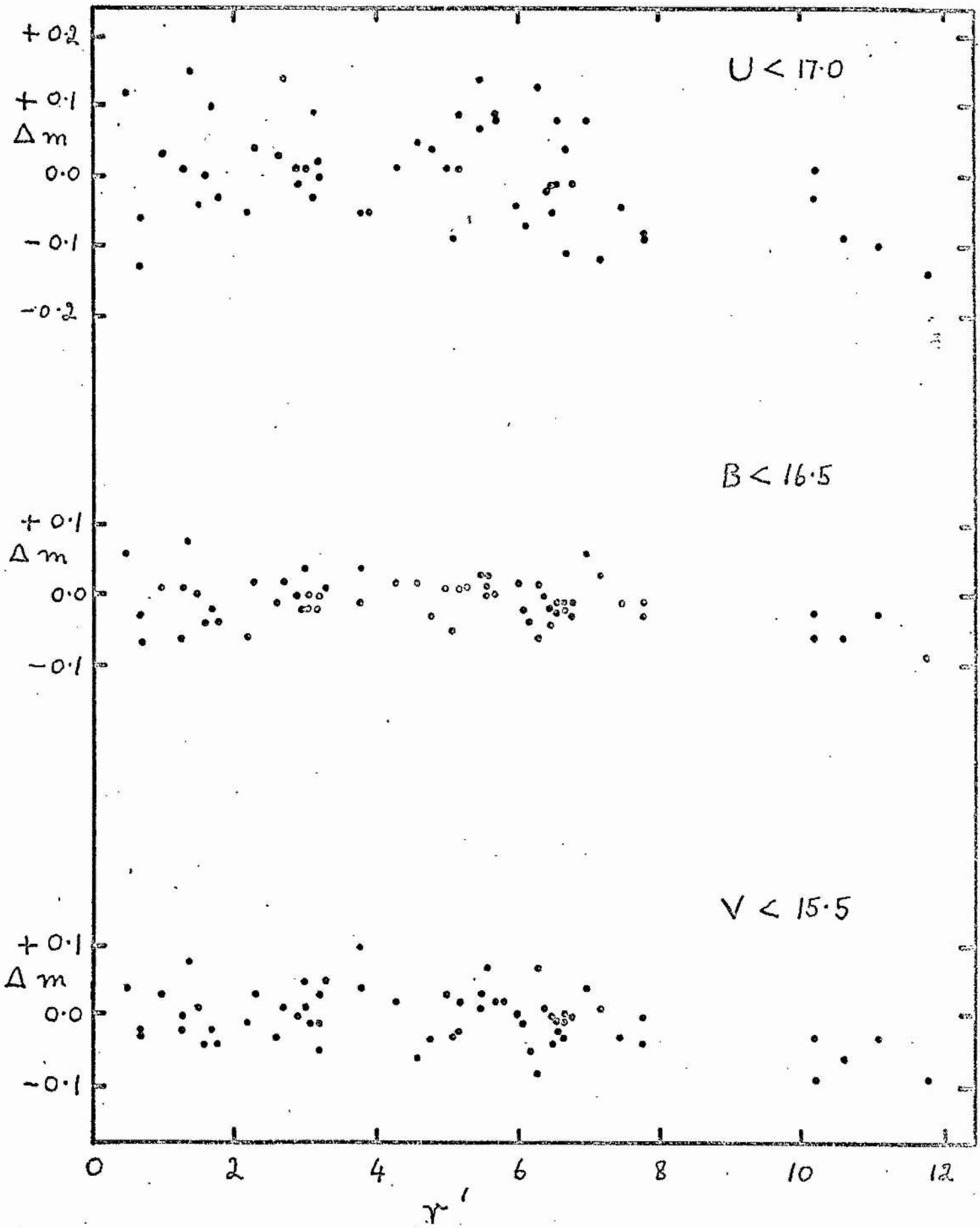
U < 17·0
B < 16·5
V < 15·5
+0·2
+0·1
Δm
0·0
−0·1
−0·2
0
2
4
6
8
10
12
r'

errors of the final magnitudes should theoretically be about half those in column 3, except for the faintest stars which are only measurable on the long exposure plates. This is not necessarily so in practice. The deduced magnitude of a given star may depend on exposure, due to sky background and crowding effects, while slight differences in the weighting of individual standard stars may result in corresponding differences in the magnitude system.

Systematic errors may be due to several causes other than the colour equations already described. The largest errors will occur at the faint end of the magnitude scale, due to error in positioning the iris curve. The error allowable from eye estimates, of the order of $0^m.01$ for the brighter stars, rises to about $0^m.1$ at most at the faint end on the long exposure plates of NGC 6383. More serious is the possibility that a small number of standards may define a systematically incorrect magnitude scale because their errors are preferentially in one direction. The U magnitudes in IC 2581 rest on only 3 standard stars with $U > 17$ and the (U-B) colour for the few faint red stars must be considered uncertain. An attempt to extend the U magnitude scale in NGC 6383 to $U = 19$ was unsuccessful; the (U-B) values for the few photo-electric standards with $U > 17.9$ are almost certainly too blue. The iris curves are well defined to the limits $V = 18.1$, $B = 19.7$, $U = 17.9$.

11. The Detection of Variable Stars.

The two bright variables in IC 2581 were originally used as local photo-electric standards, necessitating some additional observing and

complication in the reductions. It is unlikely that their variability would have been detected had they not been observed repeatedly as standards, as they are too bright for photographic observations.

The faint variable stars in NGC 6383 were detected by blinking or by plotting iris readings of one plate against those of another. (This latter procedure was undertaken for a proportion of the plates, including all the long exposure plates of NGC 6383, as a check on plate quality). Most of these stars are beyond the limit of the photo-electric sequence, so only rough magnitude estimates are possible. Variability is generally regarded as established if a star appears fainter or brighter than usual on all the plates on a given night.

The total number of observations falls far short of that required to make a complete survey for variable stars.

SECTION 3.

THE OPEN CLUSTER IC 2581.

The open cluster IC 2581 is located at $\alpha = 10^h\ 23^m\ .7$, $\delta = -57°\ 08'$ (1900); $l^{II} = 284°.6$, $b^{II} = 00°.0$. This is near the preceding end of the rich complex of young clusters and other objects which may be associated with η Carinae and the nebula NGC 3372 (Sher, 1966). The cluster is dominated by the 4th magnitude F0 Ia star, HD 90772. The only recent study of the cluster is that by Fernie (1963), (1966), who made photo-electric observations of many of the brighter stars in the cluster region. He found a distance modulus of $(m - M)_o = 11.1$, corresponding to a distance of 1.66 k pc.

1. Observations.

Table 7 gives, for the stars of the photo-electric sequence, the values of V, (B-V) and (U-B) measured photo-electrically; the total number of observations made and the number of (U-B) observations, if less; and the values of V, (B-V) and (U-B) determined photographically. Table 8 contains the photographic values of V, (B-V) and (U-B) for the remaining stars. All stars brighter than V = 15.5 and within 8' of HD 90772 have been observed, except for a few which are crowded. Magnitudes and colours of stars within about 2' of HD 90772 may be in error, especially for the fainter stars, because the standard stars were not adequate to determine corrections for plate fog caused by the

FIGURE 18.

The identification chart for IC. 2581. 74-inch reflector stopped to 44 inches. Blue light.

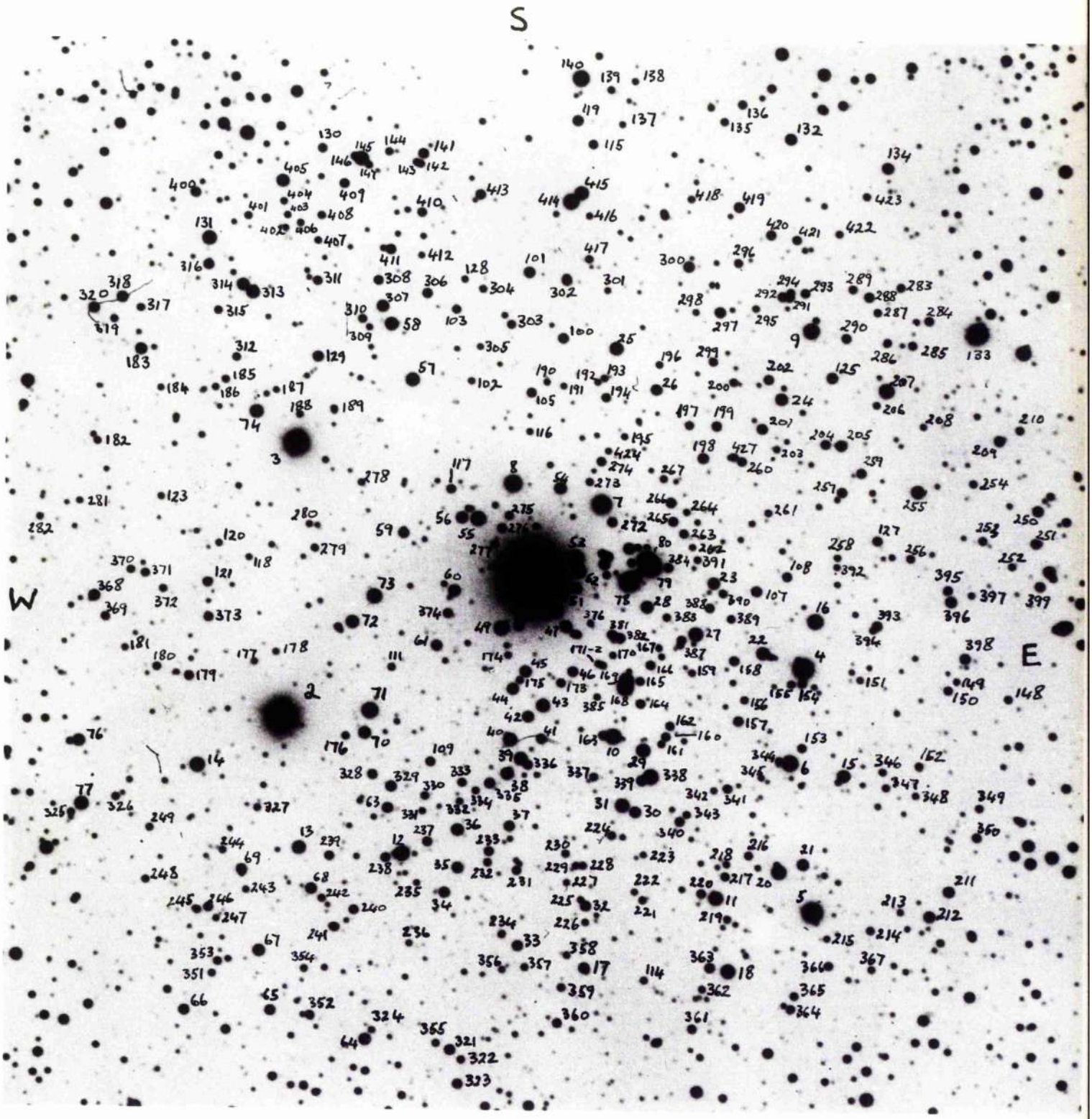
S
W
E
N

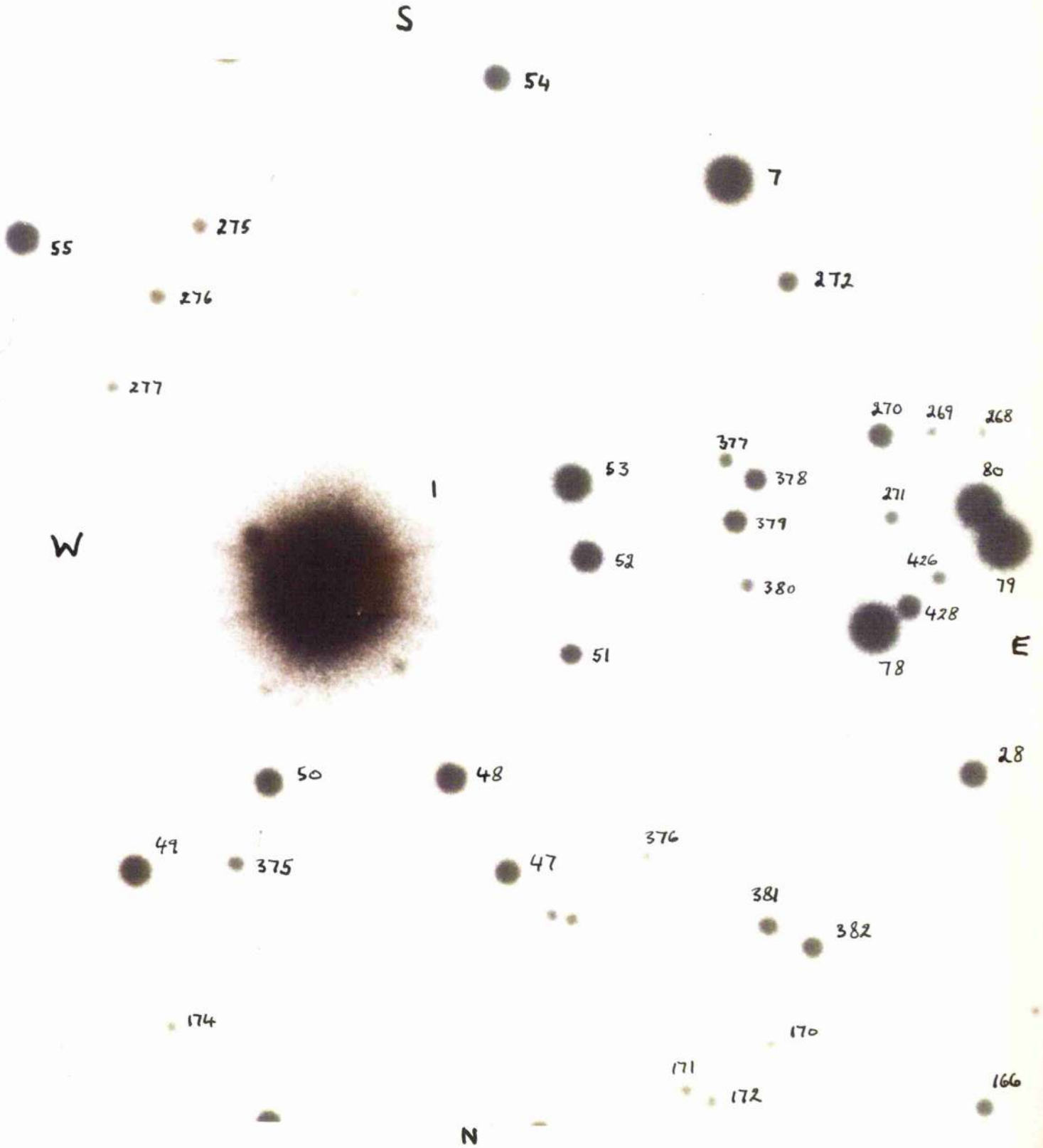
S
54
7
55
275
272
276
277
270
269
268
377
80
53
1
378
271
W
379
52
426
79
380
428
51
E
78
28
50
48
49
375
376
47
381
382
174
170
171
166
172
N

scattered light of HD 90772. The stars measured are identified on the photograph, Figure 18.

Spectral types of some of the brighter stars, estimated on 86 A/mm or 49 A/mm spectra, are given in Table 9. Successive columns give : Number assigned by Fernie, HD or CPD number, spectral type, colour excess E_{B-V}, absolute magnitude M_V and distance modulus. The relations between spectral type and intrinsic colour and absolute magnitude are from Johnson (1963), (1964) and Blaauw (1963), respectively.

2. Cluster Membership and Interstellar Reddening.

Star 5 is a foreground object on the basis of spectral type, colour and magnitude. The remaining stars of known spectral type are possible members of the cluster. The two-colour diagram, Fig. 19, shows that the stars fall in 3 main groups :

a) Stars near the standard relation for unreddened stars. These are taken to be field stars; most are type F or later, on the basis of their colours. The tendency of these stars to lie systematically above the standard line near (B-V) = 0.5, (U-B) = 0.0, may be the result of a systematic difference between the photographic and the standard ultraviolet systems.

b) Stars near the standard line displaced for reddening E_{B-V}=0.42, E_{U-B} = 0.30, from (B-V, U-B) of (+0.20, -0.70) to (+0.60, +0.40) approximately. Most of the bright probable cluster members belong to this group and these stars are regarded as possible cluster members. These stars are represented by filled circles in the colour-magnitude

FIGURE 19.

The two colour diagram for IC 2581.

The intrinsic line for dwarf stars

is shown, undisplaced and also shifted

by $E_{B-V} = 0.42$, $E_{U-B} = 0.30$.

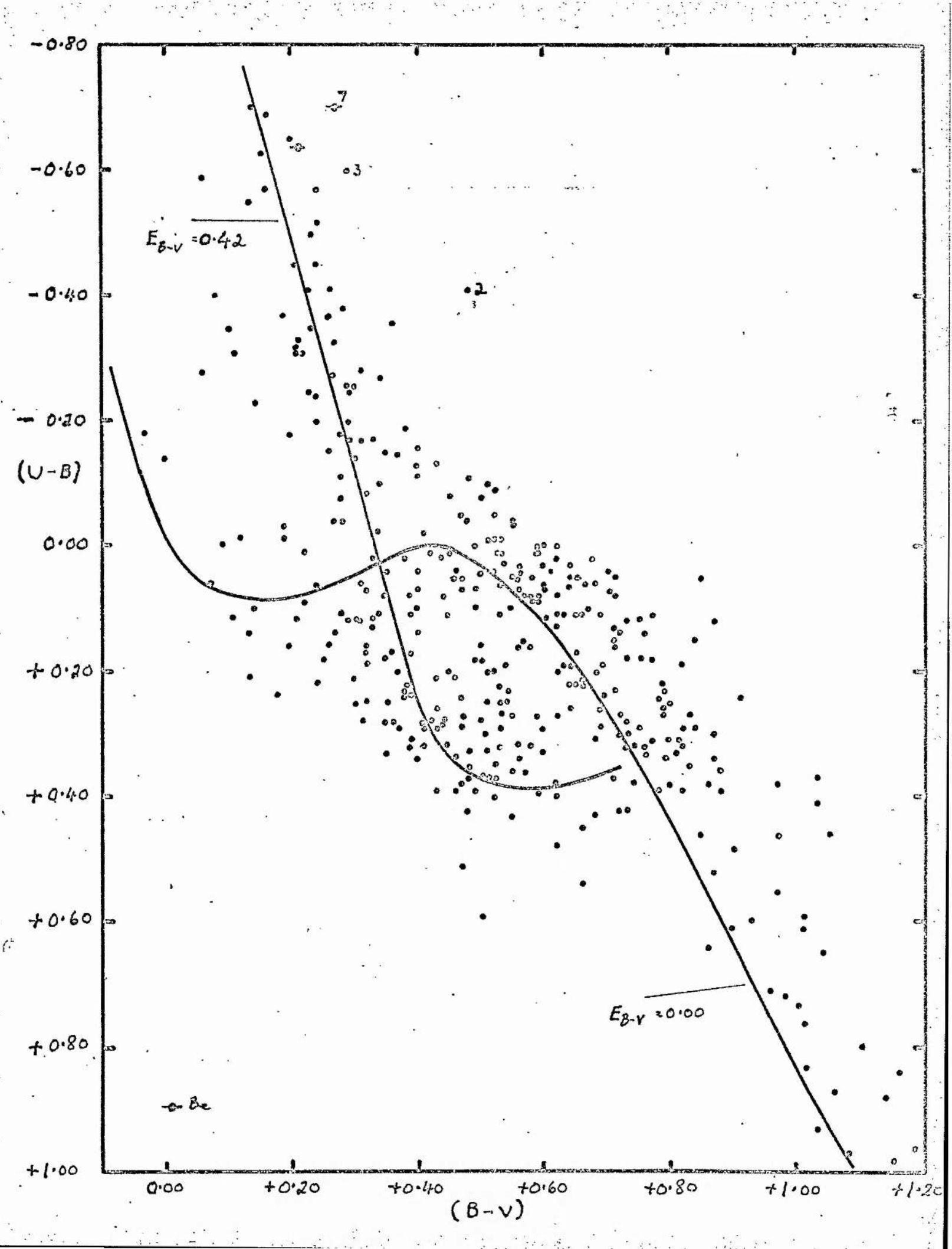
-0·80
-0·60
-0·40
-0·20
(U-B)
0·00
+0·20
+0·40
+0·60
+0·80
+1·00
0·00
+0·20
+0·40
+0·60
+0·80
+1·00
+1·20
(B-V)
E_{B-V} =0·42
E_{B-V} =0·00
7
3
2
Be

diagram of the field, Fig. 20. They define a plausible cluster sequence which could hardly be distinguished from the colour-magnitude diagram of the whole field without the ultraviolet measures.

c) Stars which fall in neither of these two areas in the two-colour diagram. These include cluster members with more than the average reddening (2, 3), stars whose colours deviate from the standard relation (2 and possibly 7) and stars whose measured colours are affected by scattered light from HD 90772.

All stars from region b) and the less discrepant of those in c) were considered as possible cluster members and plotted in the long and short wavelength colour magnitude diagrams. The effect of differential reddening was considered in appropriate cases. Most of the stars fall in a well defined sequence, with a scattering of brighter stars at a given colour. The latter, which included in particular stars with $(U - B) < -0.20$ and which were less reddened than average and stars from the region defined by $0.27 < (B - V) < 0.42$, $(U\_B) \sim 0.0$ where the cluster and unreddened field stars may both occur, were rejected if they lay more than about $0^{m}.7$ above the sequence defined by the majority of the stars. Thirteen stars which may be more reddened or whose colours are likely to be in error are regarded as probable cluster members but have been excluded from the final discussion.

The reddening of the brighter cluster members were estimated using Johnson's (1958) nomogram, with the following results :

17 stars with	$V_o < 11.0$	$E_{B-V} = 0.43$
13 stars with	$11.0 < V_o < 12.0$	$E_{B-V} = 0.41$
21 stars with	$12.0 < V_o < 13.0$	$E_{B-V} = 0.42$

FIGURE 20.

The colour magnitude diagram V, (B-V) for the IC 2581 field. The stars which fall near the intrinsic line shifted for $E_{B-V} = 0.42$ in the two colour diagram are denoted by filled circles.

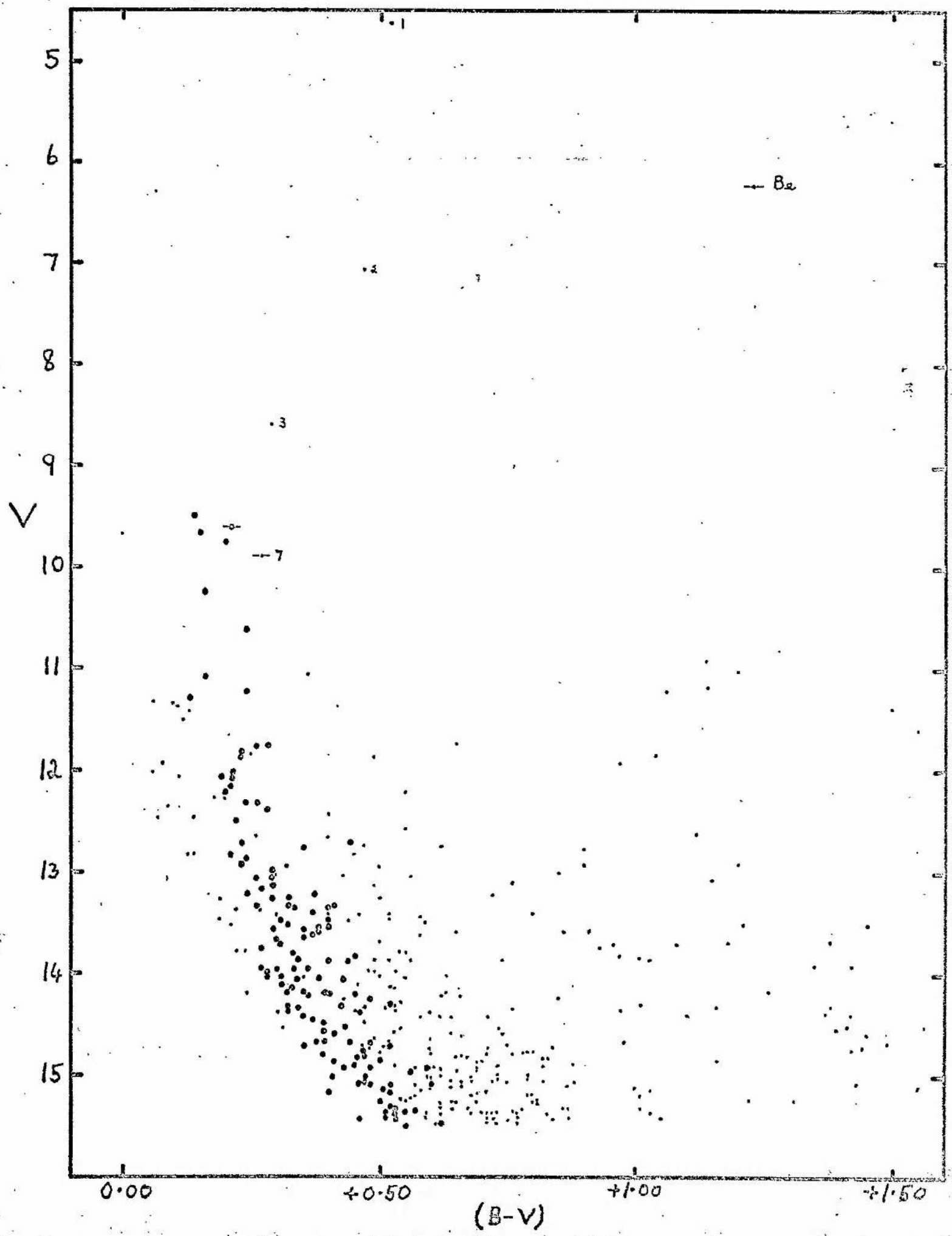
5
6
7
8
9
10
11
12
13
14
15
V
0·00
+0·50
+1·00
+1·50
(B-V)
Be
1
2
3
7

Eighty probable cluster members are contained in the region of obvious clustering which occupies approximately one-third of the area of the photometric field. Forty probable members lie in an outer zone covering the remainder of the field, except for the low star density region to the West of HD 90772. The reddenings of the probable cluster members in these two areas are :

"Cluster"	28 stars,	$V_o < 13.0$	$E_{B-V} = 0.42$
"Outer"	12 stars,	$V_o < 13.0$	$E_{B-V} = 0.42$

The mean reddening found by shifting the intrinsic line to fit the stars in region b) in the two colour diagram is $E_{B-V} = 0.42$. We adopt this as the mean reddening of the cluster.

The stars of region b) show a considerable scatter in colour excess. The individual colour excesses found from Johnson's nomogram show no correlation with position within the "Cluster" and "Outer" areas defined above, though they cover a range of $0^m.13$. The scatter may be the result of observational error and intrinsic differences in the stars themselves (Becker, 1962), as well as of small scale variations in the extinction.

The important possible cluster members, star 2 (HD 90706) and star 3 (HD 90707) lie in the low density region West of HD 90772. Seven stars from region b) of the two colour diagram fall on the outskirts of this area and five of them have slightly greater reddening than average. Seven stars from region c) which fall in the low density area have more than the average reddening. The mean reddening of three with $V_o < 13.0$ is $E_{B-V} = 0^m.55$; two of these are too bright to be cluster members and

must be foreground objects. The four fainter stars are possible cluster members with $E_{B-V} \sim 0^m.6$. The low density area is avoided by probable cluster members of normal reddening.

It appears that the low density area is the result of additional interstellar absorption. The reddenings deduced from the spectral types of star 2 ($E_{B-V} = 0^m.63$) and star 3 ($E_{B-V} = 0^m.55$) are compatible with cluster membership. They are included in the colour magnitude diagram of the cluster, but the five fainter possible members are excluded.

The existence of foreground stars, in both the low density area and the rest of the field, with magnitudes up to $1^m.5$ brighter than the cluster stars of the same colour shows that most of the interstellar absorption occurs well in front of the cluster.

The magnitude distributions of the probable cluster members in the "Cluster" and "Outer" parts of the field are markedly different:

V_o	< -3.0	-2.5	-1.5	-0.5	$+0.5$	>1.0
"Cluster"	7	2	10	14	19	25
"Outer"	1	0	1	3	10	26

The surface density of the faintest group is still at least twice as high in the "Cluster" area as outside, so it seems probable that many are genuine cluster members. It is possible that a substantial number of field stars are included among the supposed cluster members, but the similarity of the distributions of the "Cluster" and "Outer" stars in the colour magnitude diagram precludes any attempt to press the discussion of cluster membership further without additional observational criteria.

3. Stars of Particular Interest.

Fernie 1. HD 90772. Bidelman (1954) gave a spectral class, FoIa. Radcliffe spectra suggest an earlier type, perhaps A7Ia. It is too bright for photometry with the 74 inch telescope. Table 10 gives the results of photo-electric measures made elsewhere. Westerlund (1959) found a systematic difference between his measures of (B-V) for supergiants and those of Arp (1958), which he attributed to differences in the response curves of the different photometers and in the spectral energy distribution curves of reddened supergiants and of the less luminous and less reddened stars used to define the transformations from the instrumental colour system to the standard UBV system. We prefer the value of Cousins and Stoy (1964) because these observers have made the most extensive UBV measures in the Southern hemisphere.

The unreddened colour is found after allowing for the reddening of nearby bright stars; proximity to the absorbing lane renders the result rather uncertain. The best value of the reddening from stars 8, 45, 46, 54, 55, 60, 78, 79 and 80 is $E_{B-V} = 0.43$. This gives the colours of HD 90772, using the values of Cousins and Stoy:

$$(B-V)_o = 0.09 \qquad (U-B)_o = -0.32$$

The corresponding colours from Westerlund's photometry are :

$$(B-V)_o = 0.00 \qquad (U-B)_o = -0.15$$

The first value of $(B-V)_o$ but neither value of $(U-B)_o$ agrees with the intrinsic colours of A supergiants according to Johnson (1963), (1964).

Fernie 2. HD 90706. This star was classified as B3I by Feast et al

(1955), in satisfactory agreement with our estimate of B2Ib. Several UBV measures are collected in Table 10.

Fernie 3. HD 90707. B1III.

This star was found to be variable when used as a local standard. Table 10 contains the observations on ten nights. Several 49 A/mm spectra show a big range in radial velocity. The star may be an eclipsing binary.

Fernie 7. B1:V;ex

This star appears to show the extreme Be characteristics described by Schild (1966). Photo-electric measures show the star is variable; these are collected in Table 10 and were made on nine nights.

The relation between ΔV and $\Delta (U-B)$ is in the opposite sense to that of most of the variable Be stars observed by Feinstein (1968) but this is not unique. Feinstein found that Be stars are systematically redder in (B-V), for given (U-B), than are normal B stars. Schild (1966) found that the extreme Be stars had an apparently intrinsic excess in E_{B-V} of $0^m.15$ on average. Star 7 has an excess in E_{B-V} of $0^m.12$ relative to nearby stars; this may be intrinsic.

Fernie 4. B0.5Ve

This is a mild Be star, with only a filling in of Hβ

4. <u>The Distance Modulus.</u>

The quantities V_o, $(B-V)_o$ and $(U-B)_o$ have been calculated for the

FIGURE 21.

The colour magnitude diagram V_o, $(B-V)_o$ for probable members of IC 2581 showing the standard ZAMS for true distance moduli of 12.4 and 12.0.

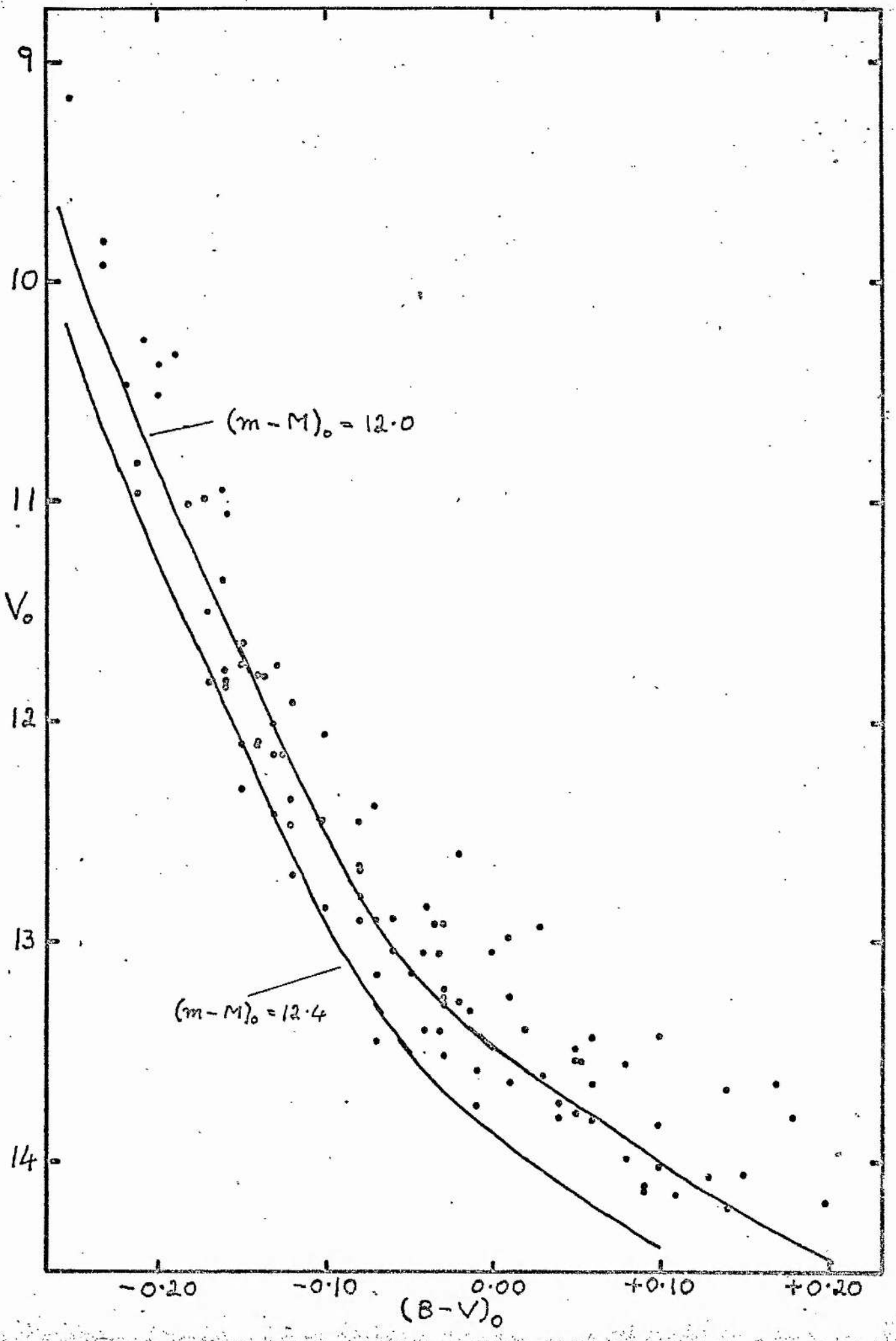
9
10
11
12
13
14
V_o
$(m-M)_o = 12.0$
$(m-M)_o = 12.4$
−0.20
−0.10
0.00
+0.10
+0.20
$(B-V)_o$

probable cluster members from the "Cluster" and "Outer" parts of the field. Johnson's nomogram was used to find $(B-V)_o$ for the brighter stars, while a mean value of $E_{B-V} = 0.42$ was assumed for fainter stars. A mean value of $E_{U-B} = 0.30$ was used to calculate $(U-B)_o$. The reddening of stars 2 and 3 was estimated from the spectral types.

Figure 21 shows two possible fits of the zero age main sequence (Johnson and Iriarte, 1958), (Blaauw, 1963) to the V_o, $(B-V)_o$ diagram of the cluster. Figure 22 gives the same two distance moduli in the V_o, $(U-B)_o$ diagram. Stars from the "Cluster" and "Outer" areas are designated by filled and open circles, respectively. Figure 23 shows the corresponding fits of the evolutionary deviation curve (Johnson, 1960) to the plot of $(V_o - M^o)$ versus V_o, constructed according to Johnson's precepts. The theoretical evolutionary deviation curves of Lindoff (1968) yield a similar result.

No single value of the distance modulus gives a satisfactory fit to the observations. Stars fainter than $V_o = 12.6$, $V = 13.9$ indicate a smaller distance modulus than those brighter than this limit, being too bright or too red to fit the same zero age main sequence. The larger value of the distance modulus, fitting stars brighter than $V = 13.8$, does not permit a satisfactory fit of the evolutionary deviation curve to the brighter stars in the cluster. The smaller value leaves stars with $12.9 < V < 13.9$ above the curve.

There are several possible explanations :

1) The photometry is in error. This would probably be an error in colour rather than in the V magnitudes, to minimise the magnitude of the error. The calibration is by non-members for $V \gtrsim 13.2$; this

FIGURE 22.

The colour magnitude diagram V_0, $(U-B)_0$ for probable members of IC 2581 showing the standard ZAMS for true distance moduli of 12.4 and 12.0.

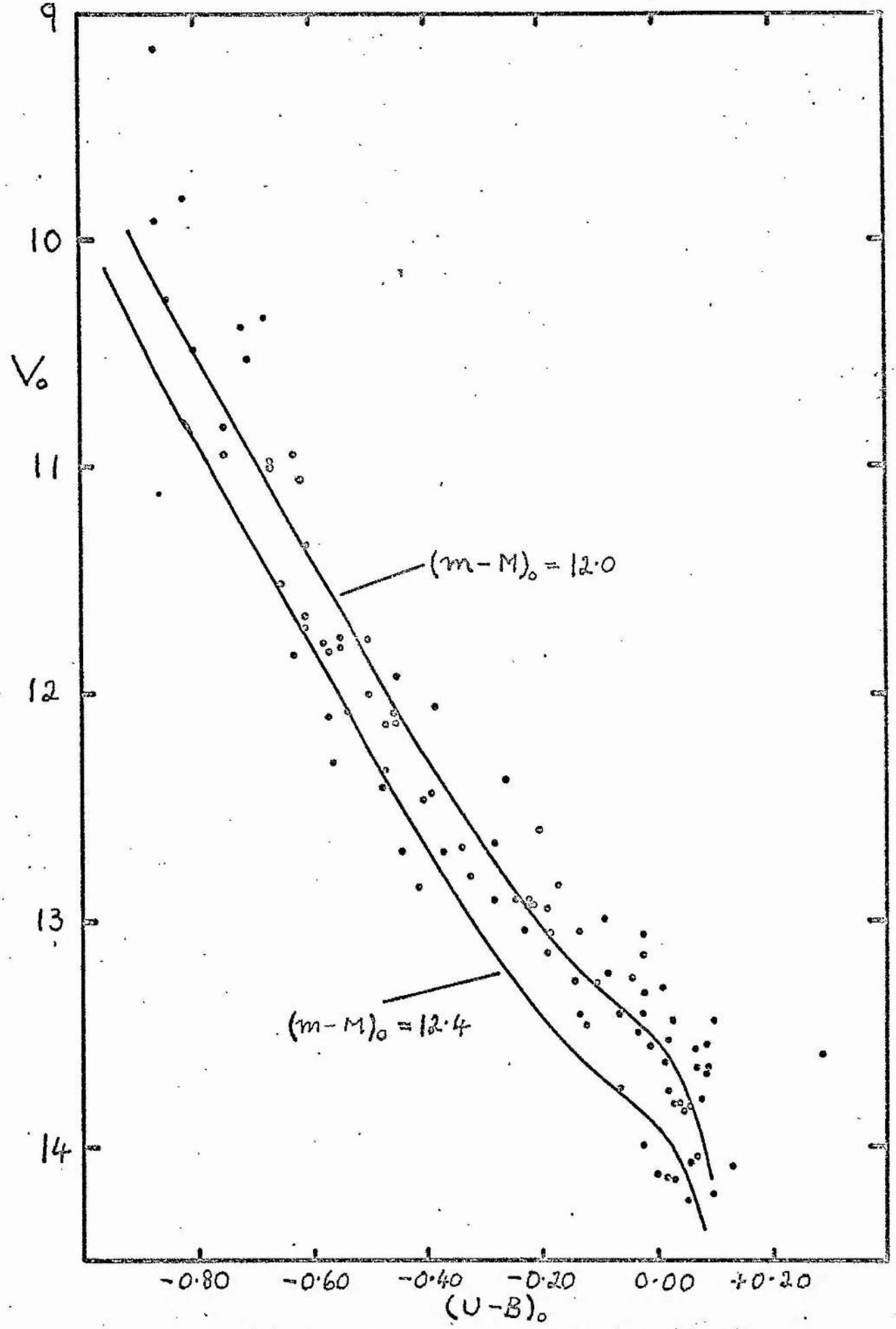
9
10
11
12
13
14
V_0
$(m-M)_0 = 12.0$
$(m-M)_0 = 12.4$
-0.80
-0.60
-0.40
-0.20
0.00
+0.20
$(U-B)_0$

should not lead to any large error in V or B, because the colour equations are well determined and the difference in colour between cluster members and the stars of the photo-electric sequence is small. If the error is at the faint end, we require (B-V) to be too red by $0^m.07$ at V = 15.5 and (U-B) too red by $0^m.15$ at V = 14.5. Such large errors seem unlikely. More complicated magnitude dependent errors, involving a smaller error at a given magnitude, cannot be ruled out. The satisfactory fit of the standard two colour relation shifted along the reddening line to the observed cluster points, the good agreement of the values of E_{B-V} derived from Johnson's nomogram for stars with $V \lesssim 14.2$ and the correct value of the limit to (U-B) at $V \sim 14.9$ argue against the occurrence of large errors in colour. We consider this explanation unlikely.

2) The faint end of the cluster sequence is contaminated by field stars. The cluster membership criterion from the colour magnitude diagram was based on the existence of a sequence in the diagram. It cannot be excluded that field stars could define a spurious sequence, in the absence of sufficient cluster members. This is only likely at the fainter magnitudes, say $V > 14$. These field stars would probably be too bright, as observed. The correct value of the distance modulus would be $\sim 12^m.4$ and the poor fit of the evolutionary deviation curve would remain.

3) The fainter stars fall above the zero age main sequence because they are still contracting and the standard evolutionary deviation curve is wrong. The lower main sequence turn off is then at about $M_V = +0^m.5$, implying a much smaller age than the nuclear age

FIGURE 23.

The evolutionary deviation diagram for IC 2581, with the standard curve fitted for true distance moduli of 12.4 and 12.0. M° is the absolute magnitude which a star of the same $(B-V)_{o}$ as the star of corrected magnitude V_{o} has on the standard ZAMS.

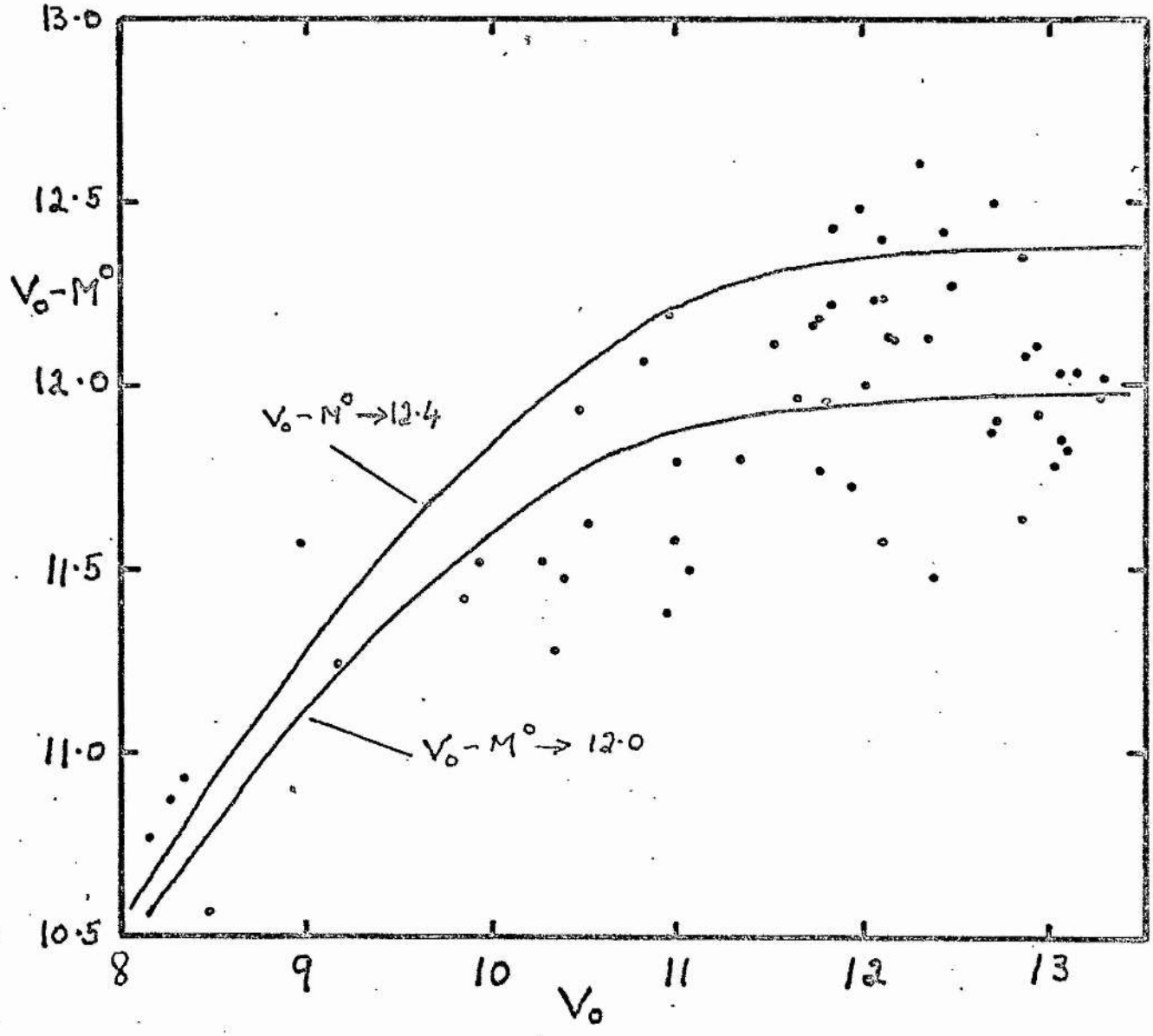
13·0
12·5
12·0
11·5
11·0
10·5
$V_o - M^o$
$V_o - M^o \rightarrow 12.4$
$V_o - M^o \rightarrow 12.0$
8
9
10
11
12
13
V_o

deduced from the bright stars evolving off the main sequence. This double explanation seems unlikely.

4) The standard zero age main sequence is wrong, in the sense that stars with $(B-V)_o \lesssim -0^m.10$ are too bright at a given colour. This would enable one to fit a zero age main sequence with $(m-M)_o = 12.0$. The stars above the value $(V_o-M^o)_{\Lambda}^{=12.0}$ in the evolutionary deviation diagram would be moved down. The stars with $V_o < 11.5$ would probably be moved down as well, but the exact shifts are not readily predicted. The standard evolutionary deviation curve will not be changed very much: Johnson's semi-empirical curve is based on clusters covering a range of ages and is in fair agreement with Lindoff's surve which is based entirely on Iben's theoretical evolutionary tracks.

Arguments given in the next section suggest that an error of this nature in the zero age main sequence is probable. We derive $(m-M)_o=12.0$ by fitting the IC 2581 sequence for $V \gtrsim 14.3$ to the corresponding section of the main sequence of the α Persei cluster, whose distance modulus is taken as 6.06 (Mitchell, 1960).

The distance moduli deduced from the spectral types of the brightest stars are :

a) From the 5 normal stars near the main sequence, Fernie 4, 8, 78, 79 and 80,

$$\overline{(m-M)_o} = 12.4$$

b) From these 5 stars and Fernie 1, 2, 3 and 7,

$$\overline{(m-M)_o} = 12.1$$

This is not inconsistent with a true distance modulus of 12.0, having regard to the uncertainties in spectral classification and the suspected error in the zero age main sequence.

We adopt $(m-M)_o = 12.0$, noting that any value in the possible range of 11.9 to 12.4 would yield essentially the same results in the comparison with theory.

5. The Zero - Age Main Sequence.

The zero age main sequence (ZAMS) is determined by fitting together the supposedly unevolved sections of cluster main sequences to cover the full range of stellar temperatures. Clusters of different ages are required to provide different sections of the main sequence. It is implicitly assumed that there is a unique ZAMS in the colour magnitude diagram. This implies that the chemical composition, insofar as it might affect the position of the ZAMS, is the same for all the clusters studied. We may add the requirement that the initial distribution of stellar rotation with luminosity on the ZAMS be the same in all cases. The sample of clusters used to define the ZAMS is small, however, and it cannot be assumed that these effects have been averaged out.

Accurate photometry of stars of well established membership is available for rather few clusters and the main practical difficulty has been to find a satisfactory overlap between the unevolved sections of main sequence which are taken to define the ZAMS over the corresponding interval of colour. Recent determinations of the ZAMS are

given by Johnson and Iriarte (1958) and by Blaauw (1963). The two determinations agree well; Blaauw has given more details of the derivation and we therefore discuss his work.

The Pleiades fits the α Persei cluster main sequence between $(B-V)_o$ = +0.10 and +0.45, with true distance moduli of 5.55 and 6.15 respectively (elsewhere we have used $(m-M)_o$ = 6.06 for the α Persei cluster, following Mitchell (1960)). The α Persei cluster fits NGC 2362 in the interval $-0.175 < (B-V)_o < 0.00$. The effects of evolution away from the main sequence are said to be apparent for $(B-V)_o < 0.10$ in the Pleiades and $(B-V)_o < -0.175$ in the α Persei cluster. The α Persei cluster is thus supposed to define the ZAMS for $-0.175 < (B-V)_o < +0.45$, extending for $0^m.275$ in $(B-V)_o$ beyond the turn-off point of the Pleiades.

This is at variance with the claim by Eggen (1965) that the α Persei cluster is very similar in stellar content to the Pleiades whose space motion is nearly the same. Additional similarities were pointed out by Kraft (1967). This differences in viewpoint is partly attributable to Blaauw's neglect of reddening in the Pleiades. Johnson and Morgan (1953) found an average reddening $E_{B-V} = 0^m.035$ for 14 brighter stars; we have found an average value of $0^m.03$ from the later photometry by Johnson and Mitchell (1958). Eggen found a slightly larger reddening on the basis of the latter photometry.

We have calculated M_V, $(B-V)_o$ and $(U-B)_o$ for the Pleiades stars, using $(m-M)_o$ = 5.55, correcting (B-V) by the individual values of E_{B-V} deduced using Johnson's nomogram for the brighter stars or by the mean value $E_{B-V} = 0^m.03$ for the fainter stars and correcting (U-B) by the mean value $E_{U-B} = 0^m.02$ for all stars. ~~We use $(m-M)_o = 6.06$,~~

FIGURE 24.

The colour magnitude diagram M_v, $(B-V)_o$ for members of the Pleiades (open circles), the α Persei cluster (crosses) and IC 2581 (filled circles), with distance moduli of 5.55, 6.06 and 12.0 respectively.

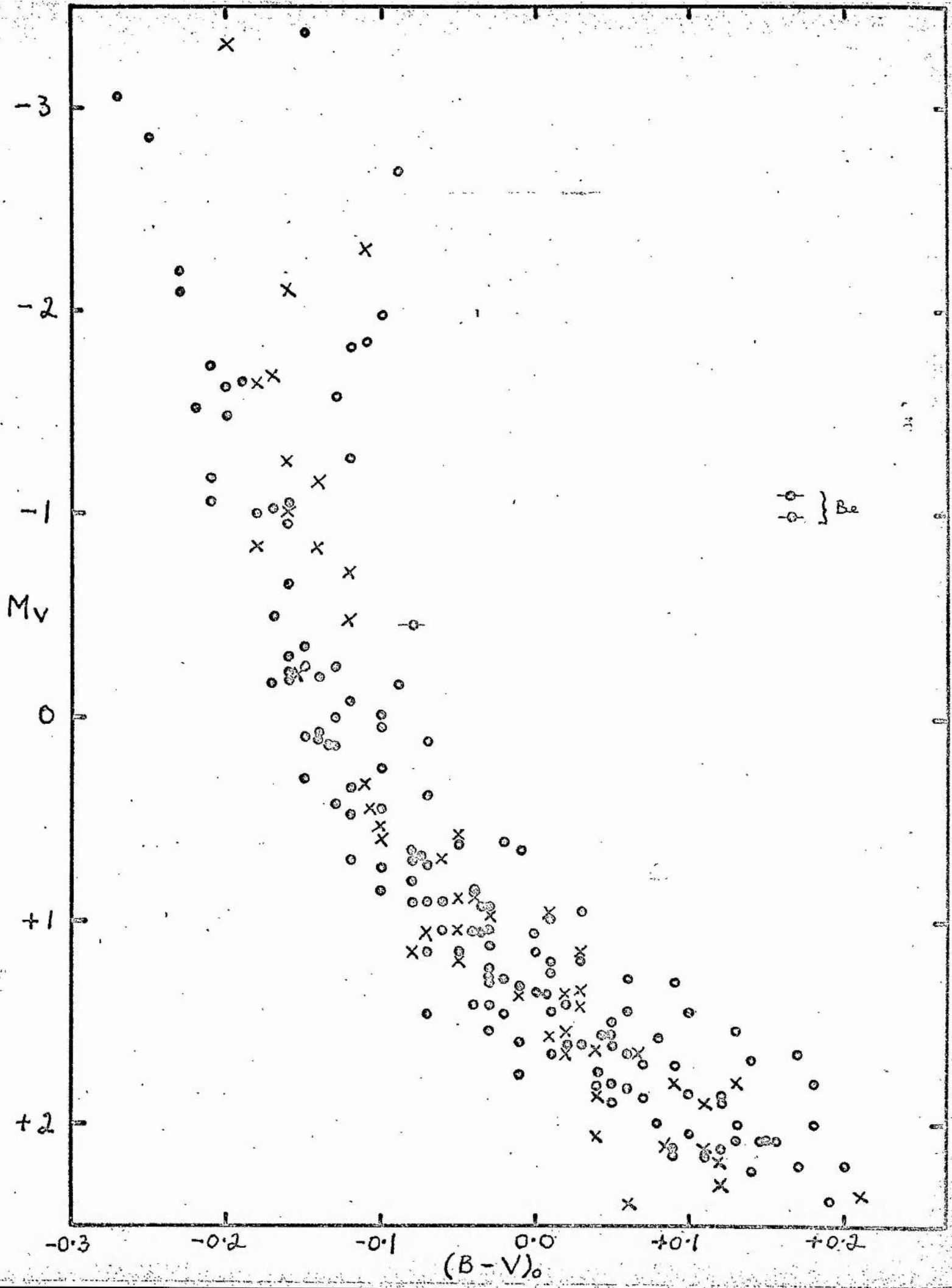
-3
-2
-1
0
+1
+2
M_V
Be
-0·3
-0·2
-0·1
0·0
+0·1
+0·2
$(B-V)_o$

~~$E_{B-V} = 0^m.02$ for all stars.~~ We use $(m - M)_o = 6.06$, $E_{B-V} = 0^m.08$ and $E_{U-B} = 0^m.05$ for the α Persei cluster.

The long and short wave colour magnitude diagrams are shown for these two clusters in Figures 24 and 25, respectively. The bluest stars in the α Persei cluster are bluer than those in the Pleiades by only about $0^m.05$ in $(B-V)_o$ or $0^m.15$ in $(U-B)_o$. The Pleiades departs from the α Persei cluster main sequence at about $M_V = +1.5$, $(B-V)_o = +0.03$, which is bluer than Blaauw found when absorption in the Pleiades was neglected. The turn off point of the α Persei cluster occurs at about $M_V = +1.2$, $(B-V)_o = -0.02$ if it is $0^m.05$ bluer than that of the Pleiades.

Blaauw's turn off point of $M_V \sim -0.6$, $(B-V)_o = -0.175$, $(U-B)_o = -0.60$ for the α Persei cluster is clearly incorrect. The bluest stars in the cluster define a sequence tangent to this colour, whereas he has found the Pleiades turn off point to be nearly $0^m.2$ redder than the bluest stars in the cluster. The assumption of homologous evolutionary tracks and constant - age loci, which seems reasonable for two fairly similar clusters, shows the implausibility of such a situation. We conclude that the ZAMS given by Blaauw is in error for $(B-V)_o \lesssim -0^m.02$.

Johnson and Iriarte used several more clusters to determine the ZAMS, but these were either too young or not observed to sufficiently faint magnitudes to relate to the Pleiades - NGC 2362 fitting. The α Persei cluster is not adequate to fill this wide gap in ages. IC 2581 has also been plotted in Figures 24 and 25, with $(m - M)_o = 12.0$. A cluster of this type would provide an important link between such

FIGURE 25.

The colour magnitude diagram M_V, $(U-B)_o$ for members of the Pleiades (open circles), the α Persei cluster (crosses) and IC 2581 (filled circles) with distance moduli of 5.55, 6.06 and 12.0 respectively.

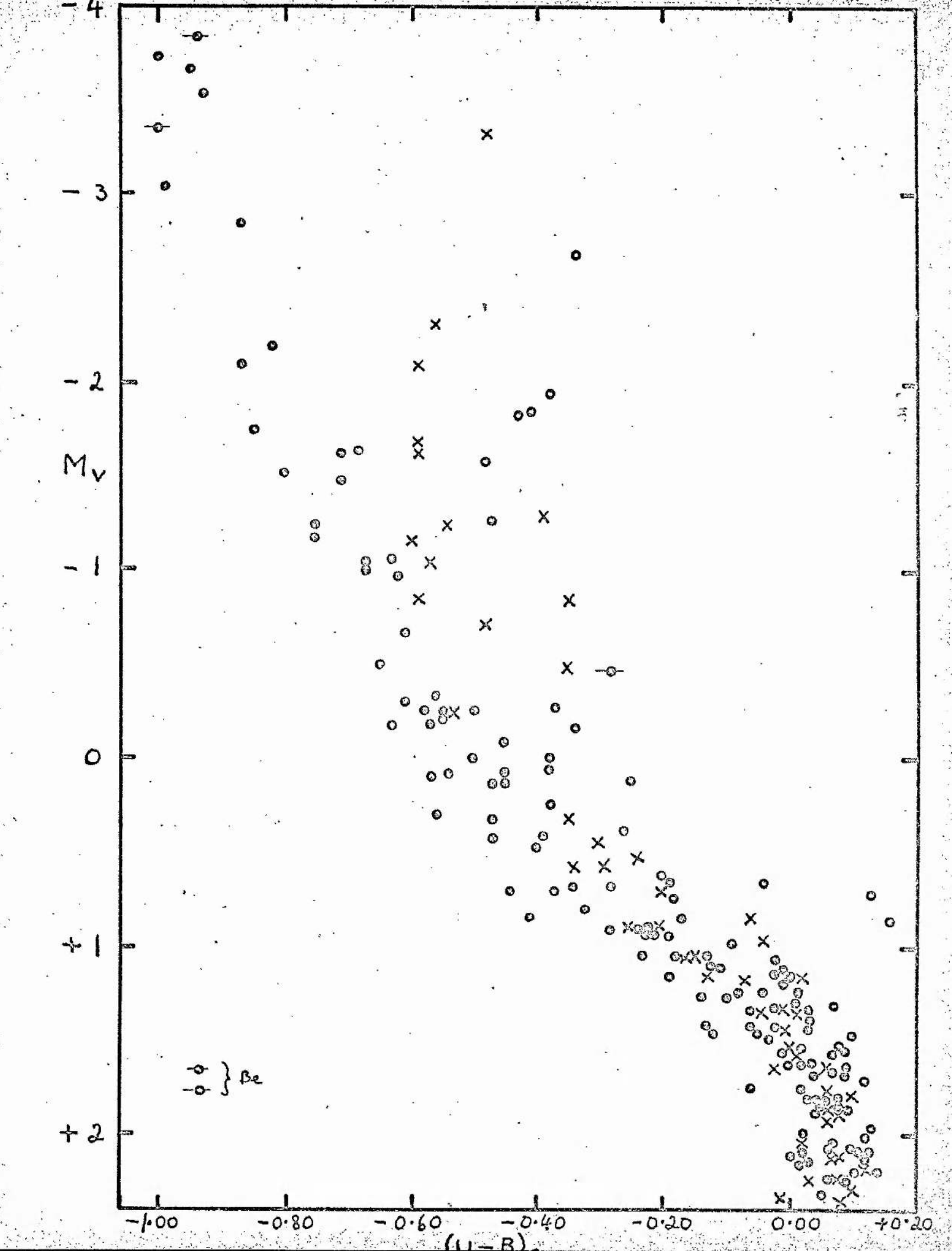
−4
−3
−2
M_V
−1
0
+1
+2
Be
−1·00
−0·80
−0·60
−0·40
−0·20
0·00
+0·20
(U−B)

clusters as the Pleiades and the α Persei cluster on the one hand and NGC 2362 and NGC 6611 on the other. One such cluster is the Double Cluster in Perseus. This was used in early determinations of the ZAMS but Schild's (1965), (1967) demonstration of substantial differences of age and distance between the two clusters and within the surrounding association may disqualify it. Other possibilities are NGC 457, NGC 3293 and NGC 4755 (K Crucis); photometric studies extending to fainter stars are needed and it remains to be seen whether cluster membership may be satisfactorily defined. All these clusters are considerably more populous than IC 2581.

6. A Comparison with Similar Clusters.

The cluster most like IC 2581 is NGC 457, which contains the FoIa star φ Cas. Pesch (1959) has published photo-electric UBV photometry of 78 stars, of which 48 were judged to be members on the basis of position in the colour-magnitude and two colour diagrams. Pesch found a distance modulus of $(m-M)_o = 12.3$ and noted the similarity of the colour magnitude diagram to that of the Perseus Double Cluster.

The long and short wave colour magnitude diagrams of IC 2581 and NGC 457 are shown in Figures 26 and 27. The distance modulus of NGC 457 has been taken as 12.1 in order to secure a fit with IC 2581. NGC 457 contains a red supergiant (M0 Ib - II; $M_V = -5.0$, $(B-V)_o = +1.65$, $(U-B)_o = +2.07$) which is not shown. The stellar content and age of these clusters is very similar. The brightest stars in one have close counterparts in the other, except for the red supergiant in NGC 457 and Fernie 3 (B1 III; EB, SB; $M_V = -5.05$, $(B-V)_o = -0.26$, $(U-B)_o = -1.00$)

FIGURE 26.

The colour magnitude diagram M_v, $(B-V)_o$ for members of IC 2581 (filled circles) and NGC 457 (open circles). The distance moduli are 12.0 and 12.1, respectively.

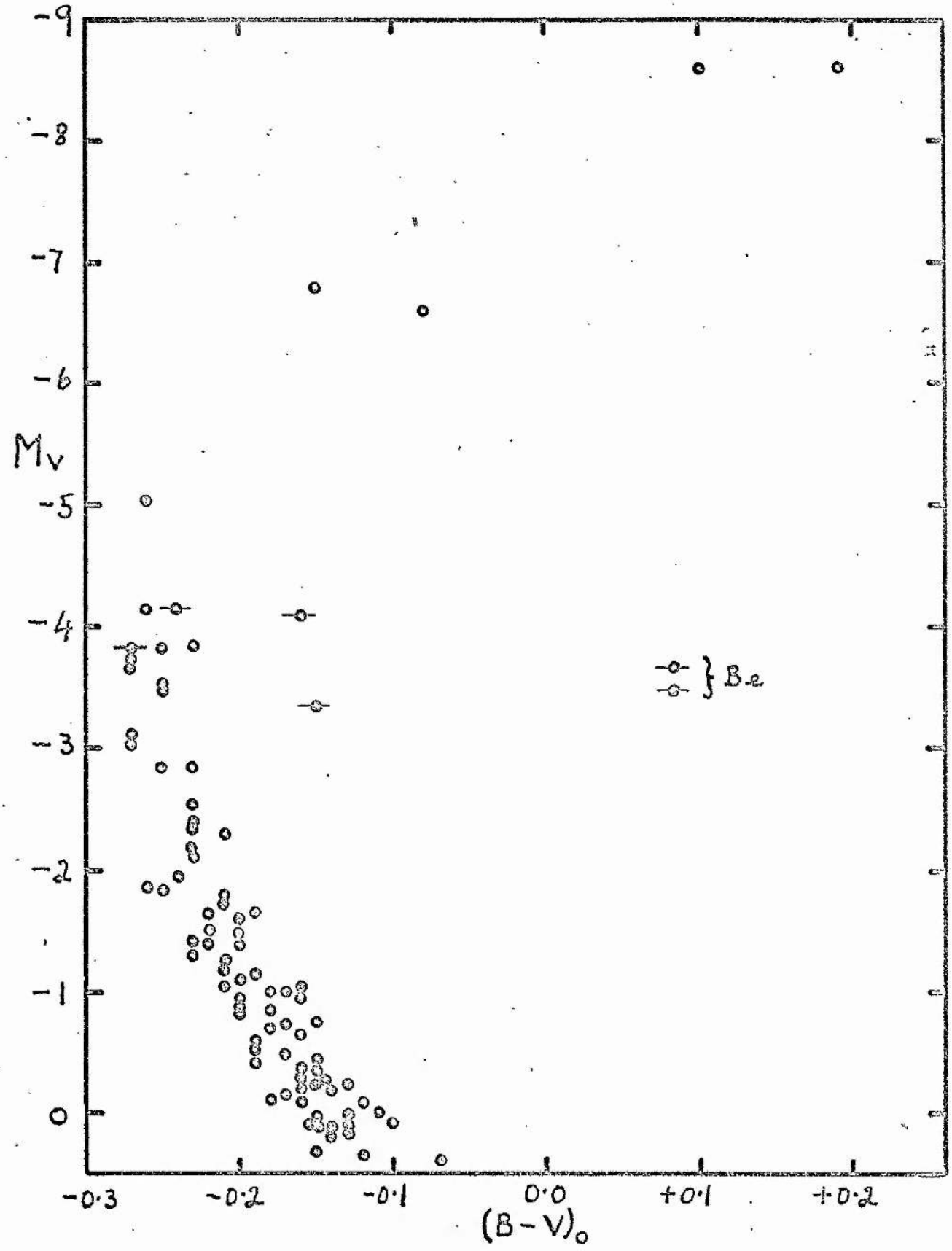
-9
-8
-7
-6
M_V
-5
-4
-3
-2
-1
0
Be
-0·3
-0·2
-0·1
0·0
+0·1
+0·2
$(B-V)_o$

in IC 2581. Two Be stars are known in each cluster. NGC 457 has 39 stars with $M_V < -0.5$, while IC 2581 has 25 stars in this range.

The composite colour magnitude diagram given by Feast (1963) for NGC 4755, NGC 3293 and the Perseus Double Cluster shows similarities. The gap between $M_V = -5$ and -6, to which Feast drew attention, contains no stars in NGC 457 or IC 2581 either. The much larger total population of the three clusters in Feast's diagram shows such features very clearly. Schild's (1965), (1967) finding that χ Persei is older than h Persei and has an age similar to that which we find for IC 2581 and NGC 457 implies that h Persei and other younger objects in the vicinity should be omitted from these comparisons.

The two Be stars in NGC 457 and Fernie 4 in IC 2581 have $M_V \sim -4.1$, while Fernie 7 has $M_V = -3.5$ or -3.9 at its brightest, depending on whether the excess reddening in (B-V) is intrinsic or is the result of additional interstellar absorption. The spectroscopic details are :

2581 - 4	B 0.5 V e	H β em
2581 - 7	B1:V:ex	Light variable
457 - 21	BO:IV:e	Light variable
457 - 39	B1.5(V)pe	Shell.

This is a rather inhomogeneous group of stars.

Schild (1966) found that the Be stars associated with χ Persei fell in two groups :

Extreme Be stars $-3.7 \lesssim M_V \lesssim -5.0$

Ordinary Be stars $-3.2 \lesssim M_V \lesssim -4.6$

(These have been made fainter here by $0^m.3$ in accordance with our treatment of IC 2581).

FIGURE 27.

The colour magnitude diagram M_V, $(U-B)_o$ for members of IC 2581 (filled circles) and NGC 457 (open circles). The distance moduli are 12.0 and 12.1, respectively.

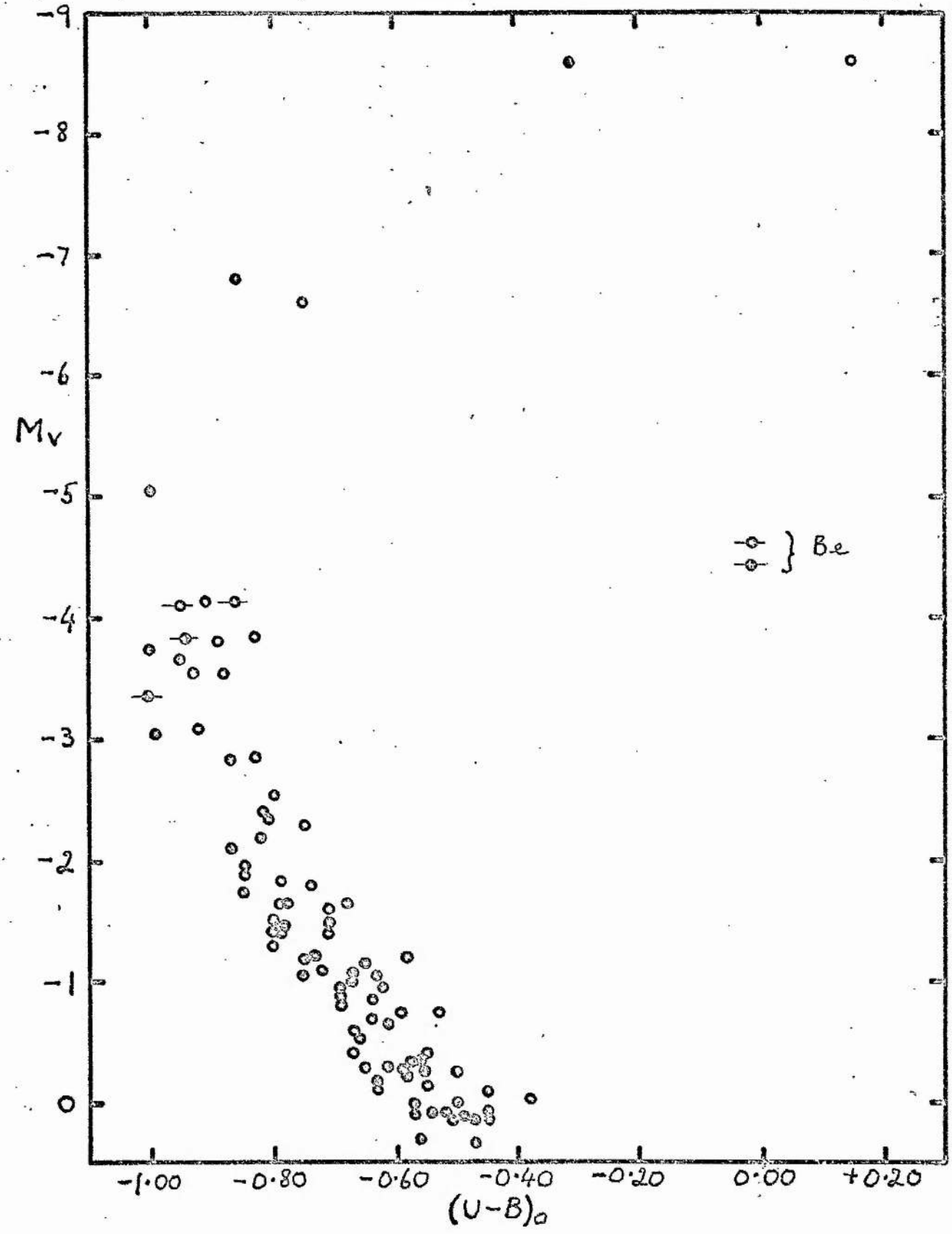
-9
-8
-7
-6
M_V
-5
-4
-3
-2
-1
0
Be
-1·00
-0·80
-0·60
-0·40
-0·20
0·00
+0·20
$(U-B)_o$

Fernie 7 in IC 2581 is relatively faint for an extreme Be star.

7. A Comparison with Stellar Evolution Theory.

Iben (1965a), (1966), (1967) has computed detailed evolutionary tracks for stars of 1.0 to 15.0 $M_\odot$. A B 0.5 V star has a mass of approximately 15 $M_\odot$ (Allen, 1963). If the brightest star near the main sequence of IC 2581 is of 15 $M_\odot$, the age is $\sim 1.2 \times 10^7$ years.

Lindoff (1968) derived synthetic colour magnitude diagrams from the calculations of Iben and others. Comparison with the colour magnitude diagrams of IC 2581 and NGC 457 gives an age of approximately 10^7 years, if Fernie 3 in IC 2581 is a member. The sparseness of the top of the colour magnitude diagram makes comparison difficult.

The B supergiants in IC 2581 (Fernie 2 : B 2.5 I b, $(B-V)_o = -0.15$, $M_{bol} \simeq -8.8$) and NGC 457 (Star 1 : B 6 I b, $(B-V)_o = -0.08$, $M_{bol} \simeq -7.8$) must be stars which have exhausted the hydrogen in their cores. We have used Harris' (1963) table of bolometric correction and log Te as a function of (B-V). Iben's (1966) star of 15 $M_\odot$ is burning helium with M_{bol} near -7.4 at the corresponding temperature. Fernie 2 is brighter than this; if this is the result of a mass larger than 15 $M_\odot$, the age will be less than the 1.1×10^7 years corresponding to the 15 $M_\odot$ model.

Stothers and Chin (1968) discuss the evolution of a 15 $M_\odot$ star treating convection and opacity differently from Iben. They assert that the blue supergiant stage follows a period as an M supergiant. The B supergiant of 15 $M_\odot$ has $M_{bol} \sim -7.6$, very similar to Iben's result. They have not calculated a complete evolutionary track and

no timescale is available. The present observations do not enable us to distinguish between the two possibilities.

The B giant in IC 2581 (Fernie 3 : Bl III, $(B-V)_o = -0.26$, $M_{bol} \sim -7.5$) might be burning hydrogen in a shell, with a corresponding age of 1.05×10^7 years if it has 15 $M_\odot$, but the short duration of that stage renders it improbable, especially as stars of this magnitude and spectral type are quite common in χ Persei and similar clusters (Schild, 1966; Feast, 1963). It is perhaps surprising that the lower edge of the gap at $M_V \sim -5$ should be defined by normal luminosity class III stars, with the Be stars slightly fainter, if the suggestion by Schild (1966), following others, that the extreme Be stars are in a state of rotational instability as the result of gravitational contraction following the exhaustion of hydrogen in the core is correct.

The explanation might be as follows. Iben's (1966) evolutionary track for a star of 15 $M_\odot$ shows little change in bolometric luminosity between the end of hydrogen burning in the core and the onset of helium burning in the core. The surface temperature increases during the stage of gravitational contraction following the exhaustion of hydrogen in the core, then decreases considerably during the short lived hydrogen shell burning stage. The rapid increase of bolometric correction with temperature means that the star may fade slightly in visual magnitude during the stage of gravitational contraction of the core and then brighten rapidly while it burns hydrogen in a shell prior to the onset of helium burning. We might then identify the normal Bl III stars just below the gap with stars about to exhaust the hydrogen in their cores, the slightly fainter Be or extreme Be stars with the stage of

gravitational contraction in the core, the gap in the colour magnitude diagram with the short lived hydrogen shell burning stage and the B type supergiants with the core helium burning stage.

Evolutionary tracks of stars contracting to the main sequence have been calculated by Iben (1965) and by Ezer and Cameron (1967). Stars of $M_V = 2.3$ (corresponding to the faint limit of the observations in IC 2581) have a contraction time of approximately 10^7 years on either theory. We would expect to find stars lying above the main sequence if the photometry were extended by a magnitude or so. If the turn off is smooth, as predicted theoretically, instead of being a sharp break as found in NGC 2264 (Walker, 1956) and in NGC 6530 (Walker, 1967) it may be difficult to distinguish. We cannot exclude the possibility that such an effect is responsible for part of the deviation from the ZAMS.

We conclude that the age of IC 2581 is approximately 10^7 years.

The A-F supergiant stars have $M_{bol} \sim -8.7$, brighter than any of Iben's 15 $M_\odot$ models. They might represent a later stage of evolution. Stothers (1966) has calculated the evolution of a 30 $M_\odot$ star. This has $M_{bol} \sim -9.3$ at the appropriate surface temperature, when its age is only 0.5×10^7 years and it is evolving very rapidly as it exhausts its helium. It seems unlikely that this is appropriate to these stars, though the scarceness of such bright A-F supergiants relative to the B and M supergiants in the other clusters of this age group suggests that it is a short lived evolutionary stage.

It is interesting that these clusters, which are old enough not to be closely involved with the gas clouds from which they presumably formed, contain such bright A-F supergiants. Stars of this type would be of

apparent photographic magnitude near 10.5 in the Large Magellanic Cloud. Early or late type supergiants with larger bolometric corrections would have to be more luminous and hence probably more massive and younger in order to have the same photographic magnitude. This may be one of the reasons for Thackeray's (1967) finding that supergiants of type B3–A5 in the LMC show a smaller concentration within diffuse nebulae than earlier and later type stars in the same brightness range, $m_{pg} < 12.2$. The small discrepancy in the late boundary of spectral type may not be significant.

8. IC 2581 and Galactic Structure.

IC 2581 is at the preceding end of the Carina complex of young clusters and gas clouds (Sher, 1966). The revised distance of 2.5 kpc places it close to the clusters associated with η Carinae, whose distance averages 2.7 kpc. The similar but more populous cluster NGC 3293 lies between the two in galactic longitude, at a distance of 2.6 kpc (Feast, 1958). The removal of IC 2581 from the region between the Sun and the η Carinae complex accentuates the lack of spiral structure marker features in this region; one cannot say whether the arm passes close to the Sun. Sher comments that the appearance of the spiral arms in external galaxies would not lead one to expect that a spiral arm should necessarily be continuous.

9. Conclusions.

IC 2581 contains up to 120 stars brighter than $V = 15.5$, $M_V = +2.3$. These include two supergiants, an eclipsing binary and two Be stars,

one of them variable in light.

$E_{B-V} = 0^m .42$ over most of the cluster.

$(m - M)_o = 12.0$, distance = 2500 pc.

The cluster may be part of the η Carinae complex.

The age is approximately 10^7 years.

SECTION 4.

THE OPEN CLUSTER NGC 6383.

The open cluster NGC 6383 is located at $\alpha = 17^h\ 28^m.2$, $\delta = -32^\circ\ 30'$ (1900), corresponding to $l^{II} = 355^\circ.7$, $b^{II} = +00^\circ.1$. Trumpler (1930a) considered it to contain not more than about 50 stars of magnitudes 10 to 16. He estimated the distance to be 2130 pc. The cluster is dominated by the 5th magnitude O star, HD 159176, which is a double lined binary. Trumpler (1930 b) remarked that the cluster, with an angular diameter of only 5'.5 and containing a few dozen faint stars grouped around a bright central star, was unusual. Magnitudes and colours were determined photographically by Zug (1937).

The first photo-electric study was made by Eggen (1961). He obtained UBV measures of 27 stars brighter than magnitude 14.0 with the Radcliffe 74-inch reflector and the 24-inch refractor at the Cape. These were selected from the brighter stars within 12' of HD 159176 and most lie to the West of that star. He found that stars fainter than V = 12 fell above the zero-age main sequence, as in the young cluster NGC 2264, suggesting that they were still contracting to the main sequence.

The (1965) measured V and (B-V) for 88 stars within 12' of arc of HD 159176 and which were brighter than V = 13.8, using Eggen's photo-electric data to calibrate the prhotgraphic photometry with the Lembang and Mt Stromlo Schmidt telescopes. He used objective prism plates to determine spectral types of many of the stars and searched for stars with H α emission. Eggen's findings were confirmed but there are no

FIGURE 28.

The identification chart for NGC 6383.

74-inch reflector stopped to 44 inches.

Yellow light.

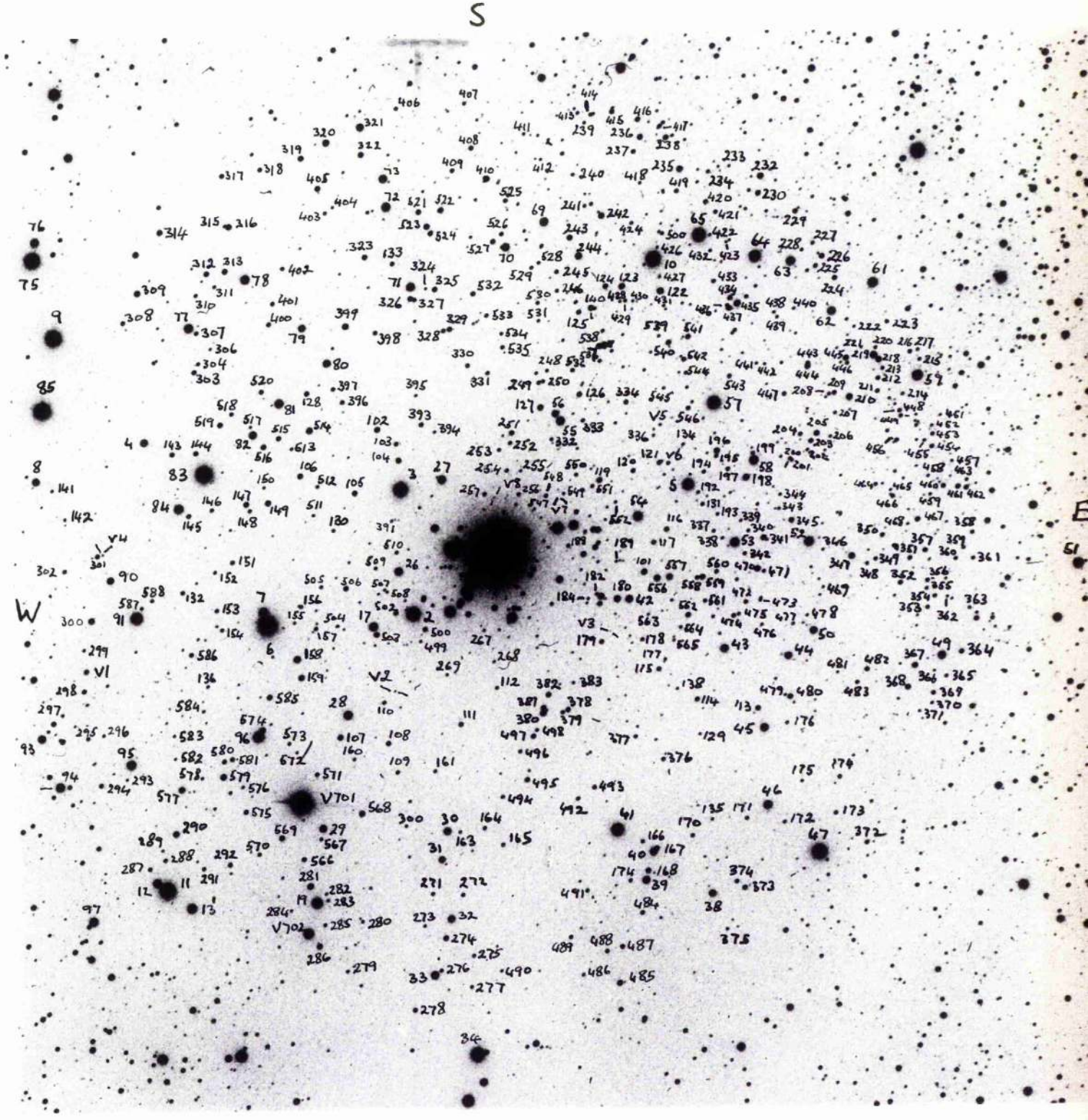
S
W
E
N

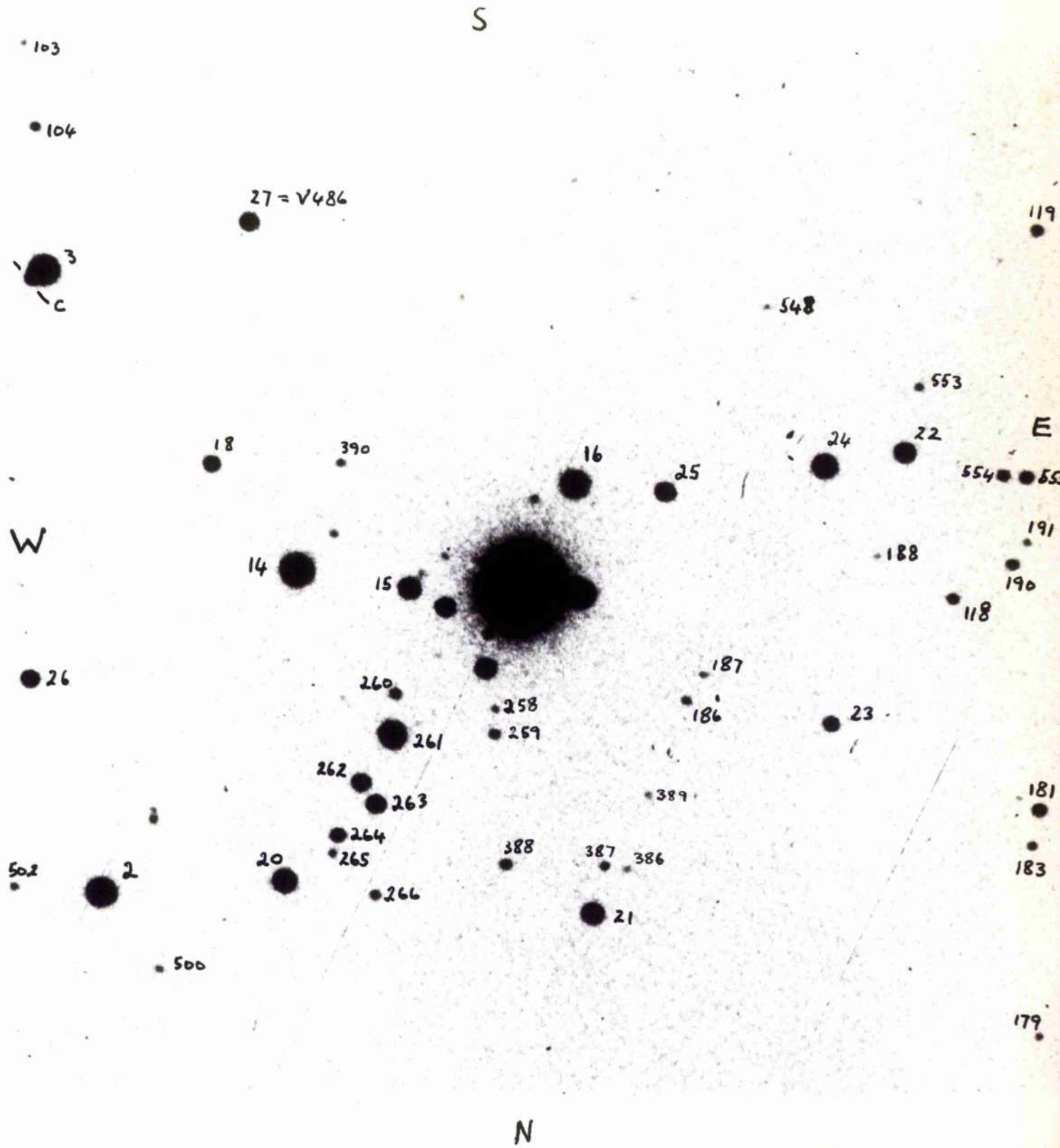
S
103
104
27 = V486
3
C
548
553
E
18
390
16
25
24
22
554
55
W
191
14
188
15
190
118
26
187
260
258
186
23
261
269
262
263
389
181
264
265
388
387
386
183
502
2
20
266
21
500
179
N

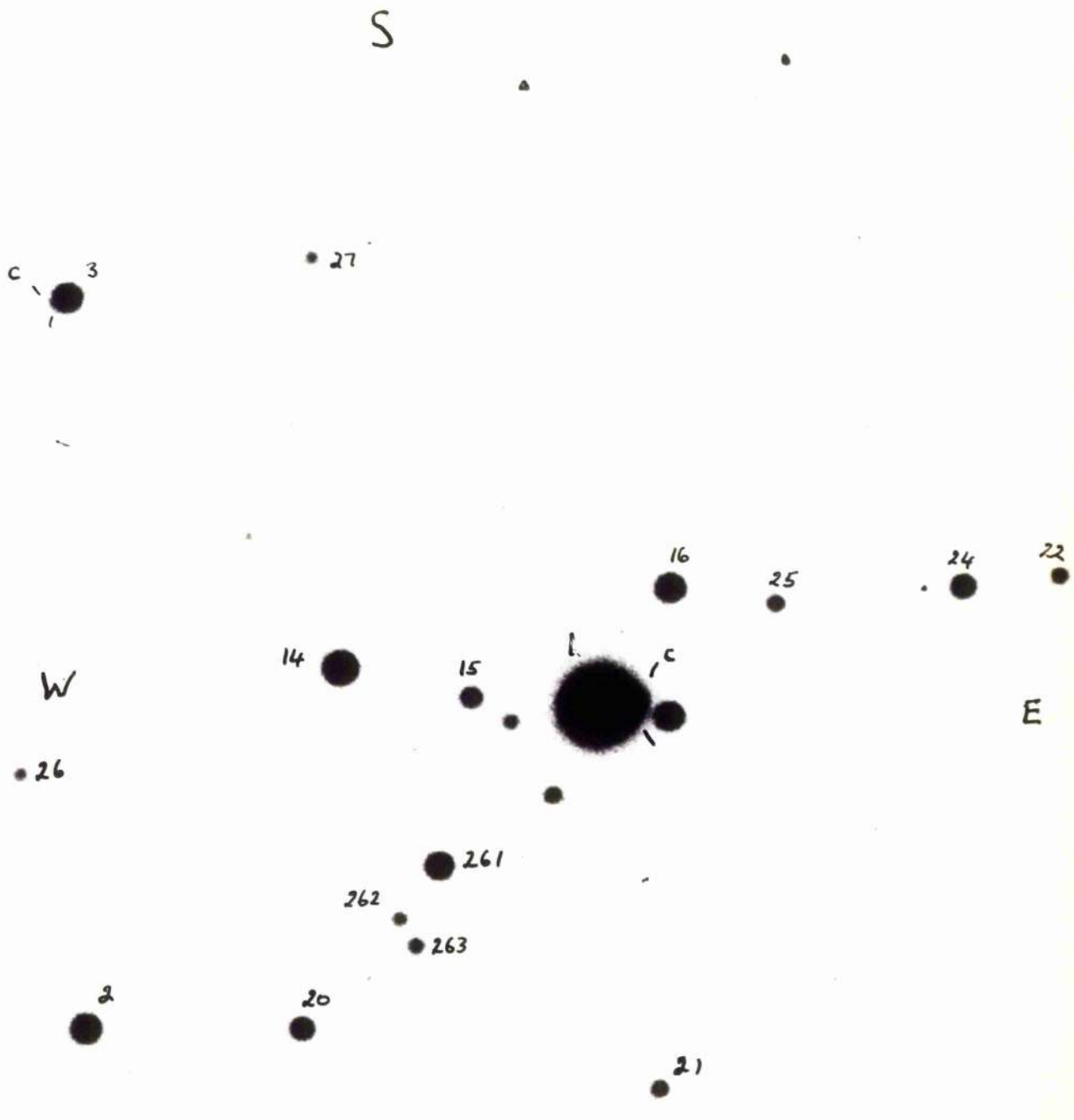
S
C
3
1
27
16
25
24
22
14
15
L
1
C
W
E
26
261
262
263
2
20
21
N

Hα emission stars brighter than V = 16.0, though analogy with NGC 2264 suggested that they should occur at V = 14.8 and fainter. One Be star was found. No decision could be made as to the possible membership of several K and M giant stars in the field.

The different observers do not agree as to the extent of the cluster. The present investigation attempts to determine the cluster membership of the stars on the basis of UBV photometry and the MK spectral types of the brighter stars.

1. Observations.

Table 11 gives the observations for the stars of the photo-electric sequence. Successive columns contain the photo-electric values of V, (B-V) and (U-B); the number of nights on which the star was observed, followed by the number of (U-B) observations if less; the photographic values of V, (B-V) and (U-B). Table 12 contains the photographic measures of V, (B-V) and (U-B) for all the other stars observed. The numbering system of Eggen and The is used for the first 99 stars. The photographic observations are complete within 10' of HD 159176 to the limiting magnitudes V = 18.1 or B = 19.7 and U = 17.9, except that a few stars which are crowded or in the vicinity of a much brighter star have been omitted. All the stars observed are identified on the photograph of the cluster, Fig. 28.

Spectral types of some of the brighter stars were determined from 86 A/mm or 49 A/mm spectra taken with the Cassegrain spectrograph on the 74-inch reflector. These are given in Table 13, whose successive columns contain : Number, HD or HDE number, spectral type, colour excess

E_{B-V}, absolute magnitude M_V from the spectral type and from Graham's (1967) Hβ photometry, respectively, and the corresponding distance moduli. The distance moduli have been calculated assuming the mean reddening of $E_{B-V} = 0^m.35$ in the case of the B type stars which are probable cluster members and the ratio of total to selective absorption is taken as R = 3.0. The relation between absolute magnitude and MK spectral type has been taken from Blaauw (1963); that between spectral type and intrinsic colour is from Johnson (1963), (1964).

2. Cluster Membership.

The spectral types show that several stars are non-members. Stars 3, 57 and 85 are foreground dwarf stars, as suspected by The. Star 9 is definitely a foreground object and, on the basis of one 86 A/mm plate, has a high velocity. Star 11 also appears to be of too low luminosity to be a member and like the first three is less reddened than the B type stars. Star 34 seems unlikely to be a member.

Three stars have spectroscopic distance moduli greater than those of the other B stars and greater than the photometric distance modulus of the cluster. Star 47 is of spectral type A3II; its relation to the cluster is uncertain. Stars 2 and 6 have luminosity Class IV and III - IV, respectively. Stars with luminosity classes which would place them above the main sequence appear to belong to the main sequences of NGC 6530 (Hiltner et al, 1965) and NGC 2264 (Morgan et al, 1965). These stars in NGC 6530 at least have very strong H lines, while the two in NGC 6383 have the relatively sharp H lines appropriate to the luminosity class. We do not expect to find stars appreciably beyond

the cluster which have not suffered considerable additional reddening; these two stars have the same reddening as the rest and their position in the colour magnitude diagram is normal, so we regard them as members.

Star 75 is about $0^m.1$ redder in (B-V) than would be expected from its spectral class and the mean reddening. It lies more than 10' from HD 159176 and it is possible that the absorption is greater; Roslund (1966 b) discovered such variations with position in a similar field nearby. Feinstein (1968) found that Be stars may be redder than normal B stars by about this amount, so the effect may be intrinsic.

All the stars with ultraviolet photometry are plotted in the two-colour diagram, Figure 29. The colours of the bluest stars are well represented by shifting the normal locus of intrinsic colours (Johnson, 1963) by $E_{B-V} = 0.35$, $E_{U-B} = 0.25$. This reddening agrees well with the values of $E_{B-V} = 0.36$, $E_{U-B} = 0.29$ deduced from the spectral types of probable cluster members.

We regard stars lying close to this line as possible cluster members. This line has $(U-B) \sim +0.40$ at $(B-V) \sim +0.50$; the stars with $(U-B) \lesssim +0.20$ are assumed to be foreground stars which are less heavily reddened. The presumed cluster stars merge with those of the less reddened field near $(B-V) = +0.70$. All stars with $V < 16.0$, $(B-V) \lesssim 1.0$ and which lie near this line are plotted as filled circles in the colour magnitude diagram, Fig. 30. The limit in colour was imposed because of increasing confusion with the field stars. There is only slight concentration of stars near the intrinsic line shifted for $E_{B-V} = 0.35$.

This sample of 'cluster' stars must be contaminated increasingly

FIGURE 29.

The two colour diagram of NGC 6383. The standard relationship for dwarf stars has been shifted for reddening $E_{B-V} = 0.35$, $E_{U-B} = 0.25$.

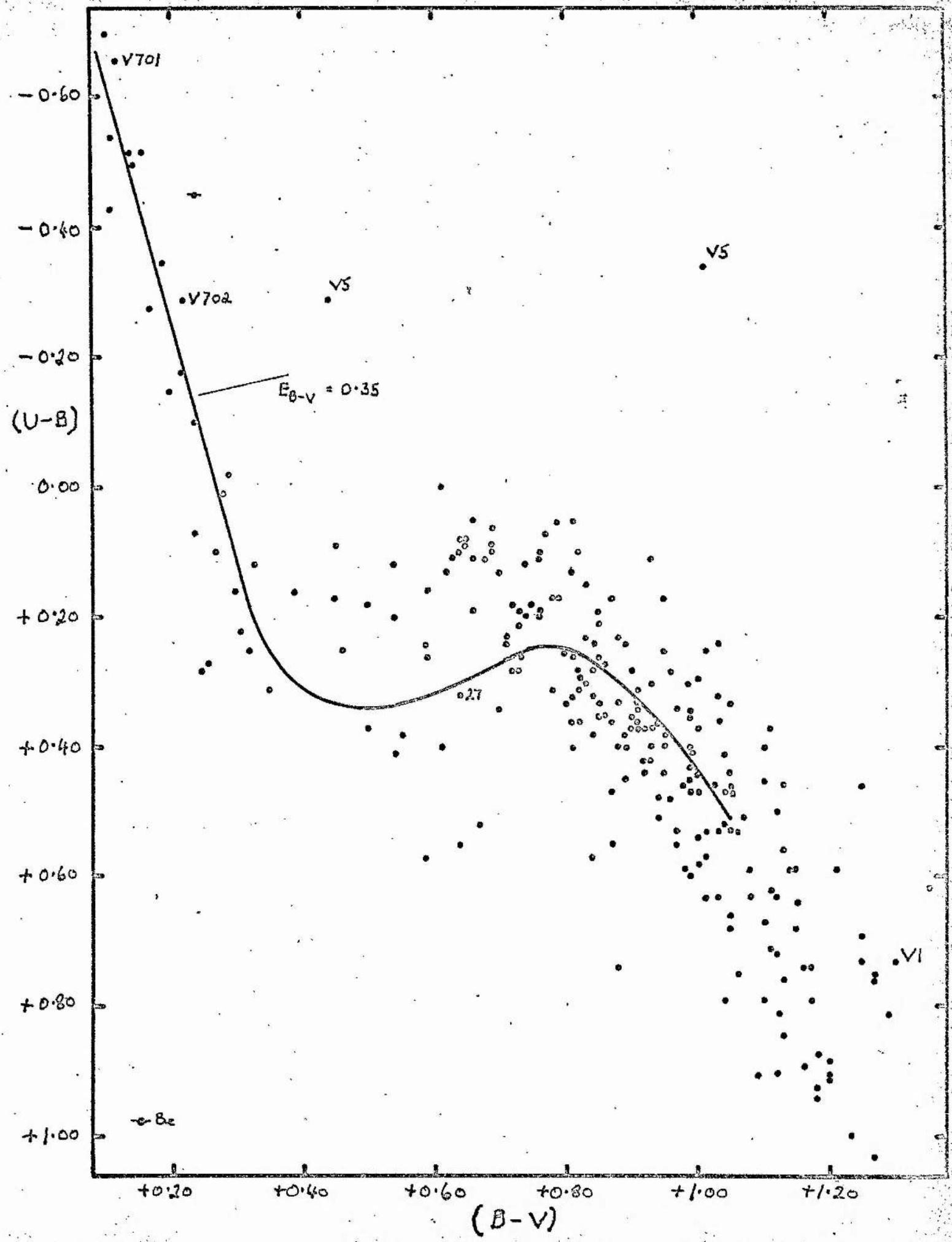
V701
V702
V5
V5
V1
E_{B-V} = 0·35
27
Be
−0·60
−0·40
−0·20
0·00
+0·20
+0·40
+0·60
+0·80
+1·00
(U−B)
+0·20
+0·40
+0·60
+0·80
+1·00
+1·20
(B−V)

by field stars at the fainter magnitudes. The surface density of B stars is about seven times that in Roslund's (1964) field, part of which was regarded as an association by The (1961). There seems no doubt that most of the B stars are members of a cluster, but it cannot be excluded that the break from the zero age main sequence near V = 12.8 is the result of a deficiency of fainter stars in the cluster.

We have eliminated several foreground stars from the colour magnitude diagrams of Eggen and The, but it is evidently impossible to eliminate all the field stars on the basis of UBV photometry alone.

The stars we regard as possible members are distributed widely over the field; they are concentrated along the direction of the star chains near HD 159176, while the NNE side of the field contains relatively few such stars.

The nuclear region of the cluster shows a well defined, though sparse, sequence in the colour magnitude diagram for $V < 13$; there is a deficiency of stars with $13.0 < V < 14.5$ and the membership of fainter stars is problematical, especially as the high density background zone (Section 3) extends as far as the nucleus.

3. The Colour - Magnitude Diagram.

The magnitudes of HD 159176 and V 701 Sco (at maximum) have been increased by $0^m.6$ in Fig. 30 to allow for their composite nature.

There is a well marked sequence to about V = 12.8, with a deficiency of stars near the zero age main sequence for the next two magnitudes. The cluster members deduced from the two colour diagram fall above the main sequence in this region and may be contracting stars.

FIGURE 30.

The colour magnitude diagram V, (B-V) for the NGC 6383 field. Stars which lie near the intrinsic line shifted for a reddening of $E_{B-V} = 0.35$ in the two colour diagram are denoted by filled circles.

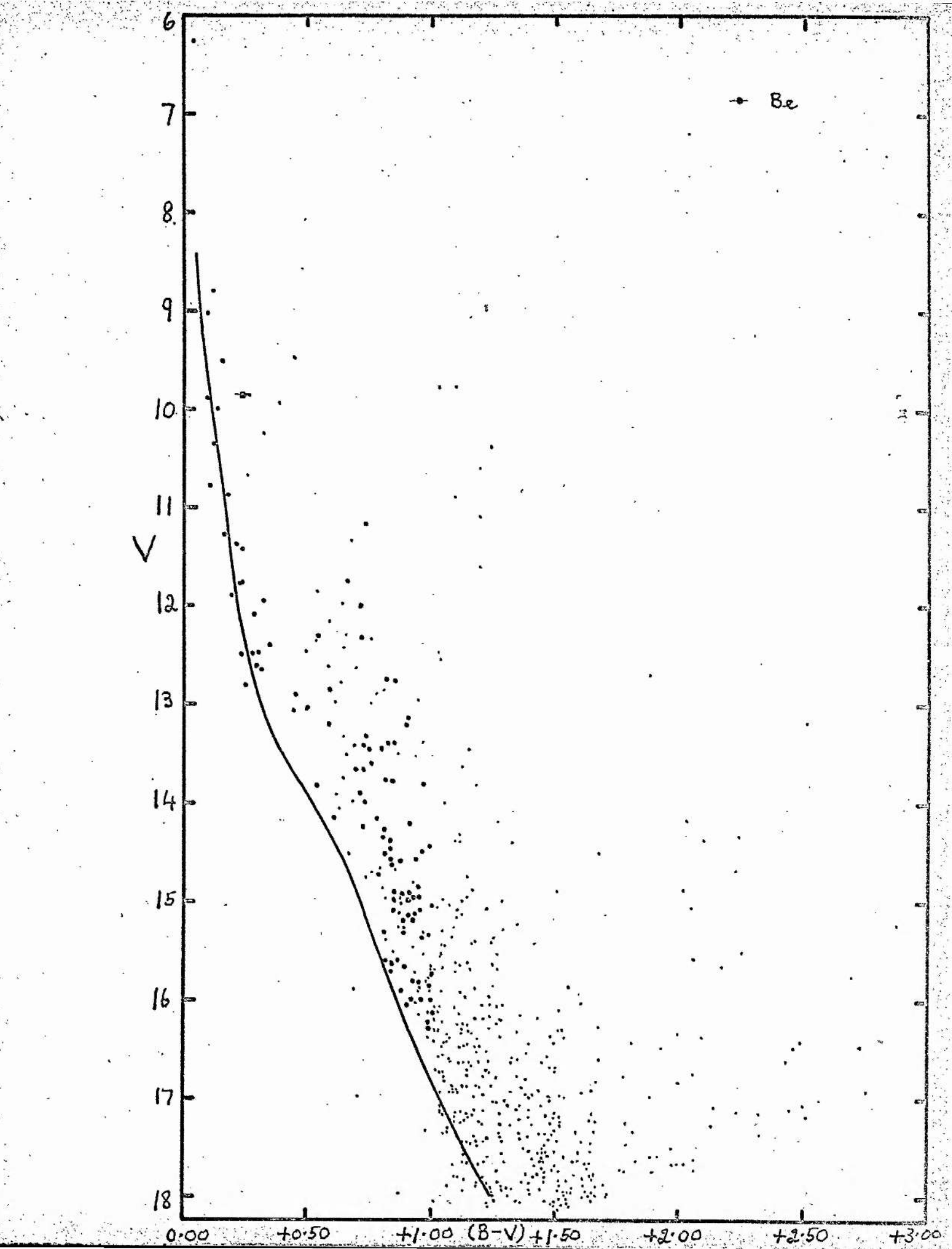
6
7
8
9
10
11
12
13
14
15
16
17
18
V
Be
0·00
+0·50
+1·00
(B-V)
+1·50
+2·00
+2·50
+3·00

The zero age main sequence (Johnson, 1963) has been fitted to the stars brighter than V = 12.8, using $E_{B-V} = 0^m.35$ and the 'normal' ratio of total to selective absorption, R = 3.0. This yields a true distance modulus of $10^m.5$. The corresponding moduli from spectral classification of the brighter stars and from Graham's (1967) Hβ photometry are $11^m.0$ and $10^m.7$, respectively. We adopt $10^m.6$ as the best value.

There are again stars near the zero age main sequence at fainter magnitudes; that is, the ZAMS plotted with $(m-M)_o = 10^m.6$, $E_{B-V} = 0^m.35$ defines the lower envelope in the colour magnitude diagram. This implies that interstellar absorption sets in at the distance of the cluster.

Examination of the Palomar Sky Atlas shows that the cluster lies in the great rift which divides the Milky Way at this longitude. A spur of higher star density extends from the South side of the rift and crosses it at this point; the centre and N and W sides of the field are in an area of relatively low density, while the high density area extends over the SE quadrant towards the centre. This is especially marked on infra red plates, which show the high density area reaching the centre of the cluster. The excess density is contributed by stars which are about $0^m.15$ redder, at given V, than those in the rest of the field. It seems likely that these are more distant stars than those of the cluster and that they are seen through a thin patch in the dense dust clouds which divide the Milky Way.

4. Variable Stars.

Three known variable stars lie in the field. They are

V 701 Sco. This is a contact binary with a period of 0.76 days. (Kukarkin et al, 1958), (Eggen, 1961), (Eggen, 1965a). Three photo-electric observations are given in Table 14; all were made, by chance, when the star was relatively faint. We assume Eggen's (1961) brightest measure represents the total light of the two stars and add $0^m.6$ to give the magnitude of a single component. Spectra at 86 A/mm and 49 A/mm show very broad shallow lines, with no sign of doubling.

V 702 Sco. Photographic observations of this suspected eclipsing star of unknown period (Plaut, 1948) are presented in Table 14. It was observed while coming out of eclipse on the night of 21 June, 1966. The magnitudes represent an average over the exposure and are correspondingly uncertain.

V 486 Sco = 27. Swope (1939) found an amplitude of $1^m.2$ in blue light. The star was usually at maximum and the period could not be established. The photo-electric and photographic observations in Table 14 show only small variations.

These three bright variables are all probable cluster members on the basis of the photometry.

Several new variables were discovered during the present investigation :

VI. Photographic observations in Table 14 show an amplitude of about two magnitudes. The (B-V) colour seems almost constant.

V6. This star is redder when faint. Table 14.

130 Stands off on some plots of iris readings on plate pairs. It deviated from the iris curves and was not used as a standard. Possibly variable.

V9. Red. Possibly variable.

V2, V3, V4, V5, V7 and V8 are noticeably bluer than most stars of similar magnitude. The variability is most pronounced in the blue and ultraviolet. Noticeable changes may occur in 24 hours. Some observations are collected in Table 14. V5, the only one bright enough for satisfactory measurement, has a very unusual colour. It cannot be excluded that this is a reddened background B star. It is unlikely that the whole group could consist of such stars, because they avoid the dense region of the star field, where the absorption is least. Their concentration near HD 159176 and in the 'cluster' part of the field suggests that they are cluster members. They may be T Tauri-like stars; their presence is consistent with The's finding that there are no Hα emission stars brighter than V = 16.0. The infra red plates show that these stars are not very red, in accordance with the finding by Blanco and Grant (1959) for Walker's (1957) variables in NGC 6530.

V4 is the S member of a close pair just to the E of 301.

5. The Nebula.

HD 159176 is near the centre of a roughly circular emission nebula of diameter 2° and is probably the principal exciting star (Sharpless, 1960). Sharpless described the nebula as amorphous and of intermediate brightness. It is much less intense than the nebulae associated with NGC 6530 and NGC 6611. There are intruding 'elephant trunk' dark nebulae at the NW end and the Palomar Sky Atlas red print shows a mottled structure. The cluster is seen projected on a region whose surface brightness is below average. Variations in the surface brightness of the nebula are partially correlated with the overall

star density, whose fluctuations are not solely attributable to patchiness in the dust clouds beyond the cluster.

Dieter (1967) found from measures of the hydrogen recombination line 158α that the radial velocity of the nebula is -8.8 ± 1.9 km S^{-1}, in fair agreement with Trumpler's (1968) velocity of -2.5 km S^{-1} for the cluster. The central star alone has a velocity of -4 km S^{-1} (Trumpler 1930 b) but the radial velocities of O stars may differ appreciably from those of the clusters to which they belong (Trumpler, 1935).

Interstellar lines in the spectrum of HD 159176 have been studied at high dispersion by Adams (1949) and by Buscombe and Kennedy (1968). They find two components in the CaII K line, with velocities -31.7, -33 and -5.1, -7 km S^{-1} respectively. The violet component has an unexpectedly large velocity for a galactic longitude near 0°. It may be that this has the same origin as the negative velocity shifts of interstellar lines in the spectra of OB stars in several associations in the Perseus arm (Munch, 1965) and in the young cluster IC 2944 in Centaurus (Thackeray and Wesselink, 1965). These velocity shifts, with the gas having a velocity 10 or 20 km S^{-1} more negative than the stars, were taken to show that the radiation from hot stars in the associations had caused the gas to expand away from the centre. Rickard (1968) has suggested that the anomalous velocities in the Perseus arm indicate a much larger scale expansion, however. If the nebula surrounding NGC 6383 had been expanding at a uniform rate of 25 km/sec relative to the cluster, it would have reached its present diameter in 8×10^5 years.

6. Relation to Neighbouring Objects.

Roslund (1964, 1966a, 1966b) has studied early type stars in a field centred on $l^{II} = 352^{\circ}.1$, $b^{II} = 2^{\circ}.3$. This lies in the Rift and Roslund found that the stars with $M_V - 2.5$ were concentrated at a distance modulus of $10^{m}.6$, corresponding to 1300 pc. The space density of all stars is roughly constant to this distance and then falls off abruptly, presumably on account of the dust clouds.

NGC 6383, at $l^{II} = 355^{\circ}.7$, $b^{II} = +00^{\circ}.1$, has a distance modulus of $10^{m}.6$ and heavy obscuration sets in just behind it. Another young cluster, NGC 6530 at $l^{II} = 006^{\circ}.1$, $b^{II} = -01^{\circ}.4$, has a distance modulus of $10^{m}.7$, and it too has a dust cloud beyond. (Walker, 1957), (Walker, 1961a).

These three objects define a section of the Sagittarius arm, 1300 pc nearer the centre of the Galaxy than the Sun in this direction. The dust clouds behind them may be analogous to the dust lanes seen on the inner side of the spiral arms in other galaxies, as Roslund (1966 b) pointed out. The Rift has an angular width of approximately 3°, corresponding to 70 pc at a distance of 1300 pc.

7. Comparison with Other Young Clusters.

Several very young clusters, containing O stars, emission nebulae and contracting stars, have been studied photometrically or spectroscopically. These include NGC 2264 (Walker, 1956), NGC 6530 (Walker, 1957), NGC 6611 (Walker, 1961 b), IC 5146 (Walker, 1959), IC 2944 (Thackeray and Wesselink, 1965) and IC 1805 (Underhill, 1967), (Vasilevskis et al, 1965 a).

Figure 31 shows the colour magnitude diagrams for NGC 6383 (filled circles) and NGC 2264 (open circles), plotted assuming that $(m-M)_o = 10^m.6$, $E_{B-V} = 0^m.35$ and $(m - M)_o = 9^m.5$, $E_{B-V} = 0^m.08$ respectively. The data for NGC 2264 are from Walker (1956), excluding stars whose membership probability is less than 0.5 (Vasilevskis et al, 1965b) but including a few stars of high probability which were not observed by Walker.

The two diagrams are rather similar: in particular the lower main sequence turn-off occurs at nearly the same absolute magnitude in each case. The fainter stars deviate more from the zero age main sequence in NGC 2264 and the distribution along the sequence is also different. The difference becomes marked below $M_V = +2$, where the membership in NGC 6383 becomes very uncertain.

NGC 6530 differs from both these clusters in containing stars as red as $(B-V)_o = 1.0$ at $M_V \sim +0.5$, while they have none redder than $(B-V)_o = 0.5$ at this magnitude. The NGC 6383 field does not contain such red stars as NGC 6530 does at a given magnitude.

Table 15 contains the following data, where available, for several young clusters : Earliest spectral type present, number of O stars, number of stars earlier than A0, number of faint variable stars detected on the basis of a few plates only (as in NGC 6383) and the colour $(B-V)_o$ at which the contraction sequence reaches the main sequence.

NGC 6383 is one of the poorest of these clusters. Only IC 5146 has fewer early type stars but it probably has more faint variable stars (this last quantity is the least certain of those tabulated).

The question of membership of faint stars in these rather loose clusters is still only partly resolved. We have seen that the fainter

FIGURE 31.

The colour magnitude diagram M_V, $(B-V)_o$ for NGC 6383 (filled circles) and NGC 2264 (open circles). The distance moduli are 10.6 and 9.5, respectively.

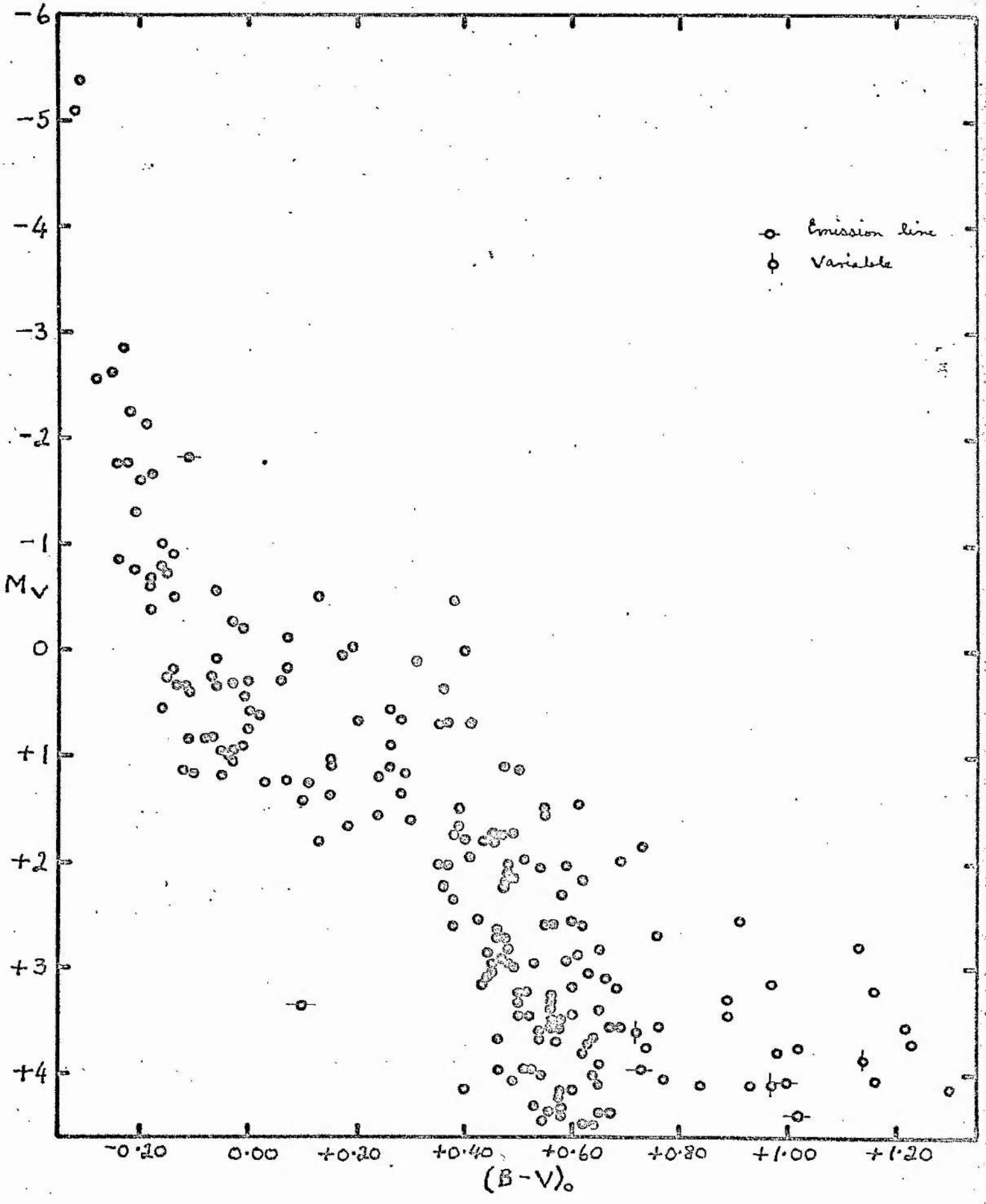
Emission line
Variable
-6
-5
-4
-3
-2
-1
0
+1
+2
+3
+4
M_V
-0·20
0·00
+0·20
+0·40
+0·60
+0·80
+1·00
+1·20
$(B-V)_o$

stars of NGC 6383 are lost in the general field in spite of the low star density. It is the only cluster for which observations are reasonably complete, a consequence of the relative faintness of the emission nebula. The colour magnitude arrays presented by Walker are incomplete at the fainter magnitudes. He has usually attempted to observe a well marked clustering which was not too badly affected by nebulosity. Dust clouds beyond the cluster are supposed to eliminate the background stars, while the foreground stars do not swamp the cluster.

The latter point was questioned by Underhill (1960) in the case of NGC 2264 but appears to have been settled in Walker's favour by the proper motion survey of Vasilevskis et al (1965 b), which showed many fewer field stars than Underhill had predicted from an extrapolation of the star density near the Sun. NGC 2264 is the nearest of the clusters studied by Walker and may be the most favourably situated in this respect.

The (1960) drew attention to the absence of clustering among stars fainter than V = 12.0 in NGC 6530. He found similar colour magnitude diagrams for the cluster region and neighbouring fields of differing obscuration, except for the bright blue stars in the cluster. (The main excess of stars in the 'clear' high density region of NGC 6383 occurs fainter than V = 16, so that there is little difference between the colour magnitude arrays of 'clear' and 'obscured' areas at brighter magnitudes). He estimated the extinction by the background cloud as about $2^{m}.2$ and suggested that some of Walker's stars above the main sequence were reddened background stars of early type. The lack of

stars with large ultraviolet excesses means that none of the reddened stars are earlier than about B8 (The), which is rather surprising. The two colour diagram of NGC 6383 is very similar; it seems preferable to attribute the scatter for the redder stars to differences in absorption among stars of later type. Walker (1961 a) obtained spectral types for eleven of these stars in NGC 6530 and found only one which could be a reddened early type star, though the classification was not accurate enough to distinguish between reddened possible cluster members and unreddened foreground stars.

The possibility that these clusters contained yellow giant stars which could be evolved members of an earlier generation was first raised by Walker (1956). He found 5 yellow giants in the NGC 2264 field. Radial velocity variations made it difficult to decide whether 3 of them were members (Herbig, 1958), (Underhill, 1958). Herbig considered 4 to be possible members. Vasilevskis et al (1965 b) obtained proper motions for 2 of the giants, which turned out to be non-members. Walker (1959) found one yellow giant whose spectroscopic absolute magnitude was consistent with membership in IC 5146. The spectroscopic luminosities or the reddening show that 2 yellow giants in NGC 6530 (Walker, 1961 a), 3 in NGC 6611 (Walker, 1961 b) and 3 in NGC 6383 are not members of these clusters. The case for the presence of evolved yellow giants in these young clusters is weak.

8. Discussion.

Iben (1965) and Ezer and Cameron (1967) have published detailed evolutionary tracks for stars contracting to the main sequence. The

comparison of theory and observation uses the relation between effective temperature and bolometric correction and (B-V), as found for normal stars, to calculate log T_e and log L, respectively, for the observed stars. The lower turn-off point of the main sequence in NGC 6383 occurs at

$$M_V = 1^m.2 \qquad (B-V)_o = -0.05$$

Eggen's (1965) tabulation then yields a bolometric magnitude + $1^m.0$ and log T_e = 4.01. The theoretical contraction time is approximately 5×10^6 years. The scarcity of bright stars and the recognition of the two brightest as rather close binaries precludes an estimation of the age from the evolution of stars off the main sequence.

Penston (1964) and Iben and Talbot (1966) have attempted to carry the comparison with theory a stage further by assigning ages to indidual stars on the basis of their position in the colour - magnitude diagram. Iben and Talbot regarded the scatter in the diagram as real and deduced a time dependence of the rate of star formation in NGC 2264 and NGC 6530.

There are several objections to this procedure :

1. The faint variable stars, which are probably T Tauri stars or related objects, have both line and continuous emission which affect the (B-V) colour and hence the deduced log T_e. (Smak, 1964), (Aveni, 1966), (Herbig, 1967).

2. Mendoza (1966) found large infra red excesses for T Tauri stars and related objects.

3. Kuhi (1964), (1966) has deduced from the emission lines and violet displaced absorption lines that T Tauri stars eject mass and may

thereby lose energy at a rate comparable with that carried by their luminous output.

The first two of these observations imply that the placing of T Tauri stars in the (M_{bol}, log Te) plane may be seriously in error. All three indicate processes which are not allowed for in the theory and may imply changes, not necessarily independent of mass, in the past evolution of stars which no longer show such phenomena.

The observed colour magnitude diagrams must contain an admixture of field stars. The area in which photometric measures were possible has generally been restricted by the bright nebulosity and the observations are incomplete at fainter magnitudes.

The comparison of theory and observation cannot be extended to the finer details of the colour magnitude diagram for the fainter stars in these clusters.

9. Conclusions.

NGC 6383 contains approximately 21 stars earlier than A0.

The lower main sequence turn off is at $(B-V)_o = -0.05$.

The contraction age is $\sim 5 \times 10^6$ years.

$E_{B-V} = 0.35$

$(m - M)_o = 10.6$

Distance = 1300 pc.

Six faint variable stars are possible members.

REFERENCES

Adams, W.S., 1949. Astrophys. J. 109, 362.

Ahmed, F., 1963. Thesis, University of Edinburgh.

Allen, C.W., 1963. Astrophysical Quantities, 2nd edition, p. 203. Athlone Press, London.

Andrews, P.J., 1965. Thesis, University of Cambridge.

Argue, A.N., 1960. Vistas in Astronomy, ed. Beer, 3, 184. Pergamon Press, London.

Argue, A.N., 1961. Mon. Not. R. astr. Soc., 122, 197.

Argue, A.N., 1963. Observatory, 83, 234.

Argue, A.N., 1964. Mon. Not. R. astr. Soc., 127, 97.

Arp, H.C., 1958. Astr. J. , N.Y., 63, 118.

Arp, H.C., 1958 a. Astr. J. , N.Y., 63, 273.

Aveni, A., 1966. Astrophys . J. , 144, 666.

Baker, J.G., 1940. Proc. Amer. Phil. Soc., 82, No. 3.

Becker, W., 1962. Z. Astrophys., 54, 55.

Bidelman, W.P., 1954. Publs astr. Soc. Pacif., 66, 249.

Blaauw, A., 1963. Basic Astronomical Data, ed. Strand, p.383. University of Chicago Press.

Blanco, V.M. and Grant, G., 1959. Publs astr. Soc. Pacif., 71, 194.

Bowen, I.S., 1960. Telescopes, ed. Kuiper and Middlehurst, p. 43. University of Chicago Press.

Burch, C.R., 1942. Mon. Not. R. astr. Soc., 102, 159.

Buscombe, W. and Kennedy, P.M., 1968. Mon. Not. R. astr. Soc., 139, 417.

Cousins, A.W.J., 1961. Cape Mimeogram No. 11.

Cousins, A.W.J. and Stoy, R.H., 1964. R. Obs. Bulls, No. 64.

Cousins, A.W.J., 1967. Private communication.

Cousins, A.W.J., 1968. Private communication.

Dieter, N.H., 1967. Astrophys. J. , 150, 435.

Eggen, O.J., 1961. R. Obs. Bulls, No. 27.

Eggen, O.J., 1963. Astrophys. J. , 138, 356.

Eggen, O.J., 1965. A. Rev. Astr. Astrophys., 3, 235.

Eggen, O.J., 1965a. Mem. R. astr. Soc., 70, 111.

Ezer, D. and Cameron, A.G.W., 1967. Can. J. Phys., 45, 3429.

Feast, M.W., Thackeray, A.D. and Wesselink, A.J., 1955. Mem. R. astr. Soc., 67, 51.

Feast, M.W., 1958. Mon. Not. R. astr. Soc., 118, 618.

Feast, M.W., Thackeray, A.D. and Wesselink, A.J., 1960. Mon. Not. R. astr. Soc., 121, 337.

Feast, M.W., 1963. Mon. Not. R. astr. Soc., 126, 11.

Feinstein, A., 1968. Z. Astrophys., 68, 29.

Fernie, J.D., 1963. Observatory, 83, 33.

Fernie, J.D., 1966. Private communication.

Finlay - Freundlich, E., 1950. Nature, 165, 703.

Finlay - Freundlich, E. and Waland, R.L., 1953. Sky and Telescope, 12, 176.

Graham, J.A., 1967. Mon. Not. R. astr. Soc., 135, 377.

Haffner, H., 1955. Mitt A.G., p.44.

Harris, D.L., 1963. Basic Astronomical Data, ed. Strand, p. 263. University of Chicago Press.

Herbig, G.H., 1958. Astr. J., N.Y., 63, 363.

Herbig, G.H., 1967. Trans. I.A.U., 13 A, 527.

Hiltner, W.A., Morgan, W.W. and Neff, J.W., 1965. Astrophys. J., 141, 183.

Hodge, P.W., 1960. Astrophys. J., 132, 341.

Iben, I., 1965. Astrophys. J., 141, 993.

Iben, I., 1965a. Astrophys. J., 142, 1447.

Iben, I., 1966. Astrophys. J., 143, 483, 505, 516.

Iben, I., 1967. Astrophys. J., 147, 624, 650.

Iben, I. and Talbot, R.J., 1966. Astrophys. J., 144, 968.

Johnson, H.L. and Morgan, W.W., 1953. Astrophys. J., 117, 313.

Johnson, H.L., 1953. Astrophys. J., 117, 356.

Johnson, H.L., 1955. Ann. d' Astrophys., 18, 292.

Johnson, H.L., 1958. Lowell Obs. Bull., 4, 37.

Johnson, H.L. and Iriarte, B., 1958. Lowell Obs. Bull., 4, 47.

Johnson, H.L. and Mitchell, R.I., 1958. Astrophys. J., 128, 31.

Johnson, H.L., 1960. Lowell Obs. Bull., 5, 17.

Johnson, H.L., 1963. Basic Astronomical Data, ed. Strand, p. 204. University of Chicago Press.

Johnson, H.L., 1964. Bol. Obs. Ton. Tac., 3, 305.

Kaye, G.W.C. and Laby, T.H., 1964. Tables of Physical and Chemical Constants, London.

Kraft, R.P., 1967. Astrophys. J., 148, 129.

Kuhi, L.V., 1964. Astrophys. J., 140, 1409.

Kuhi, L.V., 1966. Astrophys. J., 143, 991.

Kukarkin, B.V., Parenago, P.P., Efremov, Yu. I. and Kholopov, P.N. , 1958. General Catalogue of Variable Stars, 2nd edition, Moscow.

Lawrence, L.C. and Reddish, V.C., 1965. Publs. R. Obs. Edin., 3, 280.

Lindoff, U., 1968. Ark. Astr., 5, 1.

Lindsay, E.M., 1952. Irish A.J., 2, 140.

Linfoot, E.H., 1943. Mon. Not. R. astr. Soc., 103, 210.

Linfoot, E.H., 1944. Mon. Not. R. astr. Soc., 104, 48.

Linfoot, E.H., 1948. Observatory, 68, 211.

Linfoot, E.H., 1955. Recent Advances in Optics, Oxford.

Linfoot, E.H., 1956. Vistas in Astronomy, ed. Beer, 1, 351. Pergamon Press, London.

Mendoza, E., 1966. Astrophys. J., 143, 1010.

Mitchell, R.I., 1960. Astrophys. J., 132, 68.

Morgan, W.W., Hiltner, W.A., Neff, J.S., Garrison, R. and Osterbrock, D.E., 1965. Astrophys. J., 142, 974.

Münch, G., 1965. Galactic Structure, ed. Blaauw and Schmidt, p. 203. University of Chicago Press.

Penston, M.V., 1964. Observatory, 84, 141.

Pesch, P., 1959. Astrophys. J., 130, 764.

Plaut, L., 1948. Annls. Obs. Leiden, 20, 3.

Rickard, J.J., 1968. Astrophys. J., 152, 1019.

Roslund, C., 1964. Ark. Astr., 3, 357.

Roslund, C., 1966a. Ark. Astr., 4, 73.

Roslund, C., 1966b. Ark. Astr., 4, 101.

St. Andrews Observatory, 1950. Observatory, 70, 59.

Schild, R.E., 1965. Astrophys. J., 142, 979.

Schild, R.E., 1966. Astrophys. J., 146, 142.

Schild, R.E., 1967. Astrophys. J., 148, 449.

Sharpless, S.L., 1960. Astrophys. J., Suppl. Ser., 4, 257.

Sher, D., 1966. Q.Jl. R. astr. Soc., 6, 299.

Smak, J., 1964. Astrophys. J., 139, 1095.

Stock, J. and Williams, A.D., 1962. Astronomical Techniques, ed. Hiltner, p. 411. University of Chicago Press.

Stothers, R., 1966. Astrophys. J., 143, 91.

Stothers, R. and Chin, C.W., 1968. Astrophys. J., 152, 225.

Swope, H.H., 1939. Annls. Obs. Harv., 90, 231.

Thackeray, A.D., 1967. Nature, 214, 136.

Thackeray, A.D. and Wesselink, A.J., 1965. Mon. Not. R. astr. Soc., 131, 121.

The, Pik-Sin, 1960. Astrophys. J., 132, 40.

The, Pik-Sin, 1961. Contr. Bosscha Obs., 12.

The, Pik-Sin, 1965. Contr. Bosscha Obs., 32.

Trumpler, R.J., 1930a. Lick Obs. Bull., 14, 174.

Trumpler, R.J., 1930b. Publs. astr. Soc. Pacif., 42, 342.

Trumpler, R.J., 1935. Publs. astr. Soc. Pacif., 47, 249.

Trumpler, R.J., 1968. Catalogue of Galactic Clusters.

Underhill, A.B., 1958. Publs. astr. Soc. Pacif., 70, 607.

Underhill, A.B., 1960. Astrophys. J., 131, 524.

Underhill, A.B., 1967. I.A.U. Symposium No. 30, ed. Batten and Heard, p. 167.

Vanysek, V., 1964. Publs. astr. Inst. Charles University, Prague, No. 38.

Vasilevskis, S., Sanders, W.L. and van Altena, W.F., 1965a. Astr. J., N.Y., 70, 806.

Vasilevskis, S., Sanders, W.L. and Balz, A.G.A., 1965b. Astr. J., N.Y., 70, 797.

Waland, R.L., 1964. Private communication.

Walker, M.F., 1956. Astrophys. J., Suppl. Ser. 2, 365.

Walker, M.F., 1957. Astrophys. J., 125, 636.

Walker, M.F., 1959. Astrophys. J., 130, 57.

Walker, M.F., 1961a. Astrophys. J., 133, 1081.

Walker, M.F., 1961b. Astrophys. J., 133, 438.

Walker, M.F., 1964. R. Obs. Bulls., No. 82, p. 69.

Wayman, P.A., 1952. Thesis, University of Cambridge.

Weaver, H., 1962. Handb. Phys., 54, 130.

Westerlund, B., 1959. Publs. astr. Soc. Pacif., 71, 156.

Zug, R.S., 1937. Lick. Obs. Bull., 18, 89.

—oOo—

TABLE 1.

DIMENSIONS OF THE ST. ANDREWS TELESCOPES.

Dimension.		SLT Inches	JGT Inches
Primary R.O.C.,	r_h	49.5	116.45
Secondary R.O.C.,	r_s	47.25	111.72
Mirror Separation,	a	13.61	33.2
Primary - corrector,	ℓ	55.4	130.2
Primary diameter,	d_h	18.81	37.
Secondary diameter,	ds	9.6	18.75
Corrector diameter,	dc	18.5	38.25
E.F.L.,	f	45.0	106.
Iris diameter		15.0	30-37
Primary vertex-focus,	x	6.64	11.7
Iris - corrector		28	66
Dia. of primary hole		6.25	13
Dia. of corrector mask		6.9	14
Plate scale (^{11}arc/mm)		170	76.4
Material of primary : SLT		Chance Hysil	
and secondary : JGT		Pilkington Pyrex	
Material of Corrector : SLT		Pilkington White Plate Glass	
: JGT		Schott UBK 7.	

TABLE 2.

PLATES OF THE COMA CLUSTER.

SCOTT LANG TELESCOPE.

V			B		
Date 1965	Focus error (thou) KET	Focus plate	Date 1965	Focus error (thou) KET	Focus plate
9 March	0	- ?	24 Feb. R	0	
"	+½	- ?	4 April	0	
"	0		"	0:	
"	+¼		21 April R	0	
"	+½	0	"	+½	Small
4 April	0		"	+½	0 +
"	0:		23 April R	0	
21 April	0	Small	"	+1	
"	+½	"	24 April	0	
"	+½	0 +			
23 April	0				
24 April	0				

R : Plate rejected because of field error.

All plates were taken with the telescope on the East side of the pier. The exposure time was 5 minutes, but 10 minutes for the B plate on 24 February and 5½ minutes for the first V plate on 4 April.

TABLE 2. (Cont.)

PLATES OF THE COMA CLUSTER.

JAMES GREGORY TELESCOPE.

Date 1965	V. Focus error. Thou.	Seeing.	Date 1965	B. Focus error Thou.	Seeing.
18 April	+4	Poor	10 March	-4	Fair
"	0	"	"	-4	"
20 April	0	V.poor	"	-5	"
29 April	-2	Q.good	18 April	-4	Poor
"	0	"	"	-1	"
"	+2	"	20 April	0	V.poor
"	0	Fair	"	0	"
			29 April	-2	Q.good
			"	0	"
			"	+2	"
			"	0	Poor.

The exposure times were either 3 minutes or 5 minutes.

TABLE 3.

RADCLIFFE PLATES OF IC 2581.

Number	Date	Time (UT)	Exposure	Plate + Filter	Seeing
A 5024	11 Feb 1967	0132	40 sec	103aD+GG11	Rather Poor
5025	"	0134	"	"	"
5026	"	0136	"	"	"
5035	"	0245	"	"	Poor
5012	10 Feb 1967	2245	40 sec	IIaO+GG13	Quite good
5018	11 Feb 1967	0006	"	"	Fair
5019	"	0008	"	"	"
5031	"	0223	"	"	Poor
5023	"	0100	2 min	IaO+UG2	Fair
5027	"	0142	3 min	"	Rather poor
5028	"	0145	2 min	"	"
5029	"	0149	"	"	"
5032	"	0228	5 min	"	Poor
5033	"	0233	1 min	"	"
4790	19 April 1966	2048	5 min	103aD+GG11	Fair
4792	"	2104	"	"	"
4806	21 April 1966	1729	"	"	"
4815	"	2057	"	"	Fair –
5009	10 Jan 1967	0157	"	"	"
5010	"	0217	"	"	"
5034	11 Feb 1967	0240	"	"	Poor

TABLE 3 (Cont.)

RADCLIFFE PLATES OF IC 2581.

Number	Date	Time (UT)	Exposure	Plate + Filter	Seeing
A 4788	19 April 1966	2016	5 min	103aO+GG13	Fair
4789	"	2024	"	"	"
4813	21 April 1966	2038	"	"	"
4814	"	2049	"	"	Fair -
5013	10 Feb 1967	2210	5 mins	IIaO+GG13	Quite Good
5020	11 Feb 1967	0013	"	"	Fair
5030	"	0217	"	"	Poor
5016	10 Feb 1967	2307	15 min	IaO+UG2	Quite good
5017	"	2324	"	"	"
5021	11 Feb 1967	0028	"	"	Fair
5022	"	0048	"	"	"
4781	19 April 1966	1750	11 min	103aD+GG11	Fair
4805	21 April 1966	1719	10 min	"	Good
4807	"	1800	"	"	"
4816	"	2108	"	"	Fair -
5006	10 Jan 1967	0053	"	"	Fair
5008	"	0145	"	"	Fair +
4808	21 April 1966	1820	10 min	103aO+GG13	Fair
4809	"	1833	"	"	"
4810	"	1850	"	"	"
4811	"	1902	9 min	"	Fair-Poor

TABLE 3 (Cont.)

RADCLIFFE PLATES OF IC 2581.

Number	Date	Time (UT)	Exposure	Plate + Filter	Seeing
A 4812	21 April 1966	1916	10 min	103aO+GG13	Fair
5004	9 Jan 1967	2343	30 min	IaO+UG2	Fair
5005	10 Jan 1967	0014	24 min	"	"
5007	"	0119	30 min	"	Fair +
5015	10 Feb 1967	2240	"	"	Quite good
5214	31 Jan 1968	0212	20 min	103aD+GG11	Fair +
5212	"	0040	30 min	IIaO+GG13	Fair -
5213	"	0122	"	"	Fair
5068	7 June 1967	1710	45 min	IaO+UG2	Good
5069	"	1804	"	"	"

RADCLIFFE PLATES OF NGC 6383.

A 5087	9 June 1967	2121	40 sec	103aD+GG11	Fair
5106	5 July 1967	1713	"	"	Quite good
5109	"	1722	"	"	" "
5135	7 July 1967	1923	"	"	Fair +
5084	9 June 1967	2111	40 sec	IIaO+GG13	Fair
5085	"	2114	"	"	"
5086	"	2117	"	"	"
5081	"	2014	2 min	IaO+UG2	Poor

TABLE 3 (Cont.)

RADCLIFFE PLATES OF NGC 6383.

Number	Date	Time (UT)	Exposure	Plate + Filter	Seeing
A 5082	9 June 1967	2018	2 mins	IaO+UG2	Poor
5083	"	2022	"	"	"
5115	6 July 1967	0013	"	"	Fair +
4822	22 April 1966	0134	5 min	103aD+GG11	Poor
4823	"	0140	"	"	"
4828	"	0303	3 min	"	"
4977	13 Sept 1966	1708	5 min	"	Quite good
4824	22 April 1966	0155	5 min	103aO+GG13	Poor
4826	"	0216	"	"	"
4831	"	0324	3 min	"	"
4819	21 April 1966	2354	11 min	103aD+GG11	Poor
4820	22 April 1966	0008	10 min	"	"
4827	"	0255	"	"	"
4978	13 Sept 1966	1718	"	"	Quite good
4798	20 April 1966	0146	10 min	103aO+GG13	Poor
4799	"	0200	"	"	"
4800	"	0239	"	"	"
4825	22 April 1966	0205	"	"	"
4869	21 June 1966	2213	"	"	Poor
4870	"	2225	"	"	"

TABLE 3 (Cont.)

RADCLIFFE PLATES OF NGC 6383.

Number	Date	Time (UT)	Exposure	Plate + Filter	Seeing
A 4981	13 Sept 1966	1847	10 min	103aO+GG13	Poor
4979	"	1745	30 min	080-01+UG2	Quite good
4980	"	1816	"	"	"
5138	7 July 1967	2316	20 min	IaO+UG2	Fair
4867	21 June 1966	2140	14 min	103aG+GG11	Poor
4868	"	2158	"	"	"
5089	9 June 1967	2240	20 min	103aD+GG11	Fair -
5110	5 July 1967	1812	"	"	Quite good
5133	7 July 1967	1817	30 min	IIaO+GG13	Fair
5134	"	1856	"	"	"
5090	10 June 1967	0000	40 Min	IaO+UG2	Fair -
5114	5 July 1967	2348	"	"	Fair +
5072	8 June 1967	0137	60m	103aD+GG11	Quite good
5088	9 June 1967	2156	60	"	Fair +
5111	5 July 1967	1854	60	"	Good
4854	20 June 1966	2120	45	103aG+GG11	Poor
4866	21 June 1966	2103	45	"	Poor
4855	20 June 1966	2217	45	103aO+GG13	Poor
4865	21 June 1966	2002	46	"	Poor

TABLE 3 (Cont.)

RADCLIFFE PLATES OF NGC 6383.

Number	Date	Time (UT)	Exposure	Plate + Filter	Seeing
A 5071	8 June 1967	0015	60	103aO+GG13	Quite good
5113	5 July 1967	2245	60	"	Fair-Good
5137	7 July 1967	2222	60	"	Fair +
5362**	28 June 1968	0110	60	"	Fair -
5070	7 June 1967	2215	120	IaO+UG2	Quite good
5112	5 July 1967	2049	120	"	" "
5136	7 July 1967	2028	120	"	Fair +

** This plate was used only for the variable stars.

TABLE 4.

COMPUTED COLOUR COEFFICIENTS.

IC 2581

Exposure	Colour	Mag. Range.		Plate
40 sec	V	9.0 - 13.0	- 0.13	103aD
40 sec	B	9.0 - 13.5	- 0.04	IIaO
2 min	U	9.0 - 13.5	0.00	IaO
5 min	V	9.0 - 13.5	- 0.13	103aD
		12.8 - 15.0	- 0.13	
5 min	B	9.0 - 14.0	+ 0.07	103aO
		13.5 - 16.2	+ 0.09	
		9.0 - 14.0	- 0.06	IIaO
		13.5 - 16.2	- 0.01	
15 min	U	9.0 - 13.5	+ 0.03	IaO
		12.5 - 15.8	+ 0.03	
10 min	V	9.0 - 13.5	- 0.13	103aD
		12.8 - 15.5	- 0.12	
10 min	B	9.0 - 14.0	+ 0.07	103aO
		13.5 - 16.2	+ 0.08	
		14.5 - 17.2	+ 0.06	
30 min	U	9.0 - 13.5	+ 0.04	IaO
		12.5 - 16.6	+ 0.02	

TABLE 4. (Cont.)

COMPUTED COLOUR COEFFICIENTS.

IC 2581

Exposure	Colour	Mag. Range		Plate
20 min	V	9.0 - 13.5	- 0.10	103aD
		12.8 - 15.5	- 0.09	
30 min	B	9.0 - 14.0	- 0.01	IIaO
		13.5 - 16.2	+ 0.02	
		14.5 - 17.2	0.00	
45 min	U	9.0 - 13.5	0.00	IaO
		12.5 - 16.6	- 0.01	
		15.5 - 19.0	- 0.06:	
		NGC 6383		
40 sec	V	8.0 - 12.6	- 0.13	103aD
		11.0 - 14.0	- 0.15	
40 sec	B	8.0 - 13.5	+ 0.02	IIaO
		12.0 - 15.0	+ 0.04	
2 min	U	8.0 - 12.0	-	IaO
		12.0 - 15.0	- 0.13:	
5 min	V	8.0 - 13.0	- 0.14	103aD
		12.0 - 15.5	- 0.14	
5 min	B	8.0 - 13.4	+ 0.06	103aO
		12.5 - 16.5	+ 0.06	

TABLE 4. (Cont.)

COMPUTED COLOUR COEFFICIENTS.

NGC 6383

Exposure	Colour	Mag. Range		Plate
10 min	V	8.0 - 13.0	- 0.15	103aD
		12.0 - 15.0	- 0.13	
		14.5 - 17.0	- 0.16	
		8.0 - 13.0	+ 0.13	103aG
		12.0 - 15.0	+ 0.12	
		14.5 - 17.0	+ 0.12	
10 min	B	8.0 - 13.4	+ 0.07	103aO
		12.5 - 16.7	+ 0.05	
		16.0 - 18.0	-	
30 min	U	8.0 - 12.0	+ 0.07	IaO
		12.0 - 14.0	- 0.08	
		13.5 - 16.6	- 0.05	
20 min	V	12.0 - 15.0	- 0.12	103aD
		15.0 - 19.0	- 0.14	
30 min	B	12.5 - 17.0	- 0.02	IIaO
		16.0 - 20.0	- 0.04	
		17.0 - 20.5	- 0.06:	
40 min	U	12.0 - 14.0	- 0.03	IaO
		13.5 - 17.0	+ 0.08	

TABLE 5.

STANDARD ERRORS OF MAGNITUDES IN IC 2581.

Magnitude Range.	(1)	(2)	(3)
9<V<10	0.041	0.04	0.021
9<B<10	0.014	0.03	0.024
9<U<10	0.010	0.04	0.021
10<V<11	0.018	0.04	0.029
10<B<11	0.009	0.03	0.022
10<U<11	0.025	0.04	0.020
11<V<12	0.025	0.04	0.017
11<B<12	(0.000)	0.03	0.013
11<U<12	0.007	0.04	0.015
12<V<13	0.037	0.04	0.019
12<B<13	0.023	0.03	0.015
12<U<13	0.044	0.04	0.015
13<V<14	0.037	0.03	0.017
13<B<14	0.023	0.03	0.011
13<U<14	0.039	0.08	0.015
14<V<15	0.057	0.03	0.021
14<B<15	0.029	0.03	0.014
14<U<15	0.040	0.08	0.024

TABLE 5. (Cont.)

STANDARD ERRORS OF MAGNITUDES IN IC 2581.

Magnitude Range	(1)	(2)	(3)
15< V<16	0.053	0.03	0.026
15< B<16	0.029	0.03	0.015
15<U<16	0.058	0.08	0.027
16<B<17	0.056	0.05	0.016
16 <U< 17	0.047	0.08	0.030
17< B< 18	0.043	(0.05)	-
17<U<18	0.076	0.18	0.025
18<U<19	0.090	(0.18)	-

The standard errors given against B and U for the photo-electric observations (1) are those in (B-V) and (U-B), where B and U respectively fall in the stated interval.

TABLE 6.

STANDARD ERRORS OF MAGNITUDES IN NGC 6383.

Magnitude Range	(1)	(2)	(3)
9<V<10	0.011	0.04	0.02:
9<B<10	0.008	0.04	0.02:
9<U<10	0.012	0.03	0.02:
10<V<11	0.021	0.04	0.02:
10<B<11	0.011	0.04	0.017
10<U<11	0.016	0.03	0.02:
11<V<12	0.020	0.04	0.020
11<B<12	0.020	0.04	0.017
11<U<12	0.015	0.03	0.02:
12<V<13	0.019	0.04	0.020
12<B<13	0.019	0.04	0.016
12<U<13	0.030	0.06	0.038
13<V<14	0.039	0.04	0.020
13<B<14	0.020	0.04	0.017
13<U<14	0.030	0.06	0.032
14<V<15	0.046	0.04	0.030
14<B<15	0.026	0.04	0.012
14<U<15	0.044	0.06	0.045

TABLE 6 (Cont.)

STANDARD ERRORS OF MAGNITUDES IN NGC 6383.

Magnitude Range	(1)	(2)	(3)
15<V<16	0.072	0.07	0.030
15<B<16	0.036	0.05	0.016
15<U<16	0.031	0.08	0.043
16<V<17	0.040	0.07	0.05
16<B<17	0.057	0.05	0.018
16<U<17	0.100	0.08	0.069
17<V<18	0.138	0.09	0.06
17<B<18	0.091	0.11	0.021
17<U<17.9	0.118	(0.15)	0.061
18<B<19	0.177	0.11	0.026
19<B<19.7	0.104	(0.16)	0.075

The standard errors given against B and U for the photo-electric observations (1) are those in (B-V) and (U-B), where B and U respectively fall in the stated interval.

TABLE 7.

PHOTO-ELECTRIC STANDARDS IN IC 2581.

	PHOTO-ELECTRIC				PHOTOGRAPHIC		
Star	V	B-V	U-B	n	V	B-V	U-B
2	7.07	+0.47	-0.41	Std	-	-	-
4	9.60	+0.20	-0.62	2	9.61	+0.21	-0.64
5	9.77	-0.03	-0.23	2	9.68	0.00	-0.14
6	11.06	+0.19	-0.58	2	11.08	+0.16	-0.57
8	10.64	+0.25	-0.57	5	10.62	+0.24	-0.57
11	11.95	+0.06	-0.44	3	11.93	+0.08	-0.40
13	12.29	+0.17	+0.10	3	12.27	+0.18	+0.24
14	11.22	+1.11	+1.11	3	11.16	+1.14	+1.09
16	10.89	+1.15	+0.84	3	10.91	+1.14	+0.88
20	11.78	+0.24	-0.38	1	11.81	+0.23	-0.41
21	12.97	+0.27	+0.17	2	12.94	+0.32	+0.17
25	12.26	+0.23	-0.41	3	12.30	+0.24	-0.45
26	13.28	+0.23	-0.18	3	13.33	+0.26	-0.27
33	13.55	+0.21	+0.03	2	13.52	+0.21	+0.12
36	12.82	+0.24	-0.31	2	12.82	+0.21	-0.31
37	13.57	+0.29	-0.14	2	13.57	+0.29	-0.17
42	13.22	+0.23	-0.34	3	13.15	+0.27	-0.33
59	13.56	+0.37	+0.14	2	13.53	+0.40	+0.14
67	12.91	+0.24	-0.25	3	12.91	+0.23	-0.25
68	12.96	+0.86	+0.43	3	12.93	+0.90	+0.48
73	11.22	+1.07	+0.89	3	11.22	+1.06	+0.87
74	12.35	+0.06	-0.05	3	12.35	+0.09	0.00

TABLE 7. (Cont.)

PHOTO-ELECTRIC STANDARDS IN IC 2581.

	PHOTO-ELECTRIC				PHOTOGRAPHIC		
Star	V	B-V	U-B	n	V	B-V	U-B
78	9.86	+0.18	-0.64	1	(9.75	+0.20	-0.65)
79	9.62	+0.14	-0.70	1	(9.50	+0.14	-0.70)
80	10.32	+0.15	-0.67	1	(10.25	+0.16	-0.69)
100	13.39	+0.81	+0.27	3	13.40	+0.80	+0.25
101	13.09	+0.72	+0.20	4	13.10	+0.76	+0.14
102	15.18	+0.87	+0.31	2	15.19	+0.79	+0.34
103	14.18	+0.89	+0.45	3	14.22	+0.85	+0.46
105	13.67	+0.97	+0.80	3	13.71	+0.96	+0.71
107	13.63	+0.32	-0.18	2	13.65	+0.30	-0.26
108	14.09	+0.34	0.00	2	14.14	+0.33	+0.02
109	14.05	+0.41	+0.23	2	14.05	+0.43	+0.29
111	14.45	+1.62	+1.23	2	14.40	+1.73	+1.57
114	14.91	+0.69	+0.13:	2	14.87	+0.69	+0.19
115	14.22	+0.68	+0.09	2	14.23	+0.66	+0.06
116	15.25	+0.52	+0.19	2	15.30	+0.52	+0.37
117	14.33	+0.45	+0.06	2	14.20	+0.45	+0.11
118	15.35	+0.77	+0.34	2	15.34	+0.78	+0.24
119	13.44	+0.53	+0.02	2	13.40	+0.52	-0.05
120	14.94	+1.60	+1.71:	2	14.92	+1.61	+1.41
121	13.98	+0.35	+0.07	2	13.95	+0.33	+0.13
123	15.48	+0.59	+0.46	2	15.46	+0.62	+0.40

TABLE 7. (Cont.)

PHOTO-ELECTRIC STANDARDS IN IC 2581.

	PHOTO-ELECTRIC				PHOTOGRAPHIC		
Star	V	B-V	U-B	n	V	B-V	U-B
125	13.45	+0.19	+0.05	2	13.49	+0.19	-0.01
127	13.97	+0.48	-0.03	4	13.97	+0.48	-0.04
128	14.85	+2.21	+1.62	2	14.87	+2.16	+1.66
129	13.06	+1.18	+0.93	2	13.07	+1.15	+0.98
130	13.93	+1.43	+1.16	2	13.92	+1.42	+1.10
131	11.41	+1.49	+1.49	3	11.39	+1.50	+1.54
132	13.07	+0.55	+0.06	2	13.04	+0.56	+0.03
133	9.75	+0.14	-0.59	1	(9.67	+0.15	-0.63)

NOTE : The stars 78, 79, 80 and 133 had photographic measures in poor agreement with the photo-electric, attributable to crowding for the first three. The 'photographic' magnitudes quoted represent a compromise between the photo-electric and the original photographic values.

TABLE 8.

PHOTOGRAPHIC MAGNITUDES AND COLOURS IN IC 2581.

Star	V	B–V	U–B	Star	V	B–V	U–B
134	13.14	+0.49	−0.10	10	11.35	+0.10	−0.35
135	14.79	+0.71	+0.23	163	13.99	+0.53	+0.06
136	14.52	+0.43	+0.26	164	13.87	+0.56	+0.04
137	15.42	+0.87	+0.30	165	14.49	+0.39	+0.22
138	15.31	+1.01	+0.61	166	14.18	+0.32	+0.07
139	15.12	+0.51	+0.20	167	15.32	+0.53	+0.29
140	11.32	+0.06	−0.59	168	11.22	+0.24	−0.52
141	13.78	+0.24	+0.07	169	11.75	+0.28:	−0.38:
142	14.76	+0.80	+0.38	170	15.19	+0.79	+0.23
143	15.05	+0.64	+0.26	171	15.08	+0.48:	+0.36:
144	14.78	+0.78	+0.39	172	14.97	+0.65:	+0.22:
145	11.73	+0.65	+0.11	46	13.71	+0.31	−0.09
146	14.60	+1.45:	+0.93:	173	14.33	+0.47	+0.05
147	15.07	+0.60	+0.33	43	12.32	+0.26	−0.37
148	14.73	+0.71	+0.16	45	12.98	+0.29	−0.26
149	15.11	+1.55	+1.00	174	15.15	+0.58:	+0.32:
150	14.37	+0.60	+0.03	175	14.91	+0.48	+0.37
151	15.32	+0.64	+0.03	44	12.75	+0.62	0.00
152	14.59	+0.64	+0.19	40	12.16	+0.21	−0.32
153	14.37	+0.46	+0.39	41	13.75	+0.27	−0.07

TABLE 8. (Cont.)

PHOTOGRAPHIC MAGNITUDES AND COLOURS IN IC 2581.

Star	V	B-V	U-B	Star	V	B-V	U-B
154	14.37	+0.45	+0.01	71	11.05	+0.36	-0.36
155	14.73	+0.48	-0.11	176	14.80	+0.66	+0.54
156	14.40	+1.42	+1.02	177	15.36	+0.68	+0.31
157	13.52	+1.21	+0.99	178	15.37	+0.70	+0.04
158	13.99	+0.28	+0.11	179	14.04	+0.38	+0.02
159	15.15	+0.52	+0.20	180	14.40	+1.10	+0.80
160	14.31	+0.34	+0.11	181	15.44	+0.46	+0.21
161	15.00	+0.47	+0.24	182	15.02	+0.68	+0.20
162	14.36	+0.32	+0.25	183	12.61	+1.11	+1.07
29	12.08	+0.21	-0.45	184	15.46	+0.71	+0.13
185	14.92	+0.60	+0.06	216	14.35	+0.97	+0.46
186	15.33	+0.62	+0.48	217	14.36	+0.53	+0.01
187	15.42	+0.84	+0.15	218	15.05	+0.72	+0.30
188	15.06	+0.88	+0.39	219	14.88	+0.45	+0.32
189	15.25	+0.50	+0.28	220	13.64	+1.86	+2.11
57	12.28	+0.13	+0.14	221	14.40	+1.37	+1.18
190	15.38	+0.62	+0.08	222	15.36	+0.73	+0.42
191	15.48	+0.61	+0.04	223	15.37	+1.03	+0.37
192	15.27	+0.81	+0.33	224	14.56	+0.53	+0.25
193	15.16	+0.40	+0.34	32	13.21	+0.72	+0.27
194	14.32	+0.32	+0.16	225	15.24	+0.54	+0.19
195	15.27	+0.65	+0.11	226	15.02	+0.79	+0.27

TABLE 8. (Cont.)

PHOTOGRAPHIC MAGNITUDES AND COLOURS IN IC 2581.

Star	V	B-V	U-B	Star	V	B-V	U-B
196	14.69	+1.49	+1.23	227	15.32	+0.86	+0.38
197	14.43	+0.58	+0.08	228	14.91	+0.43	+0.39
198	13.00	+0.85	+0.05	229	14.89	+0.88	+0.36
199	13.86	+0.44	+0.29	230	14.82	+0.67	+0.12
200	14.75	+0.47	+0.27	231	14.39	+0.30	+0.25
201	13.64	+0.35	+0.04	232	14.70	+0.52	+0.40
202	13.95	+0.36	+0.28	233	14.04	+0.35	+0.33
24	12.74	+0.47	-0.05	35	13.21	+0.37	+0.15
203	15.39	+0.59	+0.09	34	13.46	+0.31	-0.17
204	13.99	+0.49	+0.07	234	14.98	+0.73	+0.32
205	13.32	+0.32	-0.08	235	15.25	+1.31	+0.98
206	15.10	+0.87	+0.52	236	15.40	+0.77	+0.11
207	11.83	+0.23	-0.50	237	13.70	+1.08	+0.97
208	15.49	+0.55	+0.36	238	14.10	+0.31	+0.12
209	13.58	+0.38	+0.23	239	14.10	+0.46	+0.04
210	14.81	+0.47	+0.39	240	14.18	+0.24	+0.22
211	13.26	+0.19	-0.03	241	13.83	+0.97	+0.38
212	12.94	+0.50	+0.16	12	11.02	+1.20	+1.21
213	15.38	+0.77	+0.31	242	14.92	+0.60	+0.09
214	14.79	+0.39	+0.32	243	15.34	+0.55	+0.43
215	15.33	+0.67	+0.10	69	13.46	+0.40	+0.07
244	14.70	+1.88	+1.79	275	14.56	+0.39	+0.31

TABLE 8. (Cont.)

PHOTOGRAPHIC MAGNITUDES AND COLOURS IN IC 2581.

Star	V	B-V	U-B	Star	V	B-V	U-B
245	14.75	+0.60	+0.12	276	14.29	+0.52	+0.37
246	13.86	+0.74	+0.38	277	14.79:	+0.50:	+0.59:
247	15.09	+1.43	+0.99	55	11.76	+0.26	-0.41
248	14.92	+0.59	+0.39	56	13.04	+0.43	-0.13
249	14.79	+0.76	+0.32	278	15.22	+0.56	+0.16
250	13.52	+0.32	+0.19	279	14.73	+0.84	+0.29
251	13.79	+0.55	-0.03	280	15.12	+1.00	+0.73
252	15.03	+0.73	+0.30	281	15.43	+0.72	+0.14
253	14.64	+0.49	0.00	282	15.19	+1.01	+0.59
254	14.51	+1.56	+1.67	283	14.27	+1.68	+1.78
255	12.38	+0.28	-0.18	284	14.28	+0.54	+0.03
256	14.53	+0.73	+0.28	285	14.30	+1.01	+0.76
257	13.59	+0.86	+0.64	286	14.94	+0.56	+0.34
258	15.20	+0.68	+0.06	287	14.54	+1.39	+1.13
259	13.41	+1.70	+1.92	288	13.99	+0.28	-0.11
260	13.86	+1.03	+0.93	289	14.72	+0.35	+0.18:
261	15.07	+0.75	+0.18	290	13.74	+0.93	+0.60
262	15.41	+0.51	+0.33	9	11.37	+0.11	-0.31
263	14.41	+0.35	+0.28	291	13.85	+0.34	-0.10
264	15.17	+0.69	+0.24	292	14.17	+0.35	+0.08
265	14.02	+0.31	+0.06	293	14.32	+0.42	+0.28

TABLE 8. (Cont.)

PHOTOGRAPHIC MAGNITUDES AND COLOURS IN IC 2581.

Star	V	B-V	U-B	Star	V	B-V	U-B
266	13.77	+0.22	+0.01	294	15.12	+0.64	+0.07
267	14.82	+0.83	+0.35	295	15.16	+0.71	+0.15
268	15.27	+0.60	+0.07:	296	14.18	+1.26	+0.92
269	14.90	+0.82	+0.29	297	13.33	+0.41	-0.02
270	13.07	+0.29	-0.25	298	15.35	+0.76	+0.32
271	14.67	+0.44	+0.28	299	14.58	+0.41	+0.28
272	13.96	+0.30	-0.14	300	13.37	+0.27	+0.14
273	14.91	+0.53	+0.22	301	15.47	+0.73	+0.12
274	14.01	+0.63	+0.11	302	13.78	+0.54	+0.23
53	11.29	+0.13	-0.55	303	14.42	+0.62	+0.13
54	12.87	+0.24	-0.20	304	14.95	+0.62	+0.20
305	15.41	+1.05	+0.46	332	15.25:	+0.55:	+0.27
306	13.87	+0.52	-0.09	333	14.53	+0.31	+0.28
58	12.46	+0.07	+0.06	334	15.05	+0.47	+0.38
307	12.81	+0.45	-0.08	335	13.44	+0.58	+0.16
308	14.05	+0.55	+0.05	38	12.49	+0.22	-0.31
309	15.37	+0.83	+0.27	39	12.28	+0.20	+0.16
310	14.53	+0.54	+0.25	336	13.70	+1.18	+0.96
311	14.18	+0.63	+0.19	337	14.42	+0.71	+0.37
312	14.61	+0.66	+0.45	338	11.41	+0.13	+0.21
313	11.94	+0.97	+0.55	339	13.57	+0.35	-0.15

TABLE 8. (Cont.)

PHOTOGRAPHIC MAGNITUDES AND COLOURS IN IC 2581.

Star	V	B-V	U-B	Star	V	B-V	U-B
314	12.57	+0.55	-0.04	31	12.06	+0.11	+0.12
315	14.70	+0.48	+0.33	30	13.22	+0.24	-0.24
316	13.49	+0.59	+0.01	340	13.46	+2.07	+2.39
317	15.01	+0.59	+0.08	341	14.21	+0.36	+0.17
318	13.34	+0.33	+0.12	342	15.26	+0.80	+0.31
319	15.00	+0.62	+0.02	343	14.93	+0.57	+0.08
320	13.36	+0.40	+0.04	344	15.10	+0.66	+0.22
321	13.42	+0.30	+0.21	345	15.44	+0.75	+0.12
322	14.83	+0.50	+0.37	15	12.45	+0.14	-0.23
323	13.61	+0.58	+0.05	346	15.03	+0.60	0.00
64	12.70	+0.44	+0.08	347	14.90	+0.73	+0.18
324	15.33	+0.57	+0.36	348	15.25	+0.81	+0.31
325	14.67	+0.98	+0.72	349	14.81	+0.47	+0.29
76	12.82	+0.14	+0.10	350	14.14	+0.53	+0.01
77	11.86	+0.49	+0.10	66	13.47	+0.44	+0.02
326	14.59	+0.74	+0.32	351	15.07	+0.46	+0.34
327	15.10	+0.52	+0.35	65	13.41	+0.46	+0.05
70	12.65	+0.40	-0.16	352	14.25	+0.48	+0.42
328	13.86	+0.49	+0.18	353	14.43	+0.64	+0.22
329	12.91	+1.20	+1.18	354	15.05	+0.68	+0.43
63	13.40	+0.37	+0.29	355	14.52	+1.41	+1.34

TABLE 8. (Cont.)

PHOTOGRAPHIC MAGNITUDES AND COLOURS IN IC 2581.

Star	V	B-V	U-B	Star	V	B-V	U-B
330	14.32	+1.16	+1.04	356	15.33	+0.87	+0.34
331	15.25	+0.69	+0.26	357	14.92	+0.69	+0.29
358	14.85	+1.16	+0.84	380	14.85	+0.41	+0.29
359	14.74	+0.47	+0.07	381	13.83	+0.45	+0.20
360	13.69	+1.38	+1.07	382	13.56	+0.38	-0.19
17	13.37	+0.22	+0.09	28	12.64	+0.26	+0.16
361	14.25	+0.43	+0.21	383	14.78	+0.79	+0.26
362	15.00	+0.79	+0.22	384	14.06	+0.34	-0.02
363	13.59	+0.65	+0.17	385	15.27	+0.62	+0.27
18	11.84	+0.25	+0.18	386	14.19	+0.39	+0.08
364	14.72	+0.51	+0.25	387	15.10	+0.57	+0.15
365	14.32	+1.38	+1.15	27	11.01	+0.06	-0.28
366	14.33	+0.53	+0.27	388	14.13	+0.52	+0.05
367	14.75	+1.42	+1.08	389	14.66	+0.52	+0.04
368	12.77	+0.90	+0.61	390	14.67	+0.38	+0.24
369	14.48	+0.47	+0.51	23	12.76	+0.35	+0.25
370	14.70	+0.75	+0.29:	391	14.95	+0.69	+0.11
371	14.34	+0.76	+0.33	22	12.22	+0.55	+0.05
372	15.02	+0.41	+0.32:	392	15.37	+0.71	+0.08
373	13.84	+1.01	+0.83	393	13.80	+0.33	-0.17
72	12.43	+0.40	-0.13	394	15.21	+0.56	+0.07

TABLE 8. (Cont.)

PHOTOGRAPHIC MAGNITUDES AND COLOURS IN IC 2581.

Star	V	B-V	U-B	Star	V	B-V	U-B
60	13.06	+0.26	-0.15	395	14.45	+0.37	+0.20
61	13.25	+0.50	+0.18	396	13.26	+0.32	-0.27
374	14.19	+0.39	+0.09	397	15.43	+0.71	+0.05
49	12.06	+0.19	-0.37	398	13.57	+0.38	+0.24
50	11.84:	+1.04:	+0.65:	399	13.87	+0.40	+0.10
375	14.21	+0.62	+0.11	400	13.94	+0.27	-0.04
47	13.01	+0.29	+0.12	401	14.86	+0.69	+0.14
48	12.24	+0.20	-0.18	402	15.42	+0.59	+0.09
51	13.62	+0.37	-0.15	403	15.14	+1.03	+0.41
52	12.05	+0.21	-0.33	404	15.26	+0.64	+0.05
376	15.38	+0.51	+0.30	405	12.71	+0.23	-0.35
377	14.42	+0.55	+0.10	406	15.33	+0.53	+0.11
378	13.39	+0.40	-0.11	407	15.05	+0.82	+0.32
379	13.26	+0.29	-0.20	408	14.81	+0.65	+0.05
409	14.03	+0.50	+0.04	419	13.46	+0.52	-0.01
410	13.92	+1.35	+1.14	420	13.52	+1.45	+1.40
411	13.69	+0.50	-0.08	421	14.34	+0.51	-0.01
412	15.24	+1.22	+0.91	422	15.11	+0.60	0.00
413	13.58	+0.91	+0.24	423	14.74	+1.44	+1.18

TABLE 8. (Cont.)

PHOTOGRAPHIC MAGNITUDES AND COLOURS IN IC 2581.

Star	V	B-V	U-B	Star	V	B-V	U-B
414	11.50	+0.12	-0.01	424	15.42	+0.53	+0.32
415	11.60	+1.55	+1.82	425	15.47	+0.77	+0.18
416	15.37	+0.72	+0.42	426	14.67	+0.39	+0.17
417	14.82	+0.82	+0.39	427	14.65	+0.60	+0.29
418	15.08	+0.66	+0.22	428	13.13	+0.29	-0.28

TABLE 9.

SPECTRAL TYPES IN IC 2581.

Fernie	HD/CPD.	Sp(MK)	E_{B-V}	M_V	$(m-M)_o$
1	90772	A 7 : I a	(0.43)	-8.0:	11.3:
2	90706	B 2.5 I b	0.63	-5.7	10.9
3	90707	B 1 III	0.55	-4.4	11.4
4	$-56^{\circ}3382$	B 0.5 V e	0.49	-4.0	12.1
5	$-56^{\circ}3379$	B 9 V	0.06	+0.6	8.9
7	$-57^{\circ}3261$	B 1 : V :ex	(0.43)	-3.6	12.1:
8	$-57^{\circ}3254$	B 1 V	0.50	-3.6	12.7
78	$-57^{\circ}3263$	B 0.5 V	0.48	-4.0	12.3
79	$-57^{\circ}3265$	B 0.5 V n	0.42	-4.0	12.2
80		B 0.5 V	0.44	-4.0	12.9

E_{B-V} for 1 and 7 is the mean reddening of nearby bright stars.

TABLE 10.

MAGNITUDES AND COLOURS OF BRIGHT STARS IN IC 2581.

FERNIE 1 = HD 90772.

V	B-V	U-B	Observer.
4.69	+0.49	-	Arp (1958)
4.70	+0.43	+0.16	Westerlund (1959)
4.64	+0.46	-	Fernie (1966)
4.64	+0.52	-0.01	Cousins and Stoy (1964)

FERNIE 2 = HD 90706

V	B-V	U-B	Observer
7.03	+0.42	-	Fernie (1966)
7.06	+0.47	-	Cousins and Stoy (1964)
7.07	+0.47	-0.41	Present

TABLE 10 (Cont.)

MAGNITUDES AND COLOURS OF BRIGHT STARS IN IC 2581.

FERNIE 3 = HD 90707

DATE	V	B-V	U-B	QUALITY
13 Feb 1967	8.56	+0.29	-0.59	B
16 Mar	8.55	+0.31	-0.60	B
12 April	8.65	+0.29	-0.61	B
30 April	8.63	+0.29	-0.63	A
11 May	8.61	+0.30	-0.64	B
26 May	8.93	+0.30	-0.60	A
3 June	8.78	+0.29	-0.61	B
25 Dec	8.59	+0.29	-0.59	A
27 Dec	8.60	+0.30	-0.58	A
1 Feb 1968	8.60	+0.29	-0.59	A

TABLE 10 (Cont.)

MAGNITUDES AND COLOURS OF BRIGHT STARS IN IC 2581.

FERNIE 7

DATE	V	B-V	U-B	QUALITY
21 Mar 1966	10.10	+0.21	-0.73	B
9 May	10.01	+0.24	-0.73	B
13 Feb 1967	9.93	+0.26	-0.75	B
30 April	9.80	+0.28	-0.69	A
26 May	9.87	+0.30	-0.64	A
3 June	9.91	+0.29	-0.72	B
25 Dec	9.79	+0.28	-0.68	A
27 Dec	9.77	+0.27	-0.64	A
1 Feb 1968	9.92	+0.26	-0.68	A

QUALITY A : Observed relative to bright standard.

QUALITY B : Variable local standard was assumed constant and a correction applied to reduce the values for programme stars to those found on nights when a standard tie-in was done.

TABLE 11.

PHOTO-ELECTRIC STANDARDS IN NGC 6383.

STAR	V	B-V	U-B	n	V	B-V	U-B
2	10.33	+0.15	-0.54	3	10.36	+0.14	-0.52
3	10.27	+0.31	+0.08	6	10.24	+0.33	+0.12
4	13.43	+0.96	+0.58	2	13.39	+0.97	+0.53
5	11.26	+0.17	-0.27	3	11.28	+0.17	-0.28
6	9.01	+0.11	-0.70	8	9.03	+0.10	-0.70
9	9.78	+1.03	+0.66	4	9.77	+1.03	+0.63
10	10.03	+0.12	-0.47	1	10.00	+0.14	-0.50
11	9.81	+1.19	+1.04	1	9.76	+1.22	+1.07
14	9.86	+0.13	-0.45	1	9.89	+0.11	-0.43
15	11.86	+0.18	-0.21	2	11.90	+0.20	-0.15
16	10.82	+0.15	-0.48	3	10.79	+0.11	-0.54
18	13.39	+0.83	+0.33	3	13.40	+0.82	+0.29
20	11.48	+0.24	-0.14	2	11.44	+0.24	-0.10
21	11.92	+0.71	+0.17	7,2	12.00	+0.71	+0.24
22	12.34	+0.55	+0.26	3,1	12.32	+0.55	+0.38
23	13.84	+1.01	+0.60	3,2	13.82	+0.97	+0.34
24	11.38	+0.21	-0.18	3	11.38	+0.22	-0.18
25	12.52	+0.28	+0.13	3	12.50	+0.27	+0.10
26	12.91	+0.51	+0.24	2	12.90	+0.46	+0.25
28	12.53	+0.24	0.00	3	12.50	+0.24	+0.07
29	13.57	+0.74	+0.18	3,2	13.61	+0.76	+0.20

TABLE 11 (Cont.)

PHOTO-ELECTRIC STANDARDS IN NGC 6383.

STAR	V	B-V	U-B	n	V	B-V	U-B
30	13.39	+0.85	+0.29	4	13.38	+0.84	+0.24
31	14.00	+0.69	+0.20	4	13.99	+0.69	+0.10
34	10.34	+1.24	+1.24	1	10.38	+1.24	+1.17
41	10.88	+1.11	+0.81	3	10.89	+1.10	+0.79
42	13.63	+0.76	+0.12	2	13.63	+0.76	+0.11
43	13.10	+0.47	+0.21	3	13.07	+0.45	+0.17
45	13.22	+2.46	+2.26	3	13.19	+2.51	-
50	13.50	+0.90	+0.45	2	13.50	+0.87	+0.47
52	12.30	+0.68	+0.14	2	12.30	+0.66	+0.11
53	12.32	+0.78	+0.22	2	12.35	+0.76	+0.20
54	12.29	+0.59	+0.10	2	12.32	+0.54	+0.12
55	12.80	+0.65	+0.44	2	12.79	+0.64	+0.55
56	13.79	+0.83	+0.31	3	13.78	+0.84	+0.28
57	10.64	+0.26	+0.16	3	10.67	+0.26	+0.27
58	12.38	+0.37	+0.22	2	12.40	+0.35	+0.31
69	12.76	+0.83	+0.36	2,1	12.77	+0.85	+0.21
70	13.05	+0.51	+0.26	2	13.03	+0.50	+0.37
71	12.75	+0.80	+0.37	2	12.75	+0.82	+0.31
75	9.83	+0.24	-0.40	1	9.84	+0.24	-0.45
80	13.30	+0.72	+0.16	2	13.31	+0.74	+0.20
81	12.68	+1.91	+2.16	4,3	12.70	+1.89	+2.24
83	9.53	+0.16	-0.52	3	9.52	+0.16	-0.52

TABLE 11 (Cont.)

PHOTO-ELECTRIC STANDARDS IN NGC 6383.

STAR	V	B-V	U-B	n	V	B-V	U-B
85	9.48	+0.45	+0.05	1	9.47	+0.45	+0.09
91	11.09	+1.21	+0.99	2	11.09	+1.20	+0.91
96	11.38	+0.68	+0.08	3	11.34	+0.68	+0.11
101	14.57	+0.97	+0.33	3,1	14.58	+0.94	+0.36
102	14.62	+0.83	+0.16	2,1	14.72	+0.77	+0.07
103	16.26	+1.02	+0.45	2,1	16.28	+0.99	+0.45
104	15.15	+0.93	+0.47	2,1	15.20	+0.92	+0.42
105	15.37	+1.21	+0.59	3,2	15.42	+1.17	+0.79
106	15.15	+0.87	+0.41	2,1	15.09	+0.95	+0.44
107	14.85	+0.92	+0.50	3,2	14.83	+0.95	+0.40
108	15.75	+1.21	+0.57	2,1	15.73	+1.10	+0.67
109	16.76	+1.07	-0.13:	1,1	16.73	+1.04	-
110	16.87	+0.92	-	1	16.81	+1.06	-
111	15.66	+0.90	+0.35	2	15.70	+0.84	+0.28
112	17.18	+1.10	-0.01	2	17.15	+1.05	-
113	15.33	+1.31	+1.02	1	15.40	+1.18	+0.92
114	15.96	+0.93	+0.32	2	15.99	+0.92	+0.37
115	16.11	+1.02	+0.39	1	16.08	+1.01	+0.53
116	15.65	+1.05	+0.61	3	15.62	+1.15	+0.68
117	16.15	+3.37:	-	2	16.15	+3.97:	-
118	15.02	+0.85	+0.32	3	14.98	+0.85	+0.33

TABLE 11 (Cont.)

PHOTO-ELECTRIC STANDARDS IN NGC 6383.

STAR	V	B-V	U-B	n	V	B-V	U-B
119	14.89	+0.90	+0.30	3	14.90	+0.91	+0.34
120	15.98	+0.99	+0.64	1	15.90	+1.00	+0.58
121	15.95	+0.99	+0.79	1	15.91	+1.05	+0.68
122	13.99	+0.74	+0.23	3	13.99	+0.73	+0.28
123	14.41	+1.02	+0.79:	2	14.33	+1.11	+0.90
124	15.41	+1.08	+0.72:	2	15.36	+1.09	+0.90
125	15.77	+1.07	+0.66	1	15.70	+1.01	+0.63
126	15.28	+0.86	+0.36	3	15.32	+0.81	+0.32
127	14.65	+0.83	+0.38	2	14.60	+0.88	+0.40
128	15.66	+1.16	+0.82	3,2	15.63	+1.25	+0.73
129	18.12	+1.27	-	1	18.14	+1.52	-
130	17.77	+1.47	-	1	17.35	+1.28	-
131	16.92	+1.21	+0.60	1	17.07	+1.31	-
132	16.61	+2.40	-	1	16.62	+2.43	-
133	16.42	+2.54	-	1	16.47	+2.73	-
134	17.51	+1.45	-	1	17.54	+1.50	-
135	17.98	+1.13	+0.12	2	17.83	+1.27	-
136	17.70	+2.49	-	1	17.62	+1.83	-
137	17.69	+2.05	-	1	17.78	+1.65	-
138	17.91	+1.56	-	2	17.91	+1.40	-
139	17.81	+1.71	-	1	17.99	+1.64	-
140	14.82	+1.57	+1.47	2	14.89	+1.51	+1.23

TABLE 12.

PHOTOGRAPHIC MAGNITUDES AND COLOURS IN NGC 6383.

STAR	V	B-V	U-B	STAR	V	B-V	U-B
76	12.85	+0.59	+0.24	166	17.18	+1.16	-
8	13.40	+0.73	+0.21	40	13.19	+0.59	+0.26
87	13.67	+0.70	+0.34	167	15.12	+0.87:	+0.55:
89	13.92	+0.62	+0.13	168	15.33	+0.99	+0.43
141	17.73	+1.27	-	39	13.33	+0.65	+0.08
142	17.83	+1.52	-	169	17.11	+1.35	-
143	15.81	+0.93	+0.37	170	17.08	+2.14	-
144	15.82	+0.93	+0.40	171	16.78	+1.06	-
84	12.09	+0.29	-0.02	46	12.63	+0.70	+0.13
145	15.97	+1.24	-	172	17.16	+1.10	-
146	16.71	+1.02	-	173	16.72	+1.03	+0.24
147	15.04	+1.08	+0.63	174	16.30	+1.13	+0.56
148	16.87	+1.19	-	175	17.98	+1.67	-
149	14.74	10.79	+0.17	176	17.36	+1.49	-
150	17.97	+1.71	-	177	17.58	+1.54	-
151	16.34	+1.13	-	178	17.01	+1.48	-
152	17.27	+1.41	-	179	16.06	+1.27	-
153	16.47	+1.18	-	180	14.00	+1.06	+0.53
154	17.17	+2.51	-	181	14.28	+0.81	+0.40
7	12.65	+0.31	+0.22	182	16.97	+1.48	-
155	17.79	+1.10	-	183	15.68	+1.27	+0.76

TABLE 12. (Cont.)

PHOTOGRAPHIC MAGNITUDES AND COLOURS IN NGC 6383.

STAR	V	B-V	U-B	STAR	V	B-V	U-B
156	17.25	+1.21	-	184	17.62	+1.60	-
157	16.51	+1.23	-	185	17.43	+1.22	-
158	13.75	+0.65	+0.09	186	15.65	+1.00	+0.29:
159	14.64	+0.84	+0.32	187	16.34	+1.17	-
160	17.63	+1.16	-	188	17.03	+1.26	-
161	17.15	+1.10	-	189	17.90	+1.57	-
162	18.02	+1.55	-	190	15.00	+1.29	+1.07
163	17.65	+1.63	-	191	16.25	+1.11	+0.37
164	16.77	+1.27	-	192	17.32:	+0.98:	-
165	16.90	+1.11	-	193	17.55	+1.45	-
194	17.07	+2.50:	-	224	15.69	+1.16	+0.89
195	16.77	+1.21	-	225	16.29	+1.53	-
196	14.60	+0.83	+0.23	226	15.37	+0.98	+0.46
197	16.57	+1.05	-	227	16.94	+1.61	-
198	14.20	+1.27	+1.03	228	17.37	+1.46	-
199	16.98	+1.89	-	63	12.43	+0.65	+0.08
200	16.70	+1.23	-	64	11.16	+0.73	+0.19
201	17.66	+1.63	-	229	15.56	+1.04	+0.47
202	17.60	+1.45	-	230	15.26	+1.10	+0.40
203	15.88	+1.18	+0.87	231	17.26	+1.28	-
204	16.48	+1.93	-	232	14.39	+1.11	+0.71
205	14.89	+0.85	+0.26	233	17.89	+1.62	-

TABLE 12. (Cont.)

PHOTOGRAPHIC MAGNITUDES AND COLOURS IN NGC 6383.

STAR	V	B-V	U-B	STAR	V	B-V	U-B
206	17.73	+1.90	-	234	17.06	+1.45	-
207	17.39	+1.40	-	235	14.36	+0.81	+0.26
208	17.21	+1.36	-	236	14.88	+1.17	+0.74
209	16.05	+1.29	-	237	16.15	+1.12	+0.63
210	14.38	+2.10	-	238	15.13	+1.13	+0.84
211	16.28	+1.24	-	239	17.59	+1.92	-
212	16.27	+1.68	-	240	17.34	+1.81	-
213	17.18	+1.40	-	241	17.36	+2.32	-
214	17.32	+1.50	-	242	14.69	+2.23	-
59	11.75	+0.66	+0.19	243	15.08	+1.23	+1.00
215	17.25	+1.13	-	244	13.82	+1.18	+0.94
216	16.64	+1.32	-	245	16.44	+1.50	-
217	17.54	+1.46	-	246	17.28	+2.13	-
218	14.88	+0.86	+0.27	247	17.18	+1.52	-
219	13.64	+1.13	+0.76	248	17.43	+1.15	-
220	17.23	+1.20	-	249	16.62	+1.08	-
221	18.02	+1.52	-	250	17.14	+1.50	-
222	18.07	+1.55	-	251	15.44	+1.05	+0.46
223	17.14	+2.23	-	252	16.94	+0.96	-
62	12.90	+0.78	+0.17	253	17.12	+1.04	-
61	11.99	+0.64	+0.10	254	17.04	+1.30	-
255	17.89	+1.25	-	285	17.38	+1.28	-

TABLE 12 (Cont.)

PHOTOGRAPHIC MAGNITUDES AND COLOURS IN NGC 6383.

STAR	V	B-V	U-B	STAR	V	B-V	U-B
256	17.12	+1.18	-	286	15.23	+2.87	-
257	16.77	+1.15	-	13	11.97	+0.32	+0.25
258	15.35	+0.01	-	12	13.00	+0.76	+0.10
259	15.18	+1.05	-	97	12.48	+0.28	+0.01
260	15.09	+1.11	-	287	16.62	+1.20	-
261	10.86	+0.19	-0.35	288	16.68	+1.48	-
262	12.82	+0.25	+0.28	289	17.98	+1.24	-
263	12.61	+0.30	+0.16	290	14.40	+1.12	+0.50
264	13.82	+0.54	+0.41	291	16.97	+1.22	-
265	15.88	+0.69	+0.06:	292	16.12	+1.03	+0.36
266	15.27	+0.87	+0.17	95	12.16	+0.59	+0.16
267	17.90	+1.31	-	293	18.03	+1.26	-
268	18.07:	+1.49:	-	294	16.32	+1.35	-
269	18.08	+1.50	-	94	12.54	+1.04	+0.79
270	17.86	+1.70	-	92	13.46	+1.16	+0.74
271	16.94	+1.04	-	93	13.14	+0.90	+0.28
272	16.88	+1.20	-	295	16.93	+1.08	-
32	13.42	+0.69	+0.10	296	17.65	+1.30	-
273	17.78	+1.58	-	297	17.55	+1.60	-
274	15.23	+1.35	+0.62	298	16.05	+1.21	+0.59
275	17.15	+1.15	-	299	17.63	+1.58	-
276	16.87	+1.25	-	300	14.34	+2.24	-

TABLE 12. (Cont.)

PHOTOGRAPHIC MAGNITUDES AND COLOURS IN NGC 6383.

STAR	V	B-V	U-B	STAR	V	B-V	U-B
33	12.95	+0.95	+0.38	90	13.77	+0.83	+0.30
277	17.38	+1.18	-	301	16.03	+1.61	-
278	16.06	+1.10	-	302	16.60	+1.08	-
279	17.46	+1.79	-	303	15.60	+0.81	+0.36
280	17.77	+1.66	-	304	16.93	+1.08	-
281	14.50	+1.68	+0.91	305	17.04	+1.26	-
282	17.89	+1.67	-	306	17.92	+1.29	-
283	17.67	+1.09	-	307	16.54	+1.19	-
19	11.60	+1.20	+0.88	77	12.46	+1.03	+0.32
284	18.05	+1.01	-	308	16.19	+1.22	-
309	14.52	+0.96	+0.48	339	17.77	+1.44	-
310	16.92	+1.65	-	340	17.31	+1.07	-
311	17.24	+1.10	-	341	14.86	+0.69	+0.06
312	15.16	+1.11	+0.62	342	16.99	+1.40	-
313	14.95	+1.15	+0.59	343	17.51	+1.45	-
314	14.92	+0.88	+0.23	344	17.84	+1.55	-
78	12.33	+0.72	+0.28	345	15.45	+1.06	+0.75
315	17.44	+1.19:	-	346	17.85	+1.40	-
316	14.53	+0.67	+0.52	347	14.40	+1.33	+1.08
317	15.97	+1.14	+0.59	348	17.23	+1.14	-
318	16.30	+1.02	+0.46	349	16.63	+1.45	-
319	14.94	+0.91	+0.32	350	16.23	+1.27	-

TABLE 12. (Cont.)

PHOTOGRAPHIC MAGNITUDES AND COLOURS IN NGC 6383.

STAR	V	B-V	U-B	STAR	V	B-V	U-B
320	13.89	+0.71	+0.23	351	16.12	+0.99	+0.47
321	13.44	+0.80	+0.25	352	15.82	+0.96	+0.28
322	14.95	+0.91	+0.34	353	16.83	+1.67	-
73	12.85	+0.81	+0.05	354	17.15	+2.32	-
72	12.46	+0.50	+0.18	355	17.45	+1.16	-
323	15.51	+2.25	-	356	16.69	+1.50	-
324	18.07	+1.23	-	357	15.86	+1.56	-
325	15.26	+0.89	+0.45	358	16.71	+1.15	-
326	15.42	+1.42	-	359	17.24	+1.52	-
327	16.60	+1.35	-	360	16.86	+1.13	-
328	16.01	+0.92	+0.44	361	16.99	+1.54	-
329	15.23	+0.89	+0.38	51	11.85	+0.54	+0.20
330	16.35	+1.07	-	362	17.93	+1.52	-
331	16.74	+2.06	-	363	17.50	+1.97	-
332	17.25	+1.79	-	364	15.85	+0.99	+0.34
333	16.92	+1.44	-	49	12.99	+0.61	0.00
334	15.92	+0.88	+0.33	365	17.25	+1.49	-
335	17.74	+1.78	-	366	18.03	+1.35	-
336	17.76	+1.39	-	367	14.89	+2.02	-
337	17.36	+1.44	-	368	14.86	+0.81	+0.13
338	17.55	+1.45	-	369	16.41	+1.07	+0.51

TABLE 12. (Cont.)

PHOTOGRAPHIC MAGNITUDES AND COLOURS IN NGC 6383.

STAR	V	B-V	U-B	STAR	V	B-V	U-B
370	17.48	+1.46	-	400	16.05	+0.90	+0.35
371	17.99	+1.54	-	401	16.47	+1.05	+0.44
372	16.47	+1.10	-	402	16.64	+1.16	-
47	9.93	+0.39	+0.16	403	17.08	+1.36	-
373	15.52	+0.85	+0.19	404	17.86	+1.23	-
374	16.41	+1.01	+0.25	405	15.06	+1.03	+0.53
38	13.67	+0.72	+0.18	406	16.80	+1.39	-
375	17.55	+1.29	-	407	17.23	+1.67	-
376	16.43	+1.06	-	408	16.98	+0.70	-
377	16.88	+1.37	-	409	16.45	+1.17	-
378	15.54	+1.27	+0.76	410	14.68	+0.80	+0.33
379	16.72	+1.50	-	411	17.74	+2.06	-
380	14.15	+0.61	+0.40	412	17.98	+1.31	-
381	15.32	+0.98	+0.59	413	17.15	+1.28	-
382	15.41	+1.25	+0.69	414	16.67	+1.17	-
383	17.80	+1.10	-	415	15.66	+2.17	-
384	17.80	+1.46	-	416	15.76	+2.69	-
385	17.93	+1.13	-	417	16.41	+2.49	-
386	16.62	+1.24	-	418	17.58	+1.23	-
387	15.47	+0.93	+0.11	419	16.19	+1.18	-
388	15.00	+1.13	+0.46	420	16.34	+2.00	-
389	16.47	+1.14:	-	421	16.65	+1.12	-

TABLE 12. (Cont.)

PHOTOGRAPHIC MAGNITUDES AND COLOURS IN NGC 6383.

STAR	V	B-V	U-B	STAR	V	B-V	U-B
390	15.71	+0.94	(+0.48)	422	17.43	+1.29:	-
391	17.85	+1.19	-	65	10.60	+1.20	+0.90
392	17.81	+1.21	-	423	18.00	+1.61	-
393	16.00	+1.00	+0.47	424	17.11	+1.40	-
394	17.74	+1.46	-	425	17.20:	+1.50:	-
395	17.84	+1.37	-	426	17.63	+1.22:	-
396	16.17	+1.24	-	427	17.88	+1.29:	-
397	16.46	+0.99	+0.35	428	17.92	+1.33	-
398	16.39	+1.08	-	429	17.23	+1.64	-
399	14.25	+0.73	+0.26	430	17.95	+1.54	-
79	13.44	+0.75	+0.18	431	17.63	+1.41	-
432	17.45	+1.65	-	465	18.00	+1.71	-
433	16.48	+1.12	-	466	16.39	+1.19	-
434	15.79	+0.99	+0.60	467	15.59	+2.06	-
435	14.18	+2.03	-	468	18.08	+1.53	-
436	17.01	+2.56	-	469	18.03	+1.65	-
437	15.67	+1.00	+0.54	470	14.46	+0.99	+0.41
438	17.66	+2.00	-	471	17.14	+1.65	-
439	17.45	+1.14	-	472	16.30	+1.08	+0.59
440	17.71	+1.77	-	473	17.70	+1.64:	-
441	17.63	+1.44	-	474	16.25	+1.14	-
442	17.97	+1.65	-	475	17.44	+1.61	-

TABLE 12. (Cont.)

PHOTOGRAPHIC MAGNITUDES AND COLOURS IN NGC 6383.

STAR	V	B-V	U-B	STAR	V	B-V	U-B
443	16.15	+0.95:	-	476	17.67	+1.20	-
444	15.04	+0.88	+0.74	477	17.36	+1.05	-
445	15.07	+2.05	-	44	13.52	+0.66	+0.05
446	17.28	+1.32	-	478	17.95	+1.63	-
447	16.44	+1.40	-	479	17.93	+1.45	-
448	16.84	+2.00	-	480	15.04	+1.00	+0.37
449	16.60	+1.68	-	481	17.97	+1.57	-
450	17.34	+1.59	-	482	15.73	+1.00	+0.44
451	17.95	+1.55	-	483	16.92	+1.11	-
452	17.67	+1.98	-	484	16.25	+1.14	-
453	16.92	+2.75	-	485	14.99	+0.91	+0.31
454	16.44	+1.81	-	486	17.46	+1.13	-
455	17.67	+2.02	-	487	16.22	+1.05	+0.33
456	16.38	+2.09	-	488	16.63	+1.12	-
457	17.82	+1.61	-	489	16.86	+1.09	-
458	17.64	+1.45	-	490	17.73	+1.52	-
459	17.68	+1.42	-	491	16.90	+1.10	-
460	16.19	+1.43	-	492	16.58	+1.33	-
461	15.65	+0.89	+0.24	493	16.31	+1.16	-
462	15.92	+1.12	+0.72	494	16.98	+1.18	-
463	17.44	+1.51	-	495	15.53	+0.97	+0.55
464	16.77	+1.35	-	496	16.97	+1.41	-
497	15.67	+1.05	+0.47	528	17.28	+1.52	-

TABLE 12. (Cont.)

PHOTOGRAPHIC MAGNITUDES AND COLOURS IN NGC 6383.

STAR	V	B-V	U-B	STAR	V	B-V	U-B
498	17.35	+1.36	-	529	17.11	+2.44	-
499	17.87	+1.07	-	530	16.86	+1.15	-
500	16.05	+1.25	+0.46	531	17.54	+1.65	-
501	17.81	+1.14	-	532	15.60	+0.86	+0.35
502	15.85	+0.95	+0.25	533	16.78	+1.78	-
17	12.62	+0.59	+0.57	534	17.33	+1.67	-
503	15.29	+1.29	+0.81	535	16.57	+1.47	-
504	17.71	+1.49	-	536	16.95	+1.38	-
505	17.42	+1.47	-	537	17.18	+1.46	-
506	15.61	+1.10	+0.45	538	17.55	+1.45	-
507	18.10	+1.56	-	539	17.62	+2.06	-
508	18.04	+1.46	-	540	15.32	+0.89	+0.40
509	17.50	+1.38	-	541	15.37	+1.26	+1.13
510	17.02	+1.30	-	542	16.19	+1.28	-
511	17.81	+1.46	-	543	16.36	+1.48	-
512	17.40	+1.23	-	544	16.91	+1.01	-
513	17.40	+1.36	-	545	17.67	+1.50	-
514	14.06	+0.63	+0.11	546	16.38	+1.54	-
515	15.59	+0.87	+0.36	547	17.97	+0.87	-
82	13.19	+0.90	+0.37	548	16.73	+1.24	-
516	15.10	+0.85	+0.35	549	17.86	+1.19	-
517	18.05	+1.36	-	550	17.12	+1.22	-

TABLE 12. (Cont.)

PHOTOGRAPHIC MAGNITUDES AND COLOURS IN NGC 6383.

STAR	V	B-V	U-B	STAR	V	B-V	U-B
518	16.57	+1.05	-	551	17.13	+1.12	-
519	15.18	+0.91	+0.36	552	17.79	+1.41	-
520	16.00	+0.93	+0.42	553	15.90	+0.95	+0.17
521	15.30	+1.05	+0.66	554	14.75	+1.15	+0.64
522	14.81	+0.94	+0.51	555	14.47	+0.83	+0.30
523	14.66	+0.84	+0.57	556	14.22	+0.91	+0.37
524	15.65	+1.12	+0.81	557	14.18	+0.78	+0.31
525	16.15	+1.36	-	558	16.37	+0.99	+0.30
526	16.48	+2.46	-	559	14.98	+1.05	+0.53
527	15.39	+0.82	+0.10	560	16.38	+1.28	-
561	16.94	+1.32	-	575	16.08	+1.04	+0.41
562	15.54	+1.04	+0.52	576	17.71	+1.45	-
563	18.10	+1.23	-	577	14.27	+0.79	+0.05
564	17.53	+1.40	-	578	17.79	+1.65	-
565	17.87	+1.52	-	579	14.36	+0.82	+0.29
566	16.10	+1.52	-	580	16.13	+0.99	+0.40
567	17.44	+1.19	-	581	16.18	+1.01	+0.57
568	14.76	+0.74	+0.12	582	18.05	+1.50	-
569	14.98	+0.83	+0.15	583	17.91	+1.40	-
570	16.98	+1.52	-	584	17.65	+1.13	-
571	16.54	+1.39	-	585	15.13	+0.93	+0.30
572	17.99	+1.24	-	586	16.30	+1.52	-
573	17.34	+1.07	-	587	17.58	+1.92	-
574	14.56	+0.82	+0.36	588	17.16	+1.17	-

TABLE 13.

SPECTRAL TYPES IN NGC 6383.

The	HD/HDE	Sp(MK)	E_{B-V}	M_V Sp	M_V Hβ	$(m-M)^o$ Sp	$(m-M)^o$ Hβ
1	159176	O 8 V SB2		-5.2	-5.0	10.4	10.2
2	317847	B 2 IV	0.35	-3.3	-3.0	11.6	11.3
3	317857	A 7 : pVB	0.13:	+2.0:		7.8:	
5	317853		0.30		-1.0		11.2
6	317845	B 1 III-IV	0.36	-4.2	-2.7	12.2	10.7
9	317860	K 0 IV-V	0.18:	+4:		5.2	
10	317856	B 2-3 V n	0.34	-2.0	-1.7	11.0	10.7
11	317843	K 0 III	0.21	+0.8		8.3	
14	317846	B 3 V : n	0.28	-1.7	-1.9	10.5	10.7
16	-	B 2-3 V	0.32	-2.0		11.7	
20	-		0.33		0.0		10.4
24	-	B 6 V	0.34	-0.7		11.0	
34	317848	K 3 : III	0.00:	+0.1		10.3	
47	317849	A 3 II	0.31:	-2.8		11.8	
57	317854	A 0 : V	0.26	+1.0		8.9	
75	317861	B 2-3 Vne	0.45:	-2.0		10.8:	
83	317858	B 2 V	0.38	-2.5		11.0	
85	317859	F 3 V	0.05	+3.0		6.3	
V701	317844	B 1 : nn	0.38	-3.6		11.2:	

Eggen's photometry of HD No. 159176

$V = 5.68\ (B-V) = +0.04$

has been used. Note that this was observed at the Cape and is not

TABLE 13. (Cont.)

subject to the errors which may be present in his results for the other stars observed at Pretoria.

Andrews' (1966) Hα photometry for HD 159176 gives $M_V = -6.3$, so $(m - M)_o = 11.5$.

M_V(Sp) is taken from Blaauw (1963).

TABLE 14.

VARIABLE STARS IN NGC 6383.

STAR	DATE/TIME (U.T.)	V	B-V/B	U-B/U
V701	8 Jul 1966	8.74	+0.13	-0.67
	14 Aug 1966	8.78	+0.13	-0.68
	8 Aug 1967	8.94	+0.11	-0.63
V702	22 Apr 1966	11.76	+0.20	
	19 Jun	11.78		
	21 Jun :			
	2002		13.74	
	2103	12.82		
	2140	12.52		
	2158	12.42		
	2213		12.52	
	2225		12.44	
	13 Sep	11.83	+0.22	-0.31
	9 Jun 1967	11.80	+0.17	-0.22
	11 Jun	11.81		11.77
	5 Jul	11.72	+0.26	-0.34
	7 Jul	11.76	+0.25	
V486	20 Apr 1966		13.38	
	22 Apr	12.78	+0.65	
	21 Jun	12.79	+0.62	
	8 Jul	12.60	+0.57	+0.27

TABLE 14 (Cont).

VARIABLE STARS IN NGC 6383.

STAR	DATE/TIME (U.T.)	V	B-V/B	U-B/U
	14 Jul 1966	12.59	+0.52:	
	22 Jul	12.62	+0.60	+0.27
	13 Sep	12.63	+0.63	+0.35
	9 Jun 1967	12.82	+0.63	+0.51
	5 Jul	12.75		13.81
	7 Jul	12.64	+0.74	+0.39
	5 Aug	12.69	+0.62	+0.36
	8 Aug	12.73	+0.63	+0.33
V 1	20 Apr 1966		17.19:	
	22 Apr	15.65	+1.25:	
	19 Jun	15.83	+1.32	
	21 Jun	15.89	+1.17	
	13 Sep	15.44	+1.29	+0.80:
	8 Jun 1967	15.99	+1.45	+0.68
	10 Jun	15.76		17.98
	5 Jul	17.76	+1.41	
	7 Jul		18.97	
	28 Jun 1968		19.28	
V 2	7 Jun 1967	18.7:	20.07:	
	9 Jun	18.6:		
	5 Jul	18.29:	19.09	
	7 Jul		19.6	

TABLE 14 (Cont.)

VARIABLE STARS IN NGC 6383.

STAR	DATE/TIME (U.T.)	V	B-V/B	U-B/U
V 3	7 Jun 1967		>20?	
	5 Jul		18.7	
	7 Jul		19.9	
	28 Jun 1968		19.7:	
V 5	20 Jun 1966	16.91	+0.69	
	21 Jun	17.69	+0.60	
	7 Jun 1967	17.58	+1.01	-0.34
	9 Jun	17.72:		
	5 Jul	17.38	+0.44	-0.29
	7 Jul		18.17	-0.53
	28 Jun 1968		18.44:	
V 6	20 Jun 1966	17.16	+1.22	
	21 Jun	17.10	+1.47	
	7 Jun 1967	17.15	+1.52	
	9 Jun	(16.93)		
	5 Jul	17.58	+1.58	
	7 Jul		(18.28)	
	27 Jun 1968		18.46	

TABLE 15.

CLUSTER	EARLIEST Sp.	O	NUMBER OF STARS O-B9	Var.	LOWER M.S. TURN-UP. $(B-V)_o$
IC 1805	O 5	11			
NGC 2264	O 7	1	28	50	0.00
IC 2944	O 6	9			
NGC 6383	O 8	1	21	6	-0.05
NGC 6530	O 5	3	50	70	-0.07
NGC 6611	O 6	7	64	50	-0.15
IC 5146	B 1	0	6	20+	0.0: